Project Ostrich A Feasibility Study: Detecting Buried Mines in Dry Soils Using Synthetic Aperture Radar

John V.E. Hansen
Judy Ehlen
Timothy D. Evans
Richard A. Hevenor

September 1993

U.S. Army Corps of Engineers
Topographic Engineering Center
Fort Belvoir, Virginia 22060-5546

US Army Corps of Engineers
Topographic Engineering Center

T
E
C

Project OSTRICH

REPORT DOCUMENTATION PAGE

Form Approved
OMB No. 0704-0188

1. AGENCY USE ONLY (Leave blank)	2. REPORT DATE	3. REPORT TYPE AND DATES COVERED
	September 1993	Technical Report Sep. 1990 - May 1993

4. TITLE AND SUBTITLE

Project Ostrich A Feasibility Study: Detecting Buried Mines in Dry Soils Using Synthetic Aperture Radar

5. FUNDING NUMBERS

6. AUTHOR(S)

John V.E. Hansen Judy Ehlen
Timothy D. Evans Richard A. Hevenor

7. PERFORMING ORGANIZATION NAME(S) AND ADDRESS(ES)

U.S. Army Topographic Engineering Center
Fort Belvoir, VA 22060-5546

8. PERFORMING ORGANIZATION REPORT NUMBER

TEC-0040

9. SPONSORING/MONITORING AGENCY NAME(S) AND ADDRESS(ES)

10. SPONSORING/MONITORING AGENCY REPORT NUMBER

11. SUPPLEMENTARY NOTES

12a. DISTRIBUTION/AVAILABILITY STATEMENT

Approved for public release; distribution is unlimited.

12b. DISTRIBUTION CODE

13. ABSTRACT *(Maximum 200 words)*

Metallic and nonmetallic mines were utilized to construct a minefield in arid soil at Twentynine Palms, California to assess the extent to which long-wavelength radar could be used to detect buried mines by remote sensing. Surface and subsurface mines were placed in accordance with known enemy doctrine, and the site was imaged with X-, C- and L-band radar from a Navy P-3 aircraft. This report describes the construction and physical characteristics of the test sites, and presents and discusses the results of imagery analysis.

14. SUBJECT TERMS

Ground-penetrating SAR, radar, dry soils, minefield detection, buried objects

15. NUMBER OF PAGES

108

16. PRICE CODE

17. SECURITY CLASSIFICATION OF REPORT	18. SECURITY CLASSIFICATION OF THIS PAGE	19. SECURITY CLASSIFICATION OF ABSTRACT	20. LIMITATION OF ABSTRACT
UNCLASSIFIED	UNCLASSIFIED	UNCLASSIFIED	UNLIMITED

TABLE OF CONTENTS

TABLE OF CONTENTS (continued)

LIST OF FIGURES

LIST OF FIGURES (continued)

LIST OF FIGURES (continued)

LIST OF TABLES

PREFACE

This report was prepared to reflect efforts conducted by the U.S. Army Topographic Engineering Center (TEC) in support of Desert Shield/Desert Storm between August 1990 and April 1991.

We wish to thank Marine Corps personnel from Air Ground Combat Center at Twentynine Palms, California, and particularly Range Control and the USMC 173 Marine Wing Support Squadron, for their assistance in creating and operating the test site. We also wish to thank personnel from the Foreign Science and Technology Center, Charlottesville, Virginia; the Naval Air Warfare Center, Warminster, Pennsylvania, and particularly Mr. Jim Verdi; and the Belvoir Research Development and Engineering Center, Fort Belvoir, Virginia, for their advice and assistance. Finally, a very special thank you is due to Jean Diaz, who worked so diligently preparing the final copy of this report.

Mr. Walter E. Boge was Director and LTC Louis DeSanzo was Commander and Deputy Director of the Topographic Engineering Center at the time of publication of this report.

PROJECT OSTRICH
A FEASIBILITY STUDY: DETECTING BURIED MINES IN DRY SOILS USING SYNTHETIC APERTURE RADAR

INTRODUCTION

Project Ostrich was initiated on 6 September 1990. The goal of the project was to evaluate the feasibility of using airborne (and ultimately spaceborne) ground-penetrating radars to detect buried mines. Previous investigations showed that subsurface waterways were detectable by spaceborne radars in arid soils in Chad/Egypt (McCauley et al., 1982; McCauley et al., 1986). Other investigators (Rinker, 1965; Rinker et al., 1966; Blom et al., 1984; G. Olhoeft, U.S. Geological Survey (USGS), personal communication, 1991; and L. Fullerton, Time Domains, personal communication, 1991; among others) have also shown the potential for utilizing ground-penetrating radar systems to locate subsurface artifacts in arid regions. Although a number of previous studies have been conducted to remotely detect mines, including work by the Army's Belvoir Research, Development and Engineering Center (BRDEC; Nolan, et al., 1980), none of these attempted to exploit the ground-penetrating capabilities of long-wavelength radar for this application in arid soils.

In a briefing by Walter E. Boge, Director, Topographic Engineering Center (TEC),[1] to Dr. Robert Oswald, Director of Research and Development, HQ Corps of Engineers, at the Engineer Topographic Laboratories (now renamed TEC) on 6 September 1990, TEC efforts in support of Operation Desert Shield were presented. The presentation included work being done by TEC (in conjunction with the USGS) employing hyperspectral imagery to characterize soil in Yuma, Arizona. Flights utilizing airborne X-, C-, L-, and P-band radars had shown images believed to be subsurface objects, possibly buried ordnance (G.G. Schaber, USGS, personal communication). Given the arid nature of the soil in the Yuma area and the work by previous investigators noted above, there were indications that the radar was, in fact, penetrating the surface and imaging subsurface objects. Since the soils on the Saudi Arabia/Kuwait border are highly arid (probably less than 1% moisture; see Berlin et al., 1986), the project was launched to evaluate the feasibility of detecting buried mines in such soil from airborne and spaceborne platforms.

As a result of the September 1990 meeting, Dr. Oswald directed TEC to conduct a study to determine the feasibility of using airborne, ground-penetrating radar to detect buried mines in arid soils. Given the urgent potential threats facing forces involved in Operation Desert Shield in September 1990, the study was to be done in the shortest possible time.

PROGRAM ORGANIZATION

Team Formation

On 7 September 1990, a team was put together with personnel from the Remote Sensing and Space Research Divisions of TEC's Research Institute. In time, the team drew upon personnel from other TEC elements, from the Waterways Experiment Station (WES), from the Naval Air Warfare Center (NAWC), from the U.S. Marine Corps (USMC) and from two contractors (Environmental

[1] The Engineer Topographic Laboratories (ETL) was renamed the Topographic Engineering Center (TEC) in October 1991.

Research Institute of Michigan (ERIM), Ann Arbor, Michigan; and VSE, Alexandria, Virginia). A list of team members is provided in Appendix A. The effort was designated Project Ostrich.

At the same time the project was being initiated, a team of BRDEC and WES personnel was conducting a demonstration of the Stand-off Mine Detection System (STAMIDS) at Fort Hunter Liggett, California. This provided an additional perspective to the project and allowed project personnel from both efforts to exchange information.

Sensor Platforms

Because radar wavelength and penetration depth are related (the longer the wavelength, the greater the depth of penetration), an airborne sensor platform was sought possessing either L-band (15-30 cm wavelength) or P-band radar (30-100 cm wavelength), with adequate resolution to distinguish mines with typical minefield spacing. Such systems are not plentiful in the U.S.: only two were known to be operational at the outset of Project Ostrich. Contact with the Jet Propulsion Laboratory (JPL) revealed that the National Air and Space Administration (NASA) DC-8 aircraft (which carries both L- and P-band radars) was unavailable. Discussions with ERIM on 12 September 1990 indicated that a Navy P-3 aircraft carrying X-, L-, and C-band radar might be available. A meeting at ERIM on 13 September 1990 provided additional details on the P-3 radar system. In addition to availability, the resolution of the P-3 system (1.5 m) offered major advantages. Other radar parameters, such as angles of incidence and polarization, were also taken into account. Operating parameters of the system are in Appendix B.

An in-process review meeting at TEC with personnel from the U.S. Marine Corps, ERIM, BRDEC and the Army Space Programs Office (ASPO) on 19 September 1990 provided an opportunity to review a tentative test plan and potential logistic problems anticipated. A meeting at NAWC on 20 September 1990 revealed that a fortuitous change in the aircraft's commitments made it available during the second week of October.

Test Site Selection

Preliminary discussions on potential test sites centered on two areas believed to have acceptably low soil moisture: Yuma, Arizona, and Twentynine Palms, California. Soil moisture content is very important with respect to radar penetration -- the lower the soil moisture content, the more likely the chance of penetration. For the most part, the operational area in Saudi Arabia is hyperarid, except in the rainy season (i.e. the soils probably contain less than 1.0% moisture). Fort Hunter Liggett was also considered briefly because of BRDEC's STAMIDS demonstration, but the soil characteristics were not like those described for Saudi Arabia (Berlin et al., 1986). Discussions with personnel from the USMC Combat Development Center (USMCCDC), Quantico, Virginia, led to the selection of Twentynine Palms, since it offered personnel and equipment not available at Yuma. In addition, access to Marine Corps Air Ground Combat Center (MCAGCC) is restricted, providing less interference from visitors and personnel not associated with the study. Better coordination to avoid interference between air traffic control radar systems and the airborne sensing systems was also possible at MCAGCC. On 19 September 1990, the decision was made to utilize the site at Twentynine Palms, assuming that an adequately low soil moisture content could be verified.

Initially, one study site was selected for this experiment by evaluating the surface materials map sheet in the Twentynine Palms Tactical Terrain Analysis Data Base (TTADB). This site, located

between Deadman Lake and Gypsum Ridge, comprised the only extensive area designated "sand dunes" on the surface materials map. Prior to visiting Twentynine Palms, two other sites were included as possible test sites, one located at Lavic Lake and the other at a large dry lake on the Lead Mountain 1:50,000 scale topographic map. Both were shown on the TTADB to consist of sandy soils with finer grain than soils at the Gypsum Ridge site. Although the presence of gravel is known to inhibit radar penetration, depending on particle size, no data from Saudi Arabia was available to assess comparability with respect to gravel in the two areas.[2]

A site selection survey tour of MCAGCC was made on 26 September 1990. With assistance from USMC 173 Marine Wing Support Squadron (173 MWSS), the three possible sites were visited (Lead Mountain, Lavic Lake, and Gypsum Ridge), and soil samples were collected at each for soil moisture determinations. Surface and subsurface samples from the Gypsum Ridge area contained moisture well within the probable limits of radar penetration -- the two surface samples contained 0.51% and 0.30% moisture, and the subsurface sample (4 inches), 1.14%. However, this site is not covered with sand dunes as indicated on the TTADB; it is a gently-sloping, south-facing surface covered with coarse sand and gravel. It is possibly an old alluvial fan. The samples from the dry lakes, although distinctly finer grained, contained more moisture than the samples from the Gypsum Ridge area -- the surface sample from Lavic Lake contained 0.81% moisture, and that from the Lead Mountain Lake contained 1.80% moisture. A subsurface sample collected at the Lead Mountain lake contained 7.31% moisture, which was unacceptable. Because soil moisture content is more important in these circumstances than fine grain, the Gypsum Ridge site was selected for the experiment.

In addition to the promising soil conditions, the Gypsum Ridge site was advantageously located with respect to logistic support at MCAGCC, and on 28 September 1990, the site approximately 0.5 km south of Gypsum Ridge (coordinates 78/01) was selected as the test site (see Figure 1).

After the test site was selected, soil samples were obtained from the Desert Shield theater of operations. A comparison of these samples with the Project Ostrich site samples confirmed adequate similarity for the purpose of the feasibility study (Ehlen and Henley, 1991).

Test Plan

Two invaluable sources of assistance in developing the test plan were BRDEC, Ft. Belvoir, Virginia and the Foreign Science and Technology Center (FSTC), Charlottesville, Virginia. At the request of the USMC, FSTC had prepared a classified report on Iraqi combat engineering capabilities, with emphasis on mine warfare. This report, together with discussions with the two agencies, formed the basis for the types of mines selected and their deployment in the test plan. The goal was to replicate the type of anti-tank minefield (reflecting known enemy doctrine) that could be anticipated in the Desert Shield area.

---

[2] Further work on soil samples obtained from Saudi Arabian and from Twentynine Palms has shown that the Saudi Arabian soils contain significantly more gravel than do those from Twentynine Palms (Ehlen, 1993). As the fractions > 2 mm were not sieved, information on gravel particle-size comparability is not available.

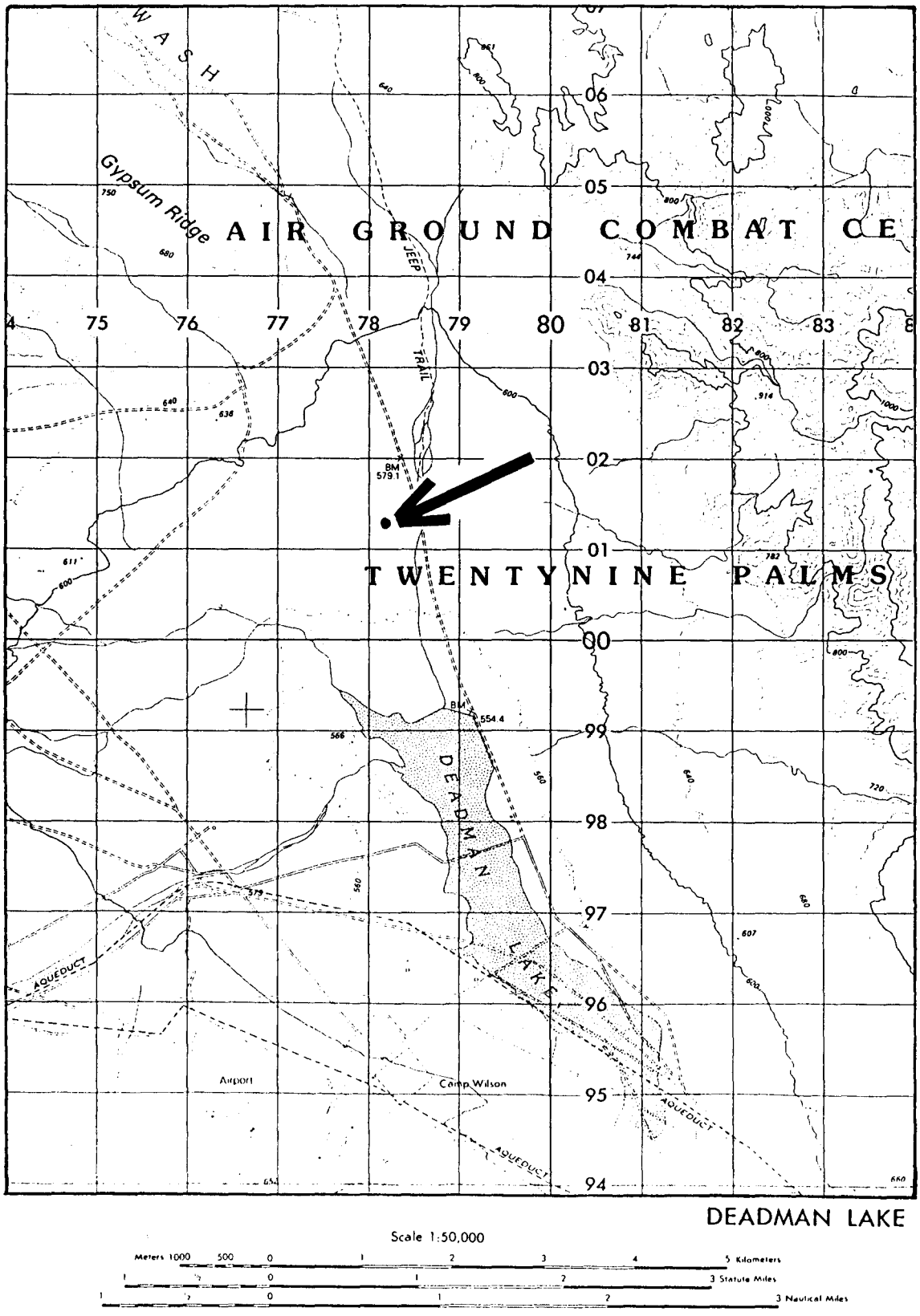

Figure 1. Map showing location of test site (arrow).

The original concept was to employ buried metallic mines only, but this was changed to include nonmetallic mines because the FSTC threat analysis indicated such mines could also be anticipated. Surface mines (both metallic and nonmetallic) were also included to obtain comparative data. The test plan included trenches with both metallic and nonmetallic mines at various depths, as well as trenches without mines. The site was designed with radar corner reflectors at the corners. The plan also included obtaining radar imagery of (1) the site prior to any soil disturbance; (2) the site after mine emplacement; and (3) the site after mine removal and restoration. The details of the test plan comprise Appendix C. Plans for soil characterization studies were also included, and involved taking both surface and subsurface samples during test operations.

A final meeting was conducted at TEC on 2 October 1990. Test plans and schedules were reviewed, and specific responsibilities for air traffic control, visitor control, photographs, logistics, and data gathering and analysis were reviewed.

Test Items

Inert metallic TM-57 and M-12 mines, approximately 12 inches in diameter, were located at the Michigan National Guard, and these mines were transported to the test site during the weekend of 6 October. Nonmetallic mines were replicated using surrogates made to BRDEC specifications. These mines were fabricated during the same weekend by VSE Corporation, Alexandria, Virginia. Photographs of both types of mines are shown in Figure 2.

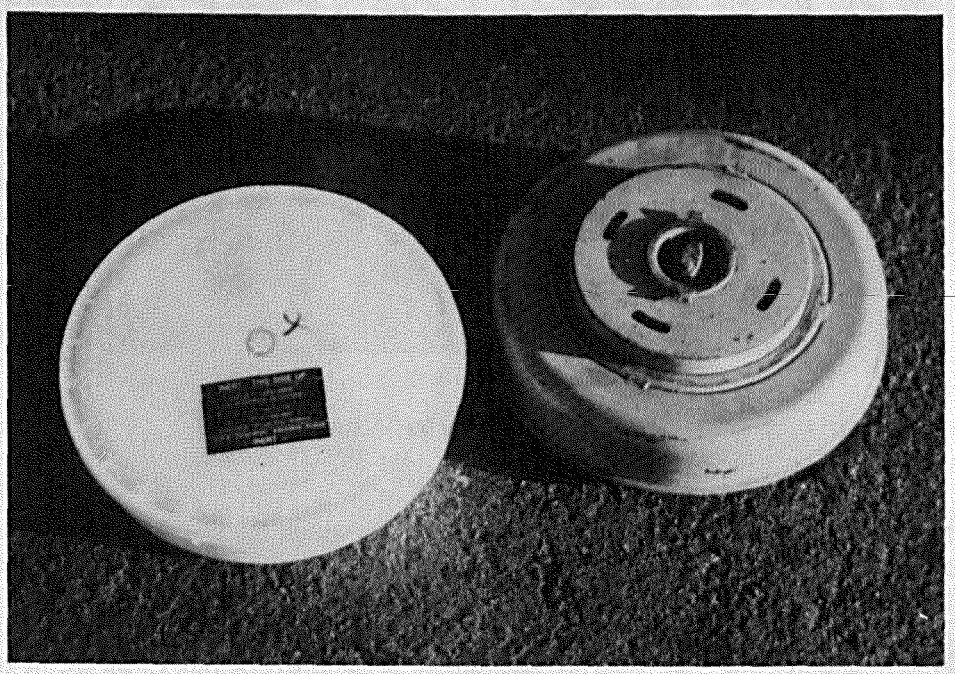

Figure 2. Nonmetallic and metallic mines.

SITE PREPARATION

Phase I

Phase I extended from 9 through 14 October 1990. In order to conform to the flight plan shown in Appendix C, personnel arrived at the site on 9 October. On 10 October, Commander, USMCAGCC, was briefed on the effort, and pledged his full support. Site preparation began the same day.

At USMCAGCC, personnel from the 173 MWSS were assigned to assist the team. First, the test site was surveyed in accordance with the test plan. A complete photographic record was made during operations. Surface corner reflectors were emplaced (Figure 3), and one corner reflector was buried just below the surface adjacent to the test site in an effort to obtain data comparing buried mine signatures with that of a known corner reflector. The first flyover was made of the bare site on the morning of 11 October. Immediately thereafter, mine emplacement operations began.

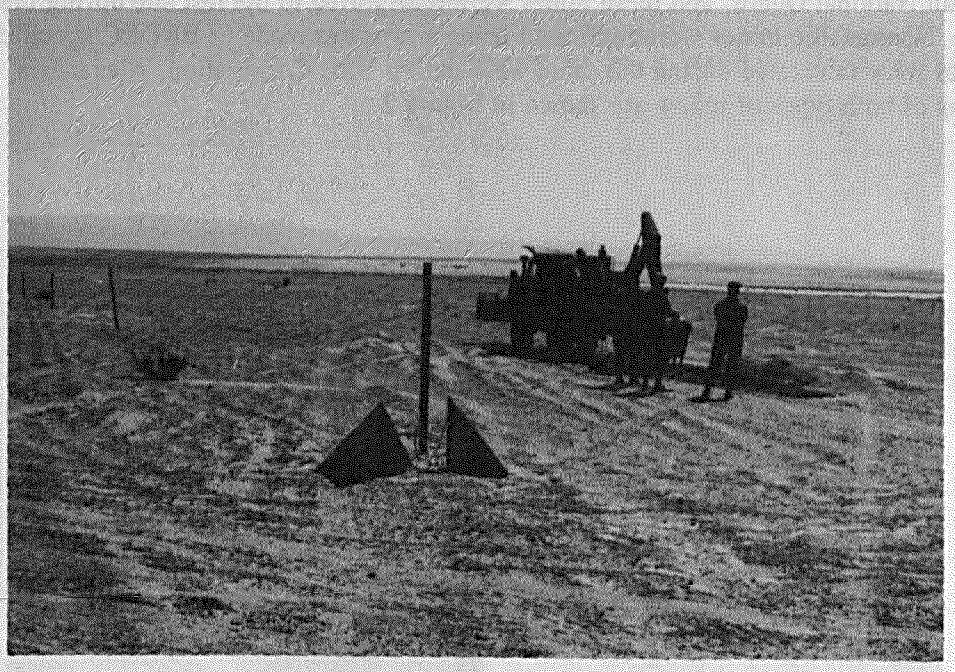

Figure 3. Corner reflectors.

The test plan required digging 12 rows of trenches in which mines could be buried. A Small Emplacement Excavator (SEE; Figure 4) was used initially, but was soon replaced by a road grader, which expedited trench digging. Each mine was surveyed in and checked for dimensional adherence to the test plan (Figure 5) and for depth (Figure 6). The majority of the mines were buried 4 inches deep, reflecting known doctrine. Mines were also buried at depths of 8 and 12 inches to simulate conditions that might result from additional sand accumulation. Operations resumed on 12 October. By late in the day, all trenches were completed with mines emplaced (Figure 7); surface mines were

Figure 4. SEE Tractor digging trench.

Figure 5. Mines being placed 5 meters apart.

Figure 6. Mines being checked for proper depth.

Figure 7. Grader burying mines.

surveyed in as well (Figure 8). All but three trenches were filled by the grader, which produced a large, relatively smooth area of disturbed soil. Soil measurements and terrain data were taken during the operation (Figures 9 and 10; and Appendix D). The P-3 aircraft arrived over the site at 1800 to begin radar imaging. Flights were made at altitudes of 7,300 and 12,400 feet.

The mines were removed on 13 October. Work proceeded rapidly since the precision with which the mines had been emplaced made their retrieval fairly easy. Site border posts and corner reflectors were removed and the surface restored as close to its original condition as possible. The flyover of the restored site occurred on 14 October.

Phase II

After Phase I was completed and later in October 1990, intelligence imagery from the Desert Shield area of operations showed what were believed to be minefields. A comparison of these images with radar images taken in Phase I of Project Ostrich showed unmistakable similarities, but also revealed some features that were not present at the test site. Accordingly, plans were made to conduct a second phase of Project Ostrich, which involved reconstructing the test site to deliberately replicate the types of features shown in the imagery from the Desert Shield area of operations, in order to obtain comparative imagery.

A revised test site plan was developed (Figure 11; see Appendix C) and on 14 November 1990, the TEC team revisited the area and constructed a new test site of the same dimensions (100x250 m), approximately 200 m south of the original test site. Radar corner reflectors were buried at different depths, and the site boundary was marked with metal stakes spaced at 8.3 m connected with a single strand of barbed wire. A single roll of concertina wire was also placed around the site, approximately 10 m outside the barbed wire fence (Figure 12). Special care was taken to disturb as little soil as possible in digging the trenches in order to simulate the operation of a Soviet mine plow. In particular, the large area of disturbed soil created in the Phase I site was not present in the Phase II site; the area of disturbed soil was confined to the trenches themselves. Additionally, two trenches perpendicular to each other were dug to obtain data on signals resulting from the disturbed soil. In all other respects (i.e. types of mines and emplacement), the sites are similar. A complete photographic record was made and soil samples were collected from corresponding locations in the Phase I site. Although soils in the Phase II site contained more moisture than those in the Phase I site, the difference was not significant.

On 6 December 1990, the site was revisited to prepare for a potential overflight by the Navy P-3 aircraft used in Phase I. The flight was intended to provide data on "aging effects" associated with disturbed soil. The site was relatively undisturbed, with the exception of some sand movement from a recent sandstorm (Figure 13). The large, unfilled trenches dug in November had been filled in (Figure 14), and an even larger X-shaped trench (approximately 20x20 m) was dug by grader north of the site. The displaced material was consistently placed on the clockwise sides of the legs of the new trench so that more data could be obtained on the disturbed soil signals. In addition, small metal castings approximately 5 inches in diameter were placed on the surface as surrogate anti-personnel mines (Figure 15). The overflight took place on 13 December 1990.

Figure 8. Surface mines being emplaced.

Figure 9. Soil sample collection.

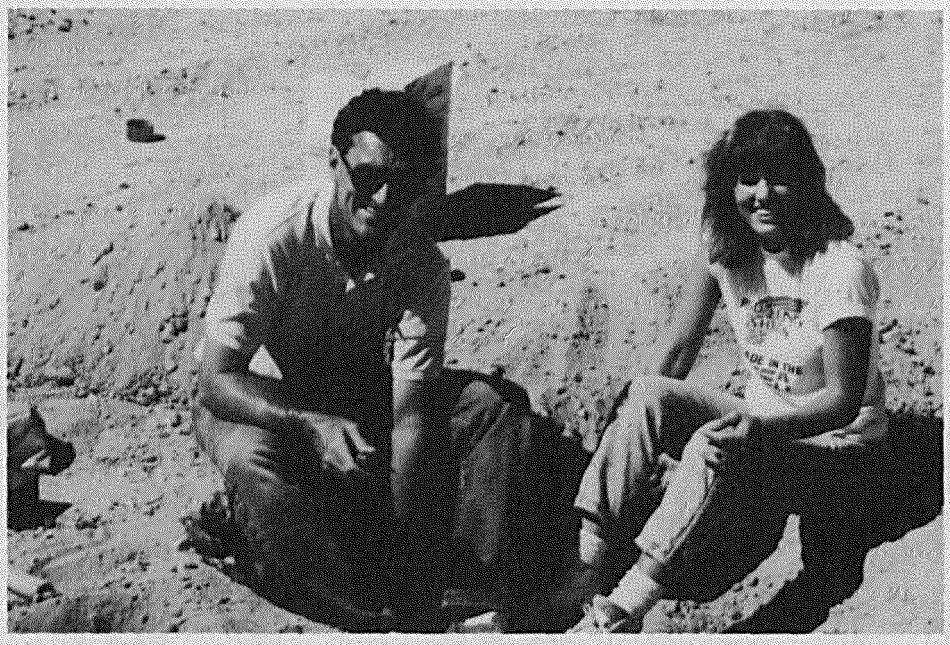

Figure 10. Soil characterization.

On 18 January 1991, the site was again revisited and a large, 20-inch radar corner reflector array was buried north of the test site. This array was buried immediately below the surface with an orientation favoring maximum strength of signal from an airborne radar viewing the ground with an approximately 40° depression angle. This array was covered with sifted, loose sand (Figure 16) to preclude the possibility of unwanted return from gravel or lower-density soil. The overflight took place on 30 May 1991. Figure 11 shows the test site as it looked in December 1992; little changed between May 1991 and December 1992.

REVIEW OF RESULTS

A total of 144 raw radar phase histories were recorded in five overflights by the NAWC P-3 aircraft. Phase histories were obtained in the X, C and L radar bands. In all of these bands, images were obtained with HH, VV, VH and HV polarizations, and at a number of angles of incidence. All the L-band phase histories and a small number of C- and X-band phase histories have been processed into finished images. The high resolution images from the Phase I test appear in Figures 17-19. High resolution imagery from the Phase II test appear in Figure 20.

Processing and image analysis concentrated on the L-band images, since greater ground penetration was expected with the longer wavelength. All of the L-band runs from October and December 1990 were processed to finished images at full resolution. These images were analyzed using existing techniques, and new algorithms were developed for use on these images (Appendices E and F). The findings of this analysis are discussed below (a summary of these results has also been reported previously by Hansen et al., 1992).

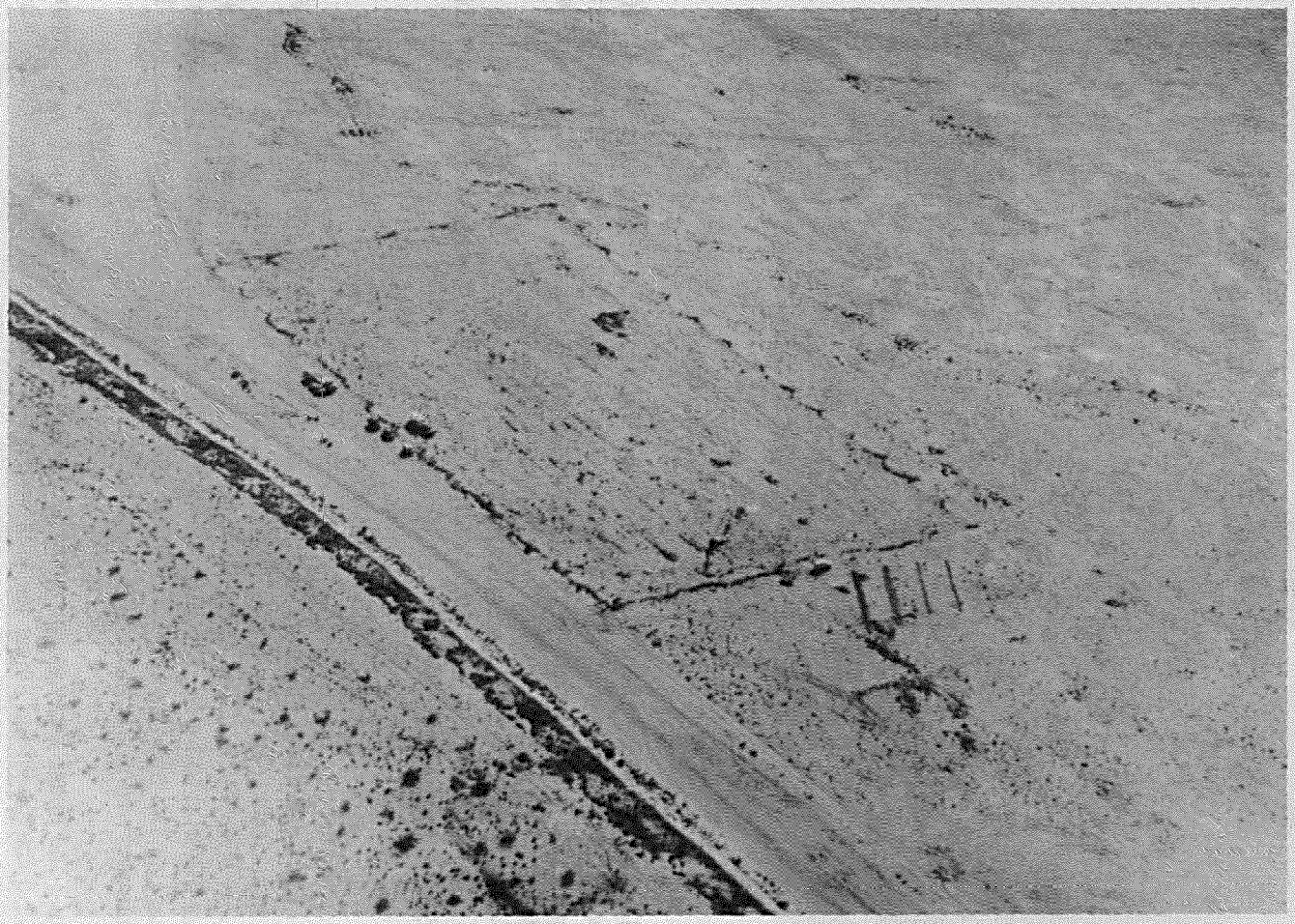

Figure 11. Aerial oblique photo showing the test site in December 1991 (courtesy of Hughes Santa Barbara Research Center).

Figure 12. Barbed wire and concertina wire surrounding Site II with corner reflector.

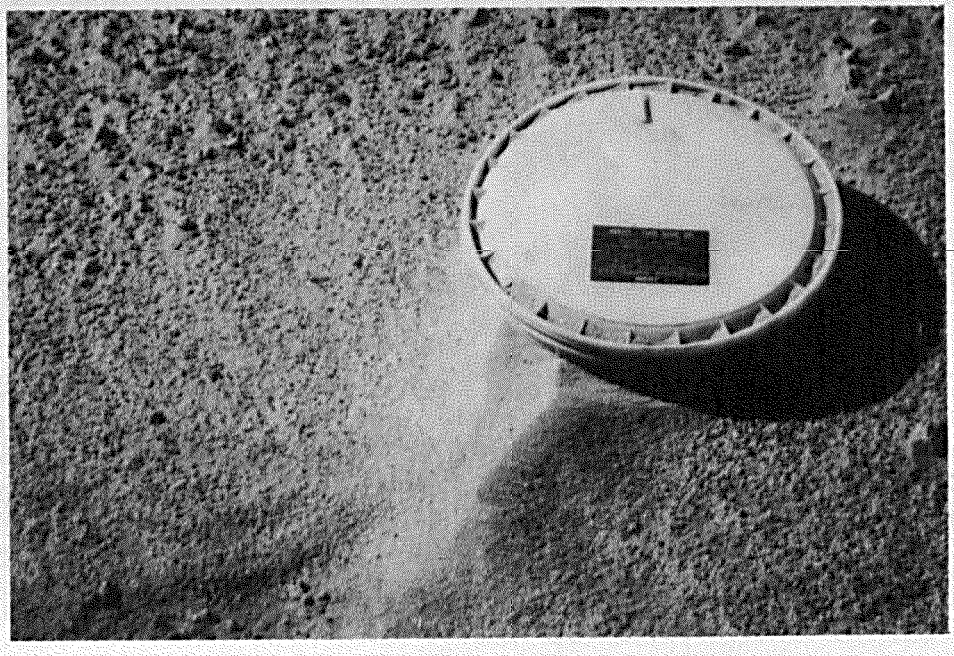

Figure 13. Effects of blowing sand on surface mine.

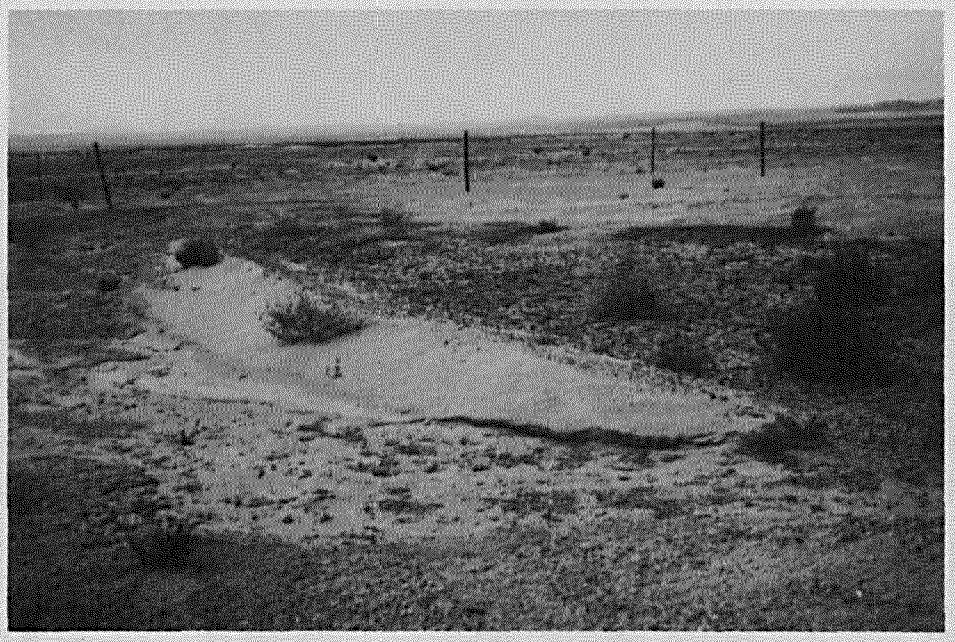

Figure 14. Open trench filled with blowing sand.

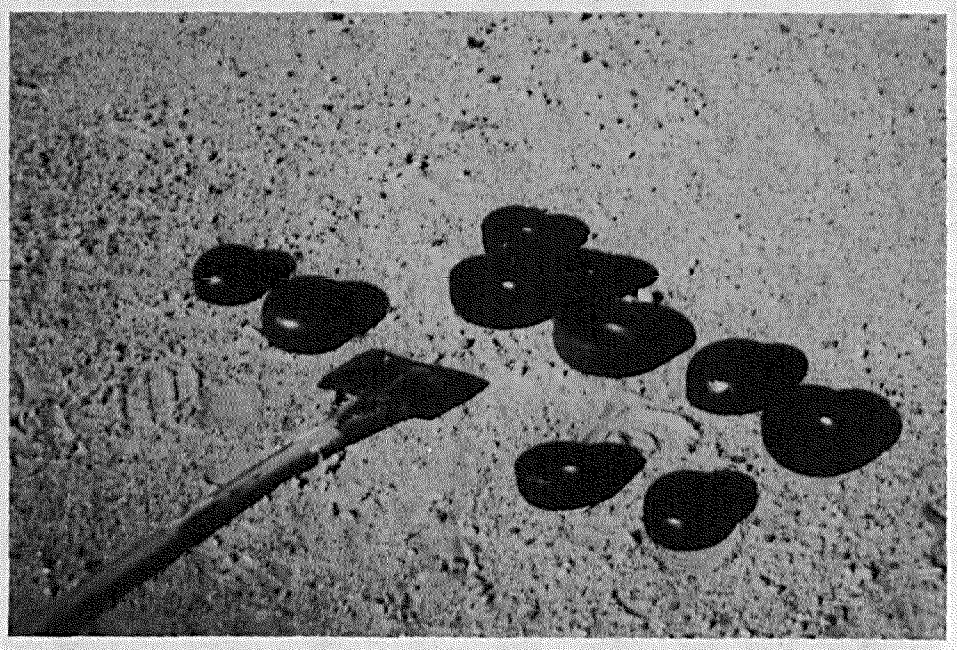

Figure 15. Surrogate scatterable mines.

Figure 16. Buried corner reflectors with sieve.

Phase I Site (October 1990)

The Phase I site was constructed on 11-12 October 1990 and imaged on 12 October 1990. Most of the trenches were dug and filled in with a road grader, producing a large area of disturbed soil (approximately 75x150 m) within the site boundaries over the trench area. Details of site construction are given in Appendix C.

As stated above, this site was imaged in three overflights. The first occurred when the site had been marked off with stakes and corner reflectors, but before mines were laid. The second occurred with the mines in place and the third occurred after the mines had been removed. The flight path of the P-3 for all of the Phase I imagery was south to north, parallel to the long axis of the site. The following results are based on analysis of the Phase I imagery. As noted above, the high resolution Phase I imagery is shown in Figures 17-19.

1. <u>There is no evidence of buried objects in the imagery</u>. No buried mines or buried corner reflectors are visible in any of the images. This is true regardless of the frequency, polarization or angle of incidence, and may be related to the basic physics and geometry of SAR (synthetic-aperture radar) imaging (see "Buried Mines" below). If signals were returned by the buried objects, they were very weak and were obscured by noise and clutter. It is possible that improvements in signal processing may yield discernable signals in the future.

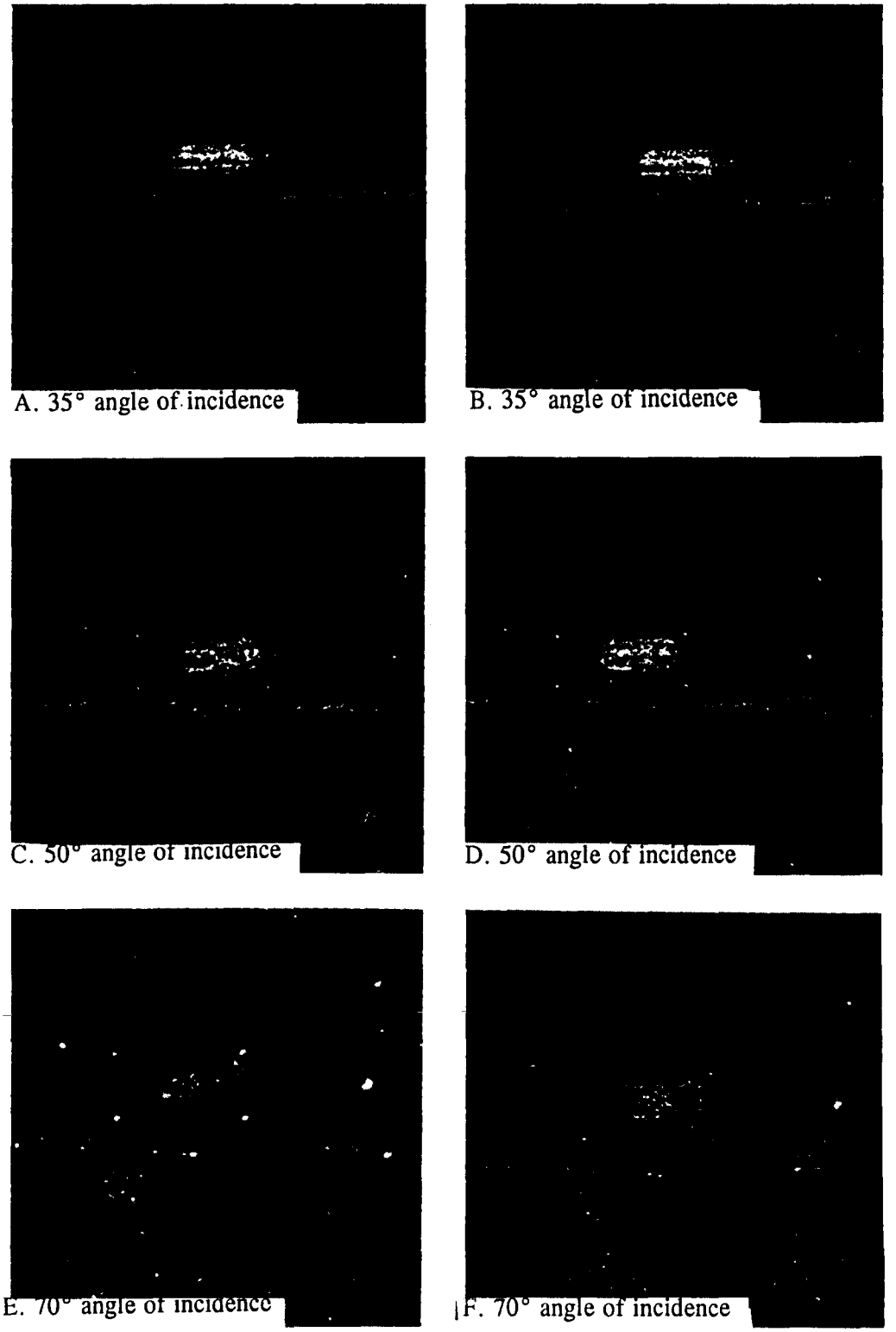

Figure 17. Phase I, L-band VV-polarization imagery

A. HV polarization, 35° angle of incidence

B. VH polarization, 35° angle of incidence

C. HV polarization, 50° angle of incidence

D. VH polarization, 50° angle of incidence

E. HV polarization, 70° angle of incidence

F. VH polarization, 70° angle of incidence

Figure 18. Phase I, L-band cross-polarization imagery

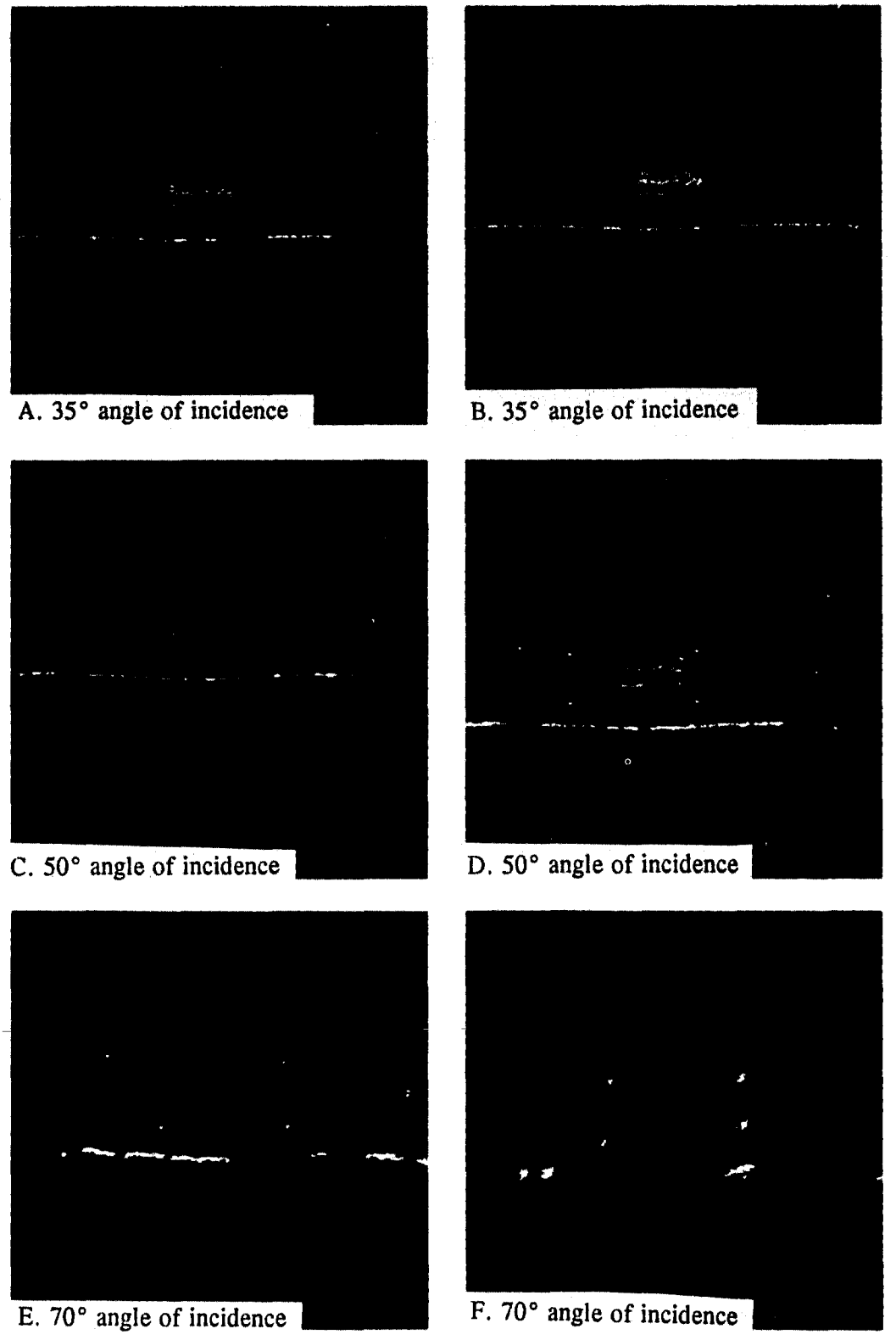

Figure 19. Phase I, L-band HH-polarization imagery

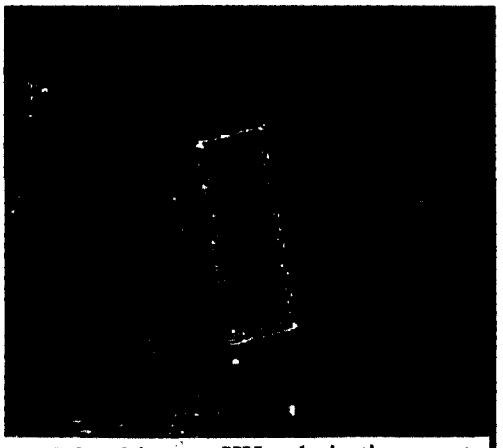

A. L-band image, HH-polarization, west-east flight line, 35° angle of incidence

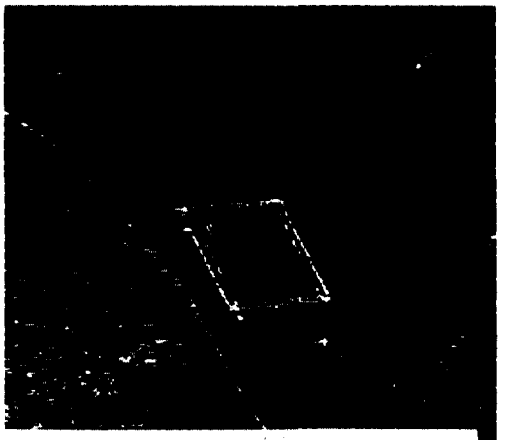

B. X-band image, HH-polarization, west-east flight line, 70° angle of incidence

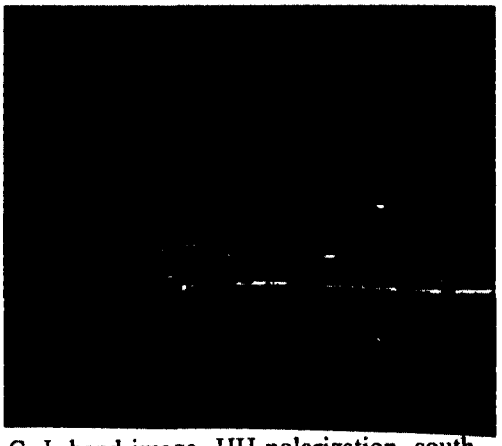

C. L-band image, HH-polarization, south-north flight line, 70° angle of incidence

D. C-band image, HH-polarization, west-east flight line, 70° angle of incidence

E. L-band image, VV-polarization, south-north flight line, 70° angle of incidence

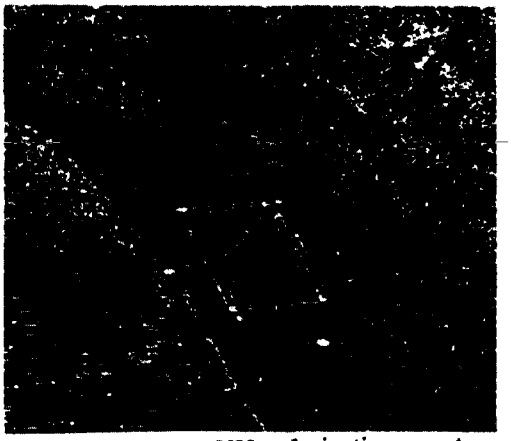

F. C-band image, VV-polarization, west-east flight line, 70° angle of incidence

Figure 20. Phase II imagery

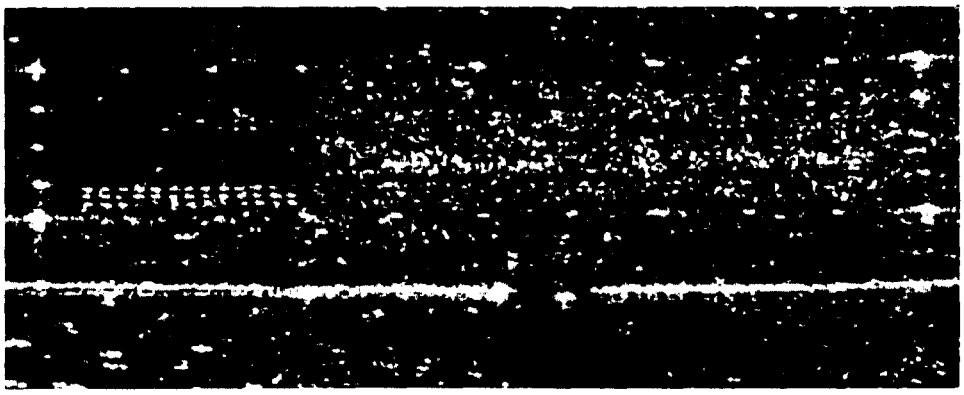

Figure 21. Phase I, C-band HH-polarization imagery.

2. Surface metal objects gave strong returns. The corner reflectors, the metal stakes bordering the site, and the metal surface mines are clearly seen and are individually resolved in a C-band image (Figure 20). Other surface objects, including metal debris scattered in the area and shrubbery, also gave strong returns. In the L-band imagery with VV polarization, the metal surface mines gave weak returns, but were not individually resolvable (Figure 17). In the cross-polarized images and in the images with HH polarization (Figures 18 and 19, respectively), the surface metal mines were not seen. The fence posts were seen on some of the L-band images as well as on the C-band image. The fence posts in the range direction (east-west) imaged better than those in the along-track direction (north-south; Figure 21). This may have been due to different orientations of the metal engineer stakes used as fence posts.

3. Nonmetallic surface mines were not detected in the L-band imagery. The nonmetallic mines located on the ground surface were not detected on any of the L-band images analyzed for either test site. A small number of these mines were detected and resolved on the C-band images (Figure 21).

4. A large area of disturbed soil gave a strong return in some of the imagery. This signal occurred over the area of the buried mines where the trenches had been covered with loose soil by the road grader. This signal was strongest with VV polarization and an angle of incidence of 35° (Figures 17A and 17B). Further discussion of this is presented under "Buried Mines," below.

Phase II Site (December 1990)

The Phase II site was constructed on 14 November 1990 approximately 200 m south of the Phase I site. The Phase II site was constructed to the same plan as the Phase I site, except that the boundary was marked with metal stakes, a single strand of barbed wire, and concertina wire. In addition, the trenches for the buried mines were dug with more care to disturb as little soil as possible to better simulate the operation of a Soviet mine plow. Thus, the largest differences between the Phase I and Phase II sites were the addition of barbed wire and concertina wire, and minimizing the area of disturbed soil.

The Phase II site was imaged by the NAWC P-3 on 13 December 1990. The high resolution imagery from this flight is shown in Figure 20. In addition to the results seen in the Phase I imagery, the Phase II imagery showed the following:

1. Strong returns were obtained from metal posts, barbed wire and concertina wire. In particular, a very bright return was seen from the single roll of concertina wire that marked the outer boundary of the site. The surface metal mines were detected quite well on one of the L-band images (Figure 22), and many of these mines were resolved.

2. Almost no returns were obtained from disturbed soil; i.e. trenches, vehicle tracks. L-band imagery shows no evidence of returns that can be attributed to disturbed soil. A possible explanation for this discrepancy in results obtained from the two sites is given in "Ground Reflection" below.

3. No evidence of buried objects (mines, corner reflectors) can be seen in the imagery. Although corner reflectors were buried at varying depths to show evidence of ground penetration, none of the objects buried on the test site, neither mines nor corner reflectors, could be identified in the imagery.

With the signal processing applied, the overall conclusions that can be drawn from analysis of the Project Ostrich Phase I and Phase II imagery are the following:

1. The synthetic aperture L-band radar system utilized in the Project Ostrich study was not able to detect small buried objects, such as mines.

2. SAR may be useful in locating surface indicators of minefields. Surface objects, such as barbed wire fences or surface metallic mines that are often associated with fields of buried mines can be detected with the type of SAR utilized in this study.

3. Strong signals from the trench area were detected in some images (possibly from the disturbed soil, surface features, or both) and may provide a potential indicator of military activity.

4. Further study of the use of ground-penetrating radar and signal processing is needed, as are improvements in radar resolution and signal processing. Although radar has been used previously to detect and to map buried objects, the failure of radar to detect relatively small buried objects in dry soils in the Project Ostrich study indicates a need for a better understanding of the mechanics of radar penetration of the ground.

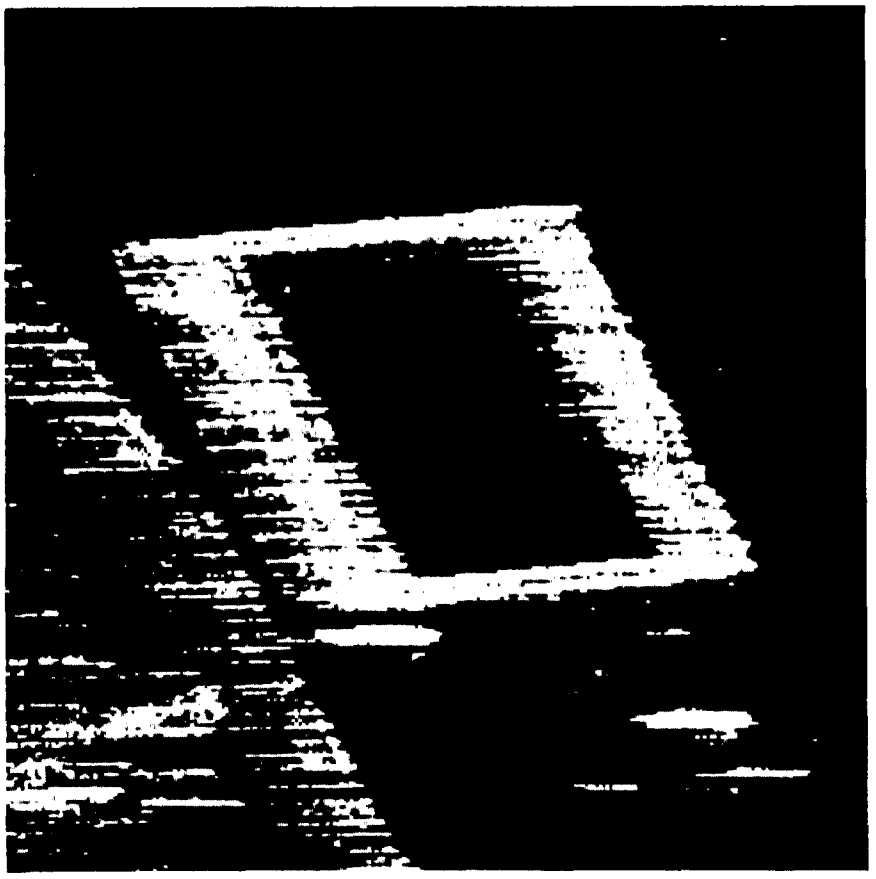

Figure 22. Phase II, L-band image, HH-polarization, west-east flight line, 70° angle of incidence.

Buried Mines

The situation pictured in Figure 23 may provide an explanation for the failure to see buried mines in the imagery. A time-harmonic electromagnetic wave is assumed incident at angle θ_i on the terrain. A mine is assumed to be buried at a depth d. The electromagnetic wave will be refracted into the terrain at angle θ_t. If the refracted wave hits the top of the mine, most of the energy will be reflected in the forward direction away from the radar. If the energy hits the side of the mine, the energy is reflected downward into the ground. There is no signal hitting the mine which is reflected in the backscatter direction, except the small edge effect that occurs at the top and bottom edges of the mine. This effect should be obtained regardless of the depth d.

Ground Reflection

The large bright return seen in some of the Phase I images, and which is particularly strong on L-band images with VV polarization (Figure 17), was not anticipated. If the ground were smooth, the incident wave should be reflected away from the radar rather than in the backscatter direction. However, a "radar rough" surface could produce a return giving the signals noted. This phenomenon is illustrated in Figure 24.

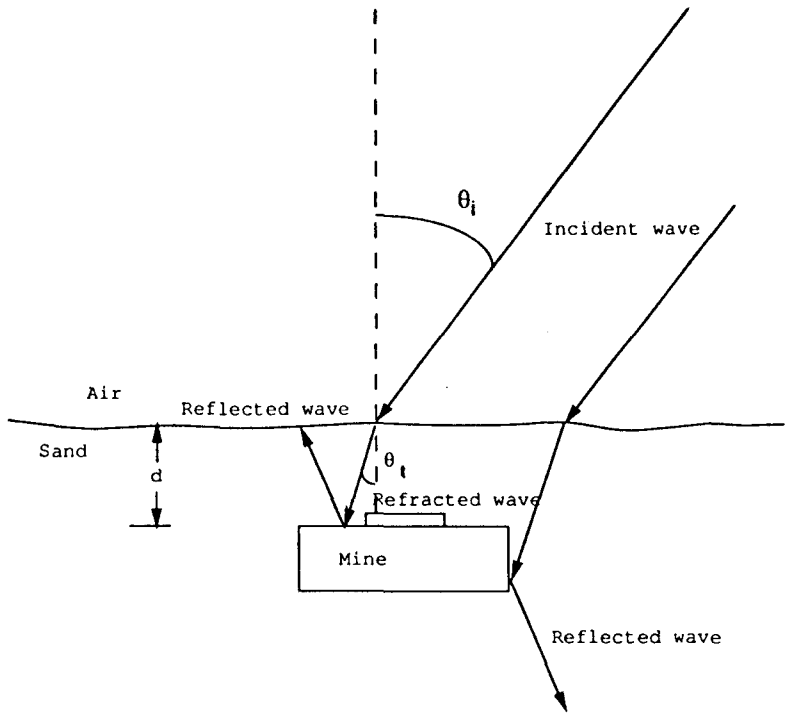

Figure 23. Radar wave reflected from buried mine.

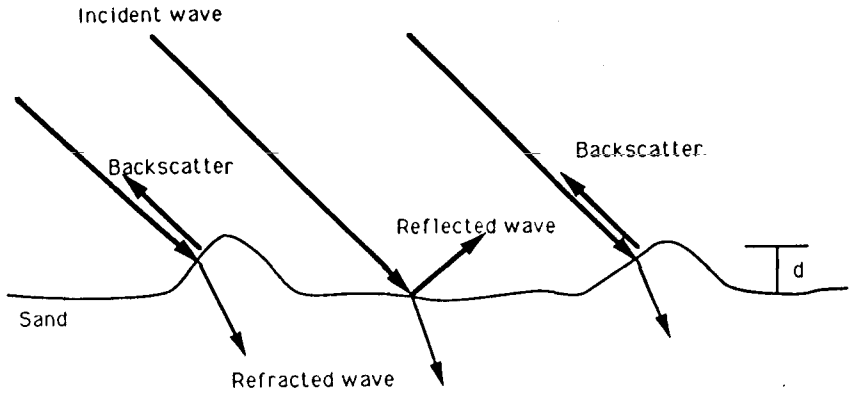

Figure 24. Radar backscatter from mounds of soil created by grader.

When the site was constructed, the eight westernmost trenches were dug using a road grader. After the mines were buried, the trenches were backfilled by having the grader push the loose soil over the trench area until the trenches were filled. In the process, small mounds approximately 6 inches high were created by loose soil pushed around the ends of the grader blade. These small mounds were oriented such as to provide a backscatter signal to the radar, and may have been responsible for some or all of the bright return seen on the imagery. If the slopes of these mounds were approximately 35° (which is likely because the angle of repose for granular particles is between 34° and 37°), the faces of these slopes would be normal to the beam of the radar when the incidence angle was 35°. If this is true, the strength of the return would be expected to become weaker as the angle of incidence increased, which is what was observed.

SUBSEQUENT EFFORTS

The efforts conducted in Project Ostrich continue to yield a number of inquiries by other agencies, indicating a wide range of interest in this area. In the latter days of Desert Storm, the increased interest in locating bunkers and other subsurface structures in Kuwait and Iraq led to Operation Groundhog, an initiative sponsored by the Office of the Secretary of Defense (OSD). The Project Ostrich site was recognized as a suitable location for some of the tests, and overflights of the area were made on 20 March 1991 utilizing the NASA aircraft mentioned previously carrying X-, L-, and P-band radars. Unfortunately, heavy rains several days before the flight generated backscatter from the moist soil and thus obscured any signals from buried objects.

In addition, on 27 March 1991, TEC convened a classified meeting of personnel involved in subterranean detection and analysis (SDA). This informal meeting confirmed interest in the Project Ostrich results, as well as in the test site itself. It was also recognized that the lessons learned from Desert Storm could contribute to the problems facing other agencies.

The effort conducted by TEC under Project Ostrich continued to produce a number of inquiries from other agencies interested in the general subject of subterranean detection and analysis. As a result, a second meeting was hosted by TEC on this subject; a classified report of that meeting is available (Hansen and Ehlen, 1992) and shows that the interest in this area is widespread. The interest in SDA extends to counternarcotics efforts, Customs Department interest in locating buried caches, treaty verification based on assessing activities occurring in subsurface structures, and to other intelligence interests. Two significant conclusions from the SDA meeting were that (1) the widespread interest in the SDA area involved several agencies external to the Department of Defense (DOD), and (2) a national focal point for SDA research appears warranted. In addition, the need for a dedicated national test site, such as the one at Twentynine Palms, would provide a standard test site for evaluating future subsurface detection systems.

CONCLUSIONS

Based on a review of the data, Project Ostrich and subsequent efforts have shown that detection of individual subsurface mines by a trained image analyst using L-band SAR images is a difficult, if not impossible, task even under the most favorable conditions of arid, barren soils. However, this is based on the signal and image-processing capabilities utilized in Project Ostrich (ERIM's and TEC's) and also reflects the conclusions from a feasibility study of limited scope, as

opposed to an in-depth research effort. Further effort, particularly in data and signal processing, or with the application of specialized image analysis techniques, could well prove useful.

The apparent lack of radar returns from the buried mines and corner reflectors on the L-band radar utilized in Project Ostrich would appear to be inconsistent with previous studies using penetrating radars (McCauley et al., 1982; Blom et al., 1984; McCauley et al., 1986). However, there are several possible explanations for this. The size of the mines used in Project Ostrich is significantly smaller than the buried objects detected in earlier studies. Polarization may prove to be a factor, and the full effect of this is not known; this is particularly relevant when substantial signals from disturbed soil are found, since such signals may also obscure returns from relatively small, buried objects. Finally, penetration and signal return are not synonymous. The shape of the object, coupled with the angle of the incoming radar signal and the immersion of the object in the soil, all could lead to penetration without a detectable return signal being received.

Although the effects of gravel-sized particles was not addressed, the detailed soil analysis comparison of the Project Ostrich test site with soils from Saudi Arabia shows many similarities (Ehlen and Henley, 1991). The low moisture content in both areas made Twentynine Palms an acceptable site for conducting minefield detection studies that would be representative of conditions found in such arid areas throughout the world. The site is also valuable in terms of its composition and its documented history, and it may well be useful to others involved in subsurface detection and analysis. The barren, arid nature of the site provides near ideal conditions for assessing the potential of penetrating radars.

The military doctrine in many nations defines minefields that are apt to leave a number of surface indicators, both in terms of disturbed soil signals, and images from other surface artifacts. Such minefields also reflect military doctrine that can prove helpful in limiting the areas of search. In addition, experience in Operation Desert Storm has shown the potential for providing soil characterization from remote sensing systems, and the value of data available from satellite imaging systems such as LANDSAT (Desert Processes Working Group, 1990a, 1990b, 1990c; Rinker and Corl, 1990, 1991a, 1991b, 1991c) and SPOT (J.N. Rinker, TEC, personal communication, 1992). The potential for long-wavelength (penetrating) radar to detect disturbed soil signals may have greater military potential than previously recognized. When coupled with the pattern-finding algorithms developed and employed in Project Ostrich, these appear to offer a tool that may assist in minefield detection. A holistic approach to the problem, including the use of expert systems, military doctrine, terrain reasoning, and visual, radar, and spectral imaging systems offers the potential for significant advances in detecting minefields in denied areas.

REFERENCES

Berlin, G.L., Tarabzouni, M.A., Al-Naser, A.H., Sheikho, K.M. and Larson, R.W. 1986. SIR-B subsurface imaging of a sand-buried landscape: Al Labbah Plateau, Saudi Arabia: *IEEE Transactions on Geoscience and Remote Sensing*, vol. GE-24, pp 595-602.

Blom, R.G., Crippen, R.E. and Elachi, C. 1984. Detection of subsurface features in Seasat radar images of Means Valley, Mojave Desert, California: *Geology*, vol. 12, pp. 346-349.

Desert Processes Working Group. 1990a. *Remote Sensing Field Guide - Desert, Landsat Thematic Mapper 165-040, 31 August, 1990*: Quantico, Virginia, U.S. Marine Corps Combat Development Center, OH O-52B.

_____. 1990b. *Remote Sensing Field Guide - Desert, Landsat Thematic Mapper 165-041, 31 August, 1990*: Quantico, Virginia, U.S. Marine Corps Combat Development Center, OH O-52C.

_____. 1990c. *Remote Sensing Field Guide - Desert, Landsat Thematic Mapper 166-040, 31 August, 1990*: Quantico, Virginia, U.S. Marine Corps Combat Development Center, OH O-52D.

Ehlen, J. 1993. *Physical Characteristics of Some Soils from the Middle East*: Fort Belvoir, Virginia, U.S. Army Topographic Engineering Center, TEC-0032.

Ehlen, J. and Henley, J.P. 1991. *A Comparison of Soils from Twentynine Palms California and Saudi Arabia*: Fort Belvoir, Virginia, U.S. Army Engineer Topographic Laboratories (now U.S.A. Topographic Engineering Center), ETL-0583.

Hansen, J.V.E. and Ehlen, J. 1992. *Subterranean Detection and Analysis (SDA)*: Fort Belvoir, Virginia, U.S. Army Topographic Engineering Center, TEC-S-001.

Hansen, J.V.E., Ehlen, J., Evans, T.D. and Hevenor, R.A. 1992. Mine Detection in very dry soils using radar: *Proceedings of the 1992 Army Science Conference, Orlando, FL*, vol. 2, pp 1-14.

McCauley, J.F., Schaber, G.G., Breed, C.S., Grolier, M.J., Haynes, C.V., Issawi, B., Elachi, C. and Blom, R. 1982. Subsurface valleys and geoarcheology of the Eastern Sahara revealed by Shuttle radar: *Science*, vol. 218, pp 1004-1020.

McCauley, J.F., Breed, C.S., Schaber, G.G., McHugh, W.P., Issawi, B., Haynes, C.V., Grolier, M.J. and Kilani, A.E. 1986. Paleodrainages of the Eastern Sahara -- the radar rivers revisited (SIR-A/B implications for a Mid-Tertiary Trans-African Drainage System): *IEEE Transactions on Geoscience and Remote Sensing*, vol. GE-24, pp. 624-648.

Nolan, R.V., Egghart, H.C., Mittleman, L., Brooks, R.L., Roder, F.L. and Gravitte, D.L. 1980. *MERADCOM Mine Detection Program 1960-1980*: Fort Belvoir, Virginia, U.S. Army Mobility Equipment Research and Development Command, Report 2294, 250 p.

Rinker, J.N. 1965. Radio echo sounding and strain rate measurement in the ice sheet of northwest Greenland: *Polar Record*, vol. 12, pp 403-405.

REFERENCES (continued)

Rinker, J.N., Evans, S. and Robin, G. de Q. 1966. Radio ice sounding techniques: *Fourth Symposium on Remote Sensing of the Environment*, University of Michigan, pp. 793-800

Rinker, J.N. and Corl, P.A. 1990. *Remote Sensing Field Guide - Desert, Landsat Thematic Mapper 166-039, 31 August, 1990*: Quantico, Virginia, U.S. Marine Corps Combat Development Center, OH O-52E.

_____. 1991a. *Remote Sensing Field Guide - Desert, Landsat Thematic Mapper 166-041, 30 August, 1990*: Quantico, Virginia, U.S. Marine Corps Combat Development Center, OH O-52F.

_____. 1991b *Remote Sensing Field Guide - Desert, Landsat Thematic Mapper 167-039, 29 August, 1990*: Quantico, Virginia, U.S. Marine Corps Combat Development Center, OH O-52G.

_____. 1991c. *Remote Sensing Field Guide - Desert, Landsat Thematic Mapper 167-040, 29 August, 1990*: Quantico, Virginia, U.S. Marine Corps Combat Development Center, OH O-52H.

APPENDIX A

PROJECT OSTRICH TEAM PARTICIPANTS

TEC

J. V.E. Hansen	Project Manager
T.D. Evans	Chief Engineer
Dr. J. Ehlen	Geologist
R.A. Hevenor	Electronic Engineer
A.E. Krusinger	Research Engineer
S. Allison	Electronic Technician

WES

J. O. Curtis	Research Physicist
L. E. Tidwell	Civil Engineer

ERIM

J. Leyden	Site Radar Engineer
G. Adams	Project Engineer

Other Contributors

1. D. Artis, B. Mandel, TEC: In-house staff
2. V. Guthrie, E. Simental, TEC: Data analysis
3. USMC Personnel, USMCAGCC, Twentynine Palms, CA: Site assistance
4. J. Verdi, K. Birney, NAWC, and P-3 Flight Personnel: Aircraft
5. R. Bernard, P. McConnell, BRDEC: Mines/technical assistance
6. R. Scholl, FSTC: Foreign technology information
7. J. F. McCauley, C.S. Breed, USGS: SIR-A experience
8. ERIM: Program assistance and data analysis
9. VSE Corp: Nonmetallic mine fabrication

APPENDIX B

P-3 RADAR SYSTEM PARAMETERS

Antenna Parameters

	X	C	L
Wavelength	3.2 cm	5.7 cm	24 cm
Frequency	9.35 GHz	5.30 GHz	1.25 GHz
Peak Transmitted Power	1.5 Kw	1.4 Kw	5.0 Kw
Azimuth Beamwidth	1.8°	3.9°	10°
Elevation Beamwidth	8.5°	15°	100°
Gain	27 dB	23 dB	23 dB
Isolation	23 dB	23 dB	23 dB

System Parameters

Bandwidth	60 MHz		120 MHz
Impulse Response Width	3 m		1.5 m
Sidelobes		30 dB Taylor	
Pulse Width		4 microseconds	
Peak Duty Cycle		1.6%/4 KHz	
A/D Quantization		6 bit I&Q	
Sample Rate	62.5 MHz		125 MHz
	(2.4 m/sample)		(1.2 m/sample)
Samples		4096 I&Q/Channel	
Slant Range Swath	9.8 km/channel		4.9 km/channel
Maximum Range		18.8 km @ 8 KHz	
		37.6 km @ 4 KHz	
PRF		proportional to velocity up to 350 kts	
Clutterlock		12 sec time constant	

APPENDIX C

TEST SITE CONSTRUCTION AND OPERATIONS

Overview

The test site was constructed to simulate a Soviet-doctrine deliberate minefield. Soviet doctrine allows for placing mines at varying intervals; however, mines were placed in trenches at set, measured intervals to facilitate image analysis. As stated previously, two test sites (Phase I and Phase II) were constructed. The two sites, although very similar, were not identical; but because the Phase II site is still in existence, the following discussion refers to the Phase II site. Differences between the two sites are noted where they exist.

Test Site Configuration

Location of Test Site

The test site is located on the Marine Corps Air Ground Combat Center (MCAGCC) at Twentynine Palms, California. The site as constructed occupies an area approximately 300 m long by 150 m wide, and is located in the Gypsum Ridge Training Area, south of Gypsum Ridge itself. The site coordinates are 34°20'30"N, 116°9'00"W.

Test Site Layout

The test site contains two minefield areas, each 150x30 m (Figure C1). These minefield areas are separated from each other by a 20 m corridor and from the test site boundaries by 10 m corridors. In addition, there are two areas within the test site where surface mines are located. These areas are separated from the minefields by a 20 m corridor. The minefield area on the eastern side of the site contains only metal mines, while the western minefield area contains only nonmetallic mines.

Each of the minefield areas consists of two parallel mine rows. Each mine row is 10 m wide and 150 m long and contains three parallel trenches in which mines are placed. The trenches are 5 m apart. The mine rows are separated by a 10 m corridor. Each trench in the metal minefield area contains 18 mines in the first 100 m spaced at 5 m intervals with the first mine placed at the northern end. Each trench in the nonmetallic minefield area contains 20 mines in the first 100 m spaced at 5 m intervals starting at the northern end. The remaining 50+ m of the trenches in both minefield areas is empty. The mines buried in the first mine row (first set of three trenches) of each minefield are buried such that the tops of the mines are 4 inches below the ground surface. The buried mines are placed in the trenches at a spacing of 5 m. The trenches are backfilled.

In the first trench in the second mine row (second set of three trenches), the mines are buried such that the tops of the mines are 4 inches below ground level. In the second trench, the mines are buried such that the tops are 8 inches below ground level, and in the third, the tops are 12 inches below ground level.

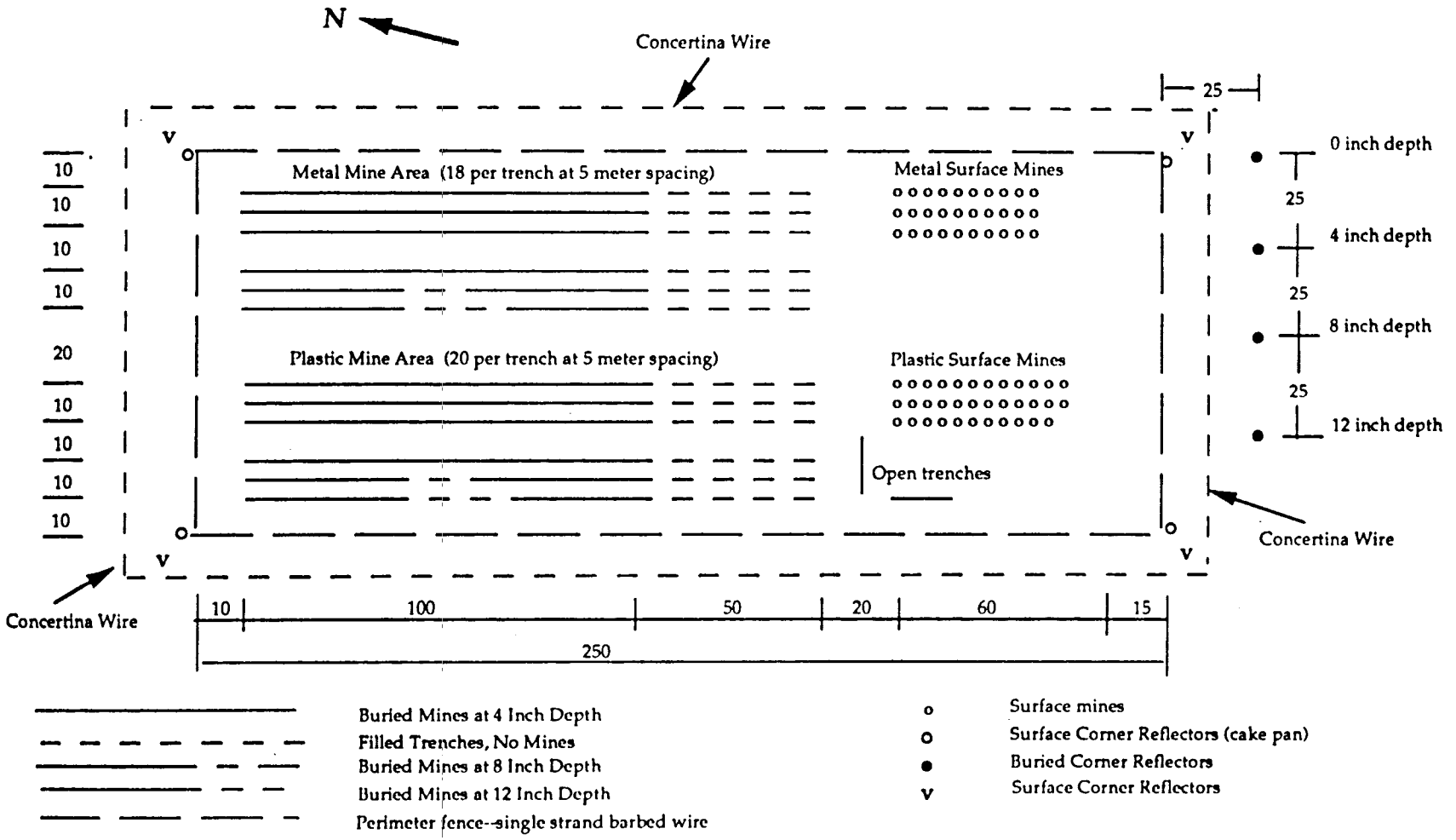

The site is also surrounded by concertina wire 15 meters outside the barbed wire perimeter

All dimensions are in meters except as indicated

Figure C1. Test Site layout as of 15 November 1990.

The surface mines are placed in three parallel lines. Each of these lines begins 20 m from the trenches in the first mine row in each minefield. The lines are spaced 5 m apart and the mines are placed in the lines at a spacing of 5 m. There are 10 mines in each line in the metal surface mine area (in the Phase I site, there were 13 mines in each line). In the nonmetallic surface mine area, there are 12 mines in the first two lines, and 11 mines in the third line (in the Phase I site, there were 13 mines in each line).

Two trenches are located south of the nonmetallic minefield area. These trenches are perpendicular to each other, and were left open with the soil excavated from them to one side (Figure C2).

Test Site Marking and Fencing

The test site was marked with corner reflectors at the four corners. These reflectors are trihedrals constructed of 0.25-inch aluminum plate, and are 60 cm high. The reflectors were oriented facing due south at a 10° angle from the horizontal and were placed so as to be 5 m from the perimeter in either direction (Figure C3). In addition, four corner reflectors were buried along the southern boundary of the site (Figure C1). All of the reflectors were relocated on 18 January 1991; see "Modifications to Site" below.

The test site is fenced with metal engineer stakes set at an interval of 8.3 m and strung with a single strand of barbed wire. In addition, concertina wire was placed around the perimeter of the site 5 m outside of the corner reflectors. The concertina is secured at approximately 50 m intervals with metal engineer stakes. In the Phase I site, the engineer stakes were placed 25 m apart, and no barbed wire or concertina wire were present.

Buried Reflectors

Four corner reflectors were buried at the southern end of the site, 25 m from the single-strand barbed wire fencing the site, and outside the concertina wire perimeter (Figure C1). These reflectors were buried at varying depths, and were oriented to face due south. The easternmost reflector was buried so that the topmost point of the reflector was at the surface of the ground (Figure C4). The second reflector is located 25 m to the west and was buried so that the top-most point was 4 inches below the ground surface. The third reflector is 25 m west of the second and was buried so that the topmost point was 8 inches below the ground surface. The westernmost reflector is 25 m west of the third, and was buried with the topmost point 12 inches below the ground surface.

The buried reflectors were relocated on 18 January 1991 (see "Modifications to Site" below).

Test Site Construction

Once the location of the test site was determined, a 250x100 m area was marked off using metal engineer stakes. These stakes were set at an interval of 8.3 m (25 m in the October 1990 site), using a 50 m tape measure. The corners of the rectangle were set at 90° by measuring the hypotenuse of the triangle formed by the stakes set at 25 m from the corner stake along each of the perpendicular sides.

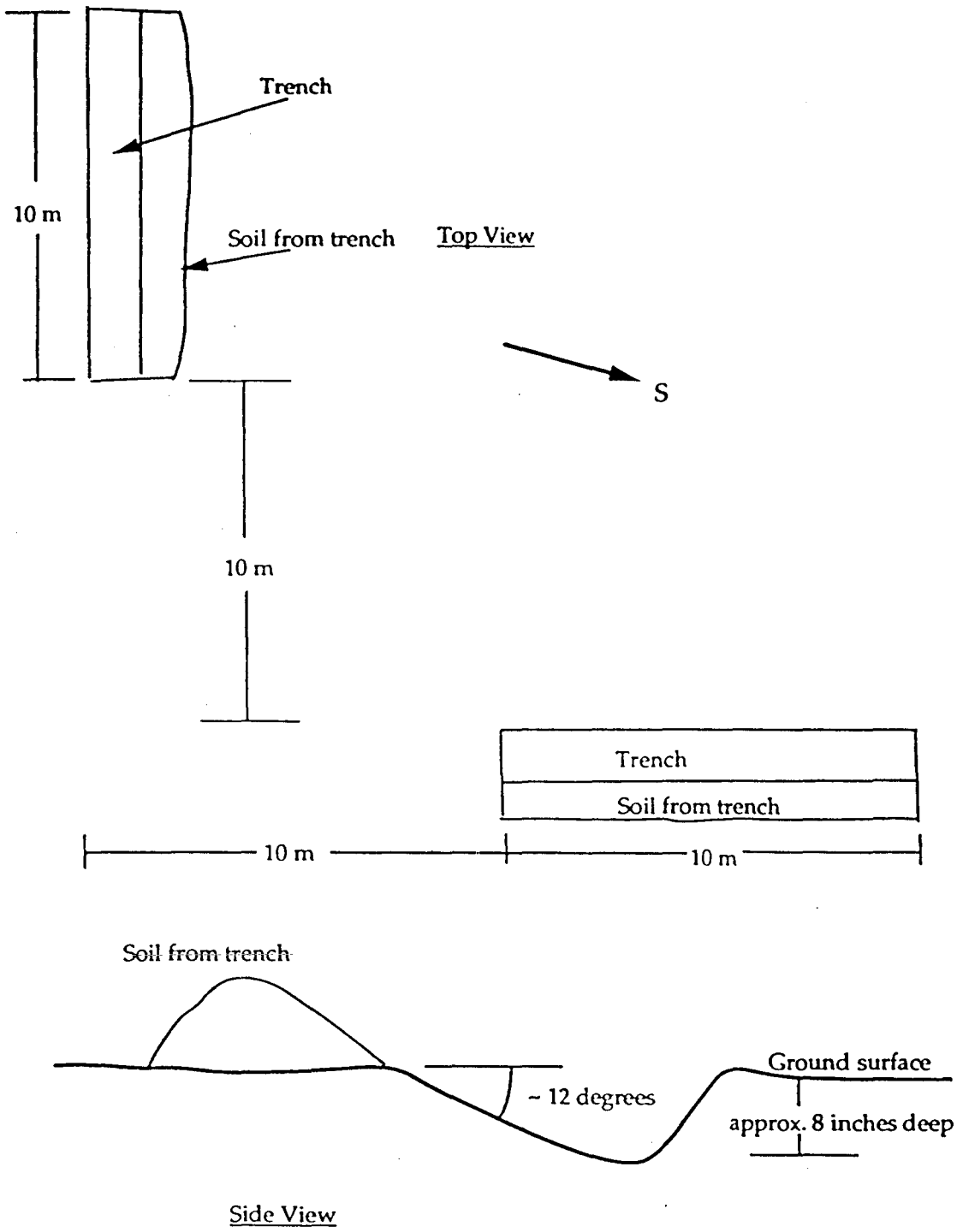

Figure C2. Configuration of open trenches.

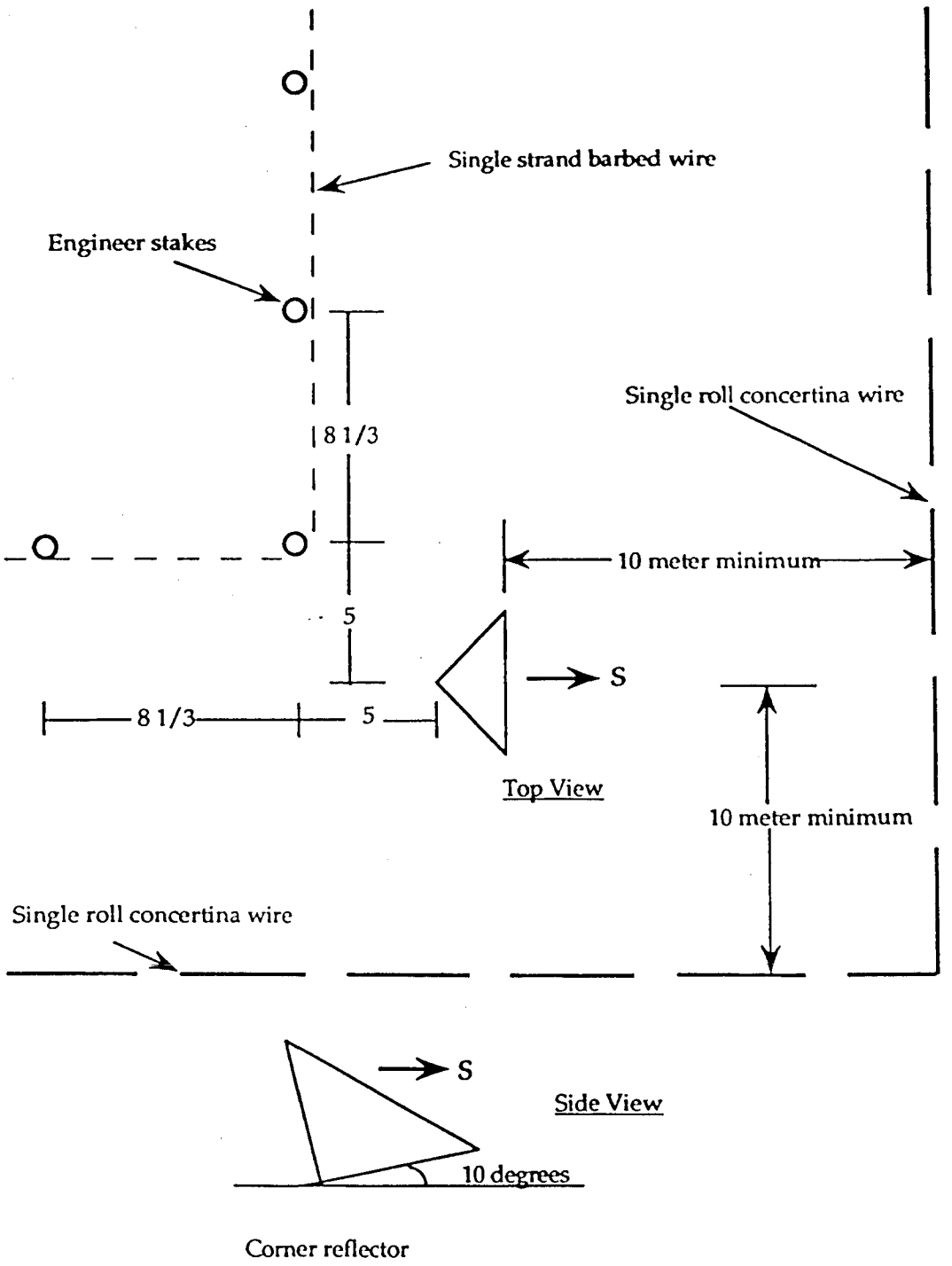

Figure C3. Orientation of surface corner reflectors (15 November 1990 through 17 January 1991).

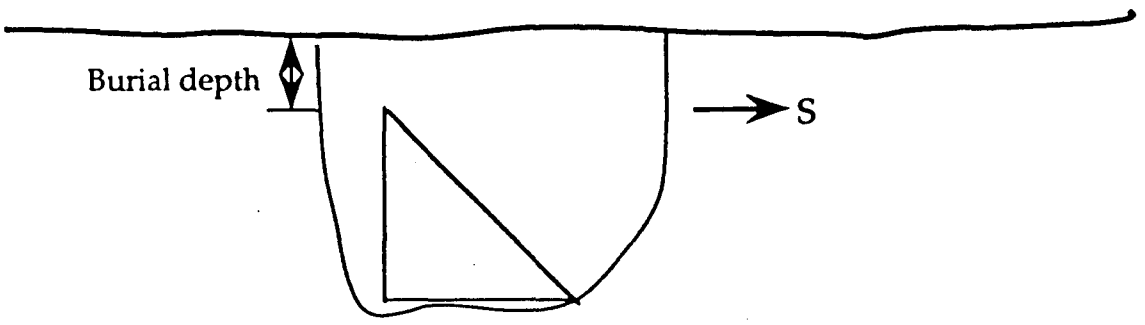

Figure C4. Orientation of buried corner reflectors.

Construction of the minefields began by laying out parallel trenches. The starting point of each trench begins 10 m from the northern and eastern edges of the test site. The first trench was laid out parallel to the eastern boundary, and is 10 m from that boundary. All other trenches are parallel to the first trench, at the designated spacing from the preceding trench. All spacings were measured with premeasured ropes and the line of each trench was marked by placing fluorescent, red-colored wooden blocks on the ground at appropriate intervals. Spacing of the trenches was measured from the eastern edge of the preceding trench to the eastern edge of the new trench.

Trenches were dug with a grader (the four easternmost trenches in the Phase I site were dug by a backhoe). The first mine is at the beginning of the trench. The remaining mines in each trench were placed at 5 m intervals. The mines were placed using a mine-measuring rope, which has markings every 5 m. The depth of the tops of the mines was measured using a wooden depth gage.

Once the mines were placed in the trenches at 5 m intervals and the depth of each mine was checked with the depth gage, the trenches were backfilled with the grader. This was done in such a way as to produce the least amount of soil disturbance between the trenches (in the Phase I site, all but the three easternmost trenches were filled en masse by the grader, which produced a large, relatively smooth area of disturbed soil).

Modifications to Site

The test site was modified on 6 December 1990 with the addition of simulated scatterable metal mines. These objects are cast iron pipe end caps, 4.5-5.5 inches in diameter, and are pictured in Figure C5. The 6 December 1990 modifications to the test site are shown in Figure C6.

The test site was further modified on 18 January 1991. Six holes were dug between the metal mine area and the nonmetallic mine area, then refilled. In addition, two of the four buried corner reflectors were dug up. Together with the four surface corner reflectors, they were reburied in arrays at the northern end of the test site. When the holes were refilled, the soil was strained through 0.25-inch mesh hardware cloth to remove large clumps and gravel. The layout of these arrays is shown in Figure C7 and the orientation of the buried reflectors in the ground is shown in Figure C8. The 18 January 1991 site configuration with modifications is shown in Figure C9.

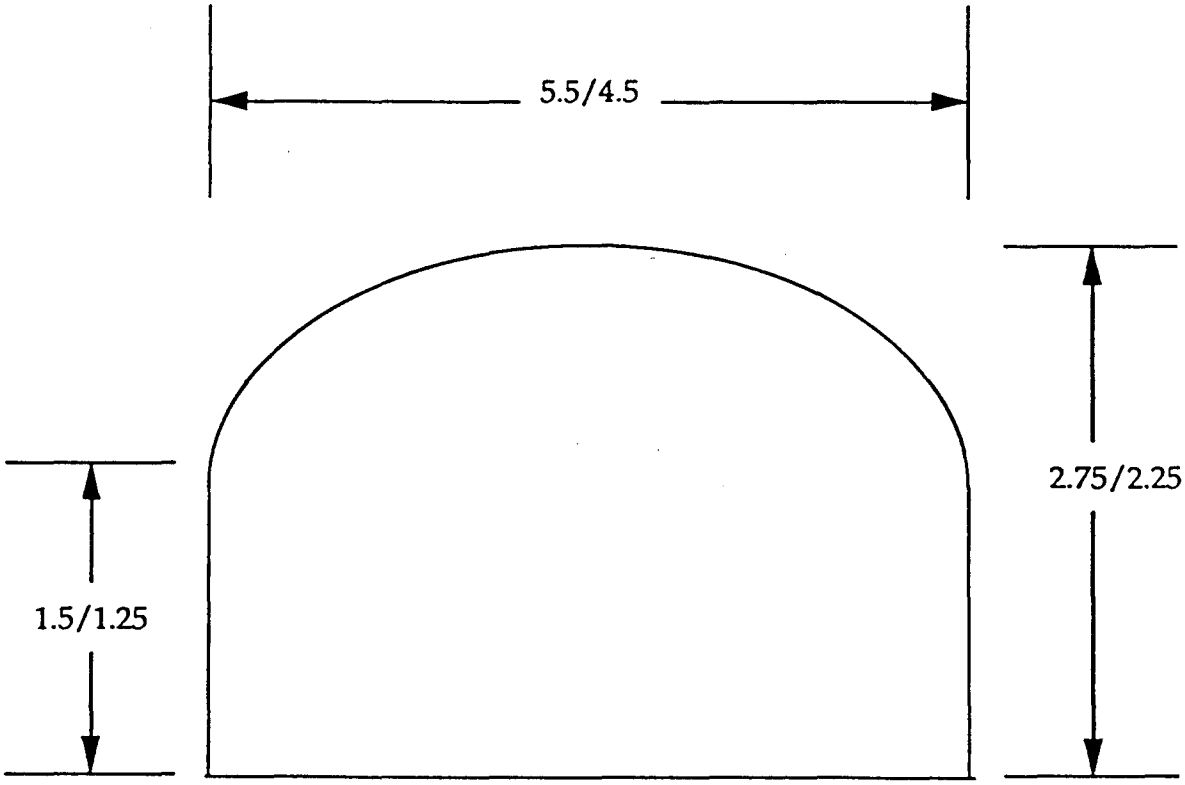

Figure C5. Metal scatterable mine surrogates (5.5 inch/4.5 inch).

Mines

The metal mines are U.S. M-20 and M-21 training mines, obtained from the Ammo Center at Twentynine Palms Marine Corps Air Ground Combat Center (MCAGCC). The nonmetallic mines are surrogates, manufactured by VSE Corporation, Alexandria, Virginia, to have approximately the same size, shape and radar cross-section as standard nonmetallic mines. These surrogates consist of a sealed plastic container approximately 12 inches in diameter and 3 inches deep filled with a mixture consisting of 80% nylon granules and 20% RTV 3112 silicone rubber, and a small styrofoam disk to simulate an air gap. The physical characteristics of these surrogates are given in Table C1.

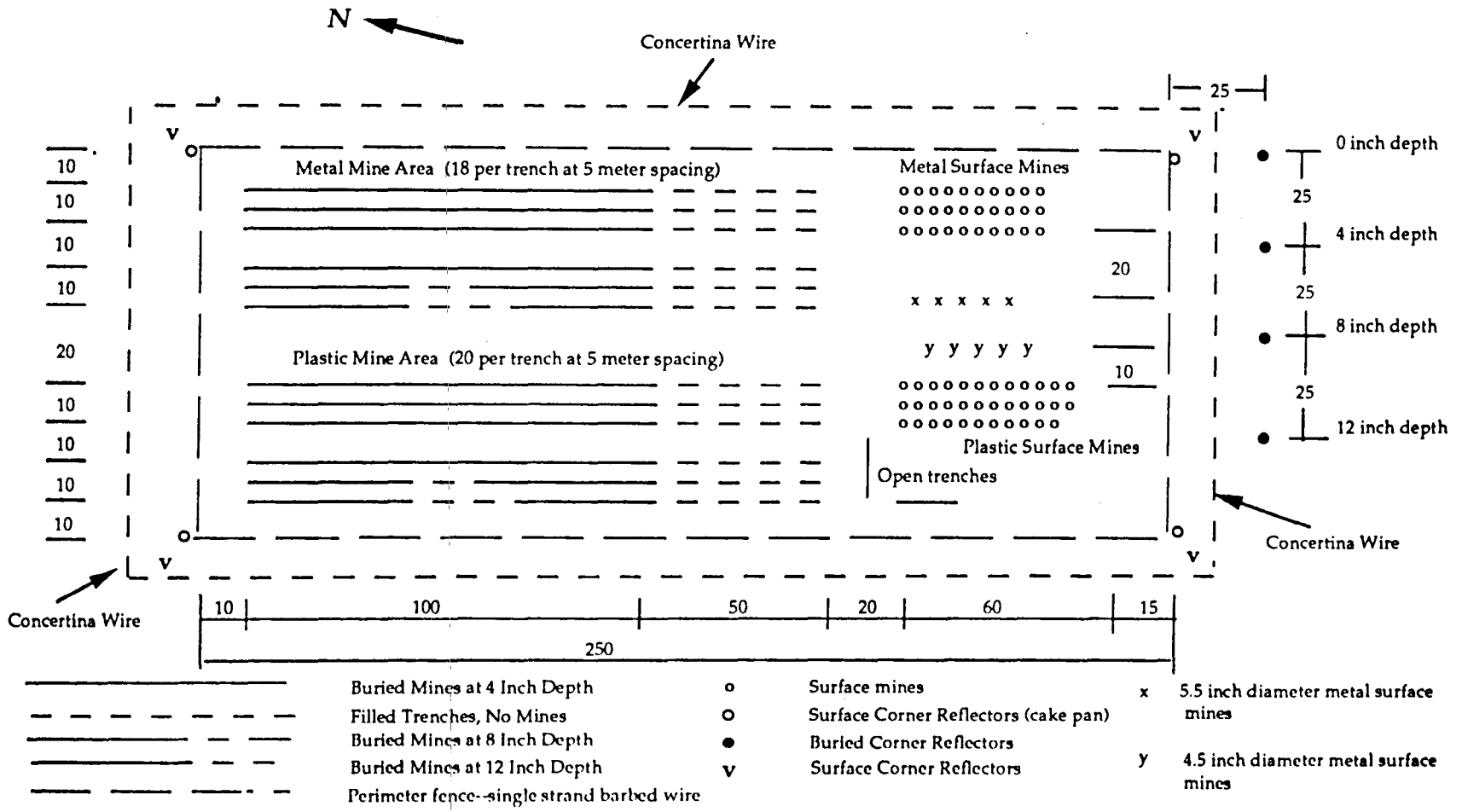

The site is also surrounded by concertina wire 15 meters outside the barbed wire perimeter

All dimensions are in meters except as indicated

Figure C6. Test site layout as of 6 December 1990.

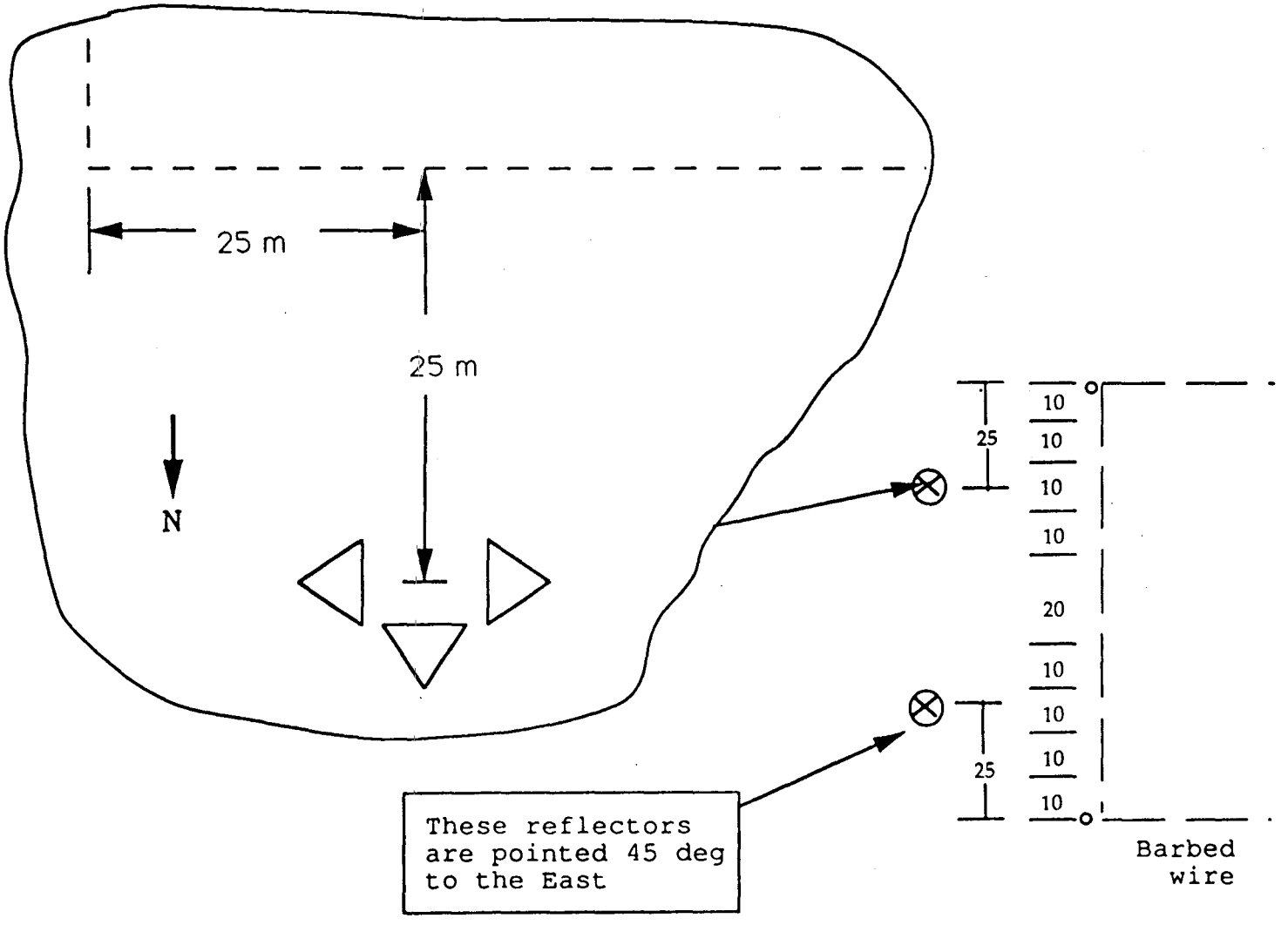

Figure C7. Location of buried reflectors as of 18 January 1991.

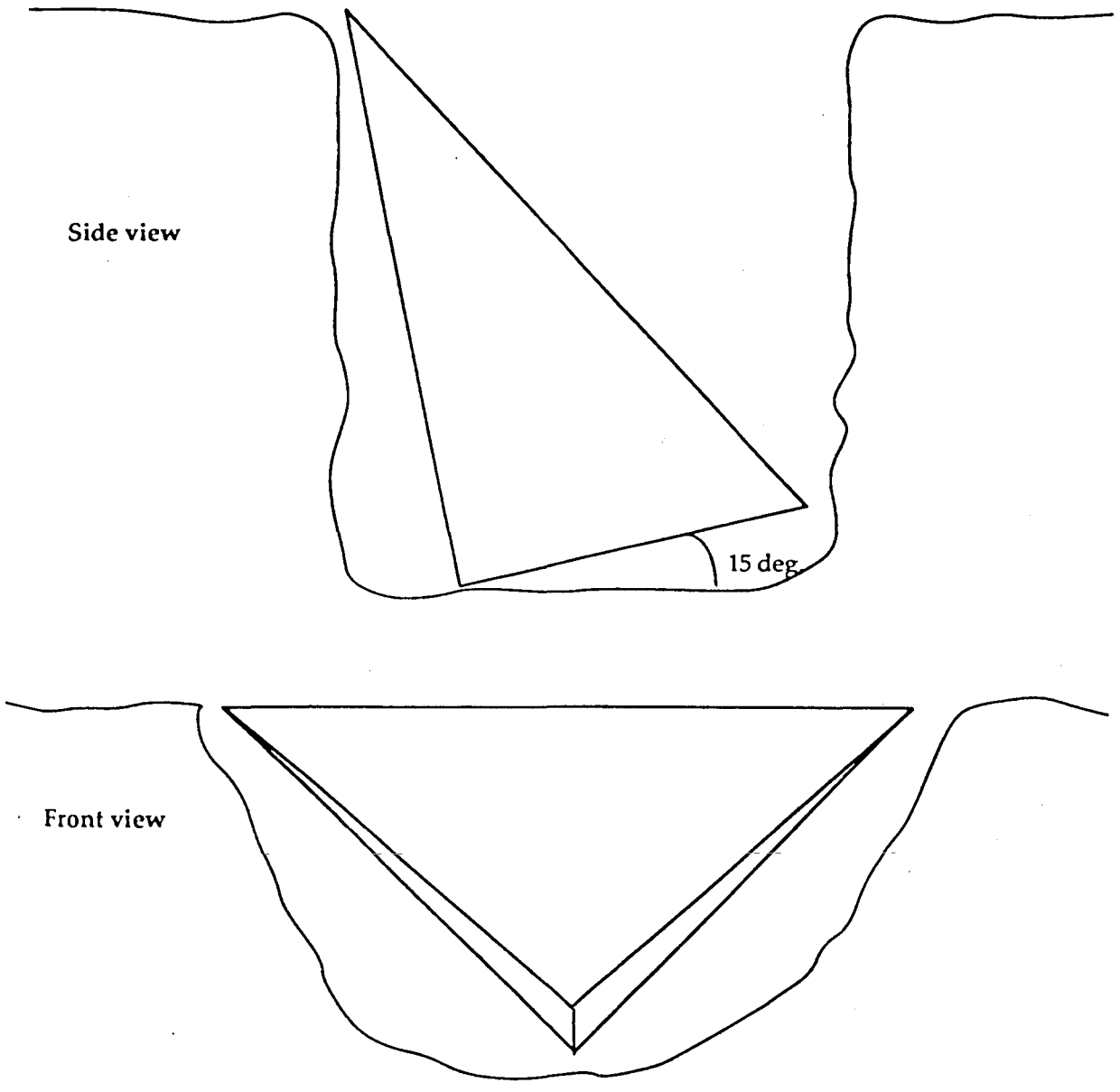

Figure C8. Orientation of reflectors buried on 18 January 1991.

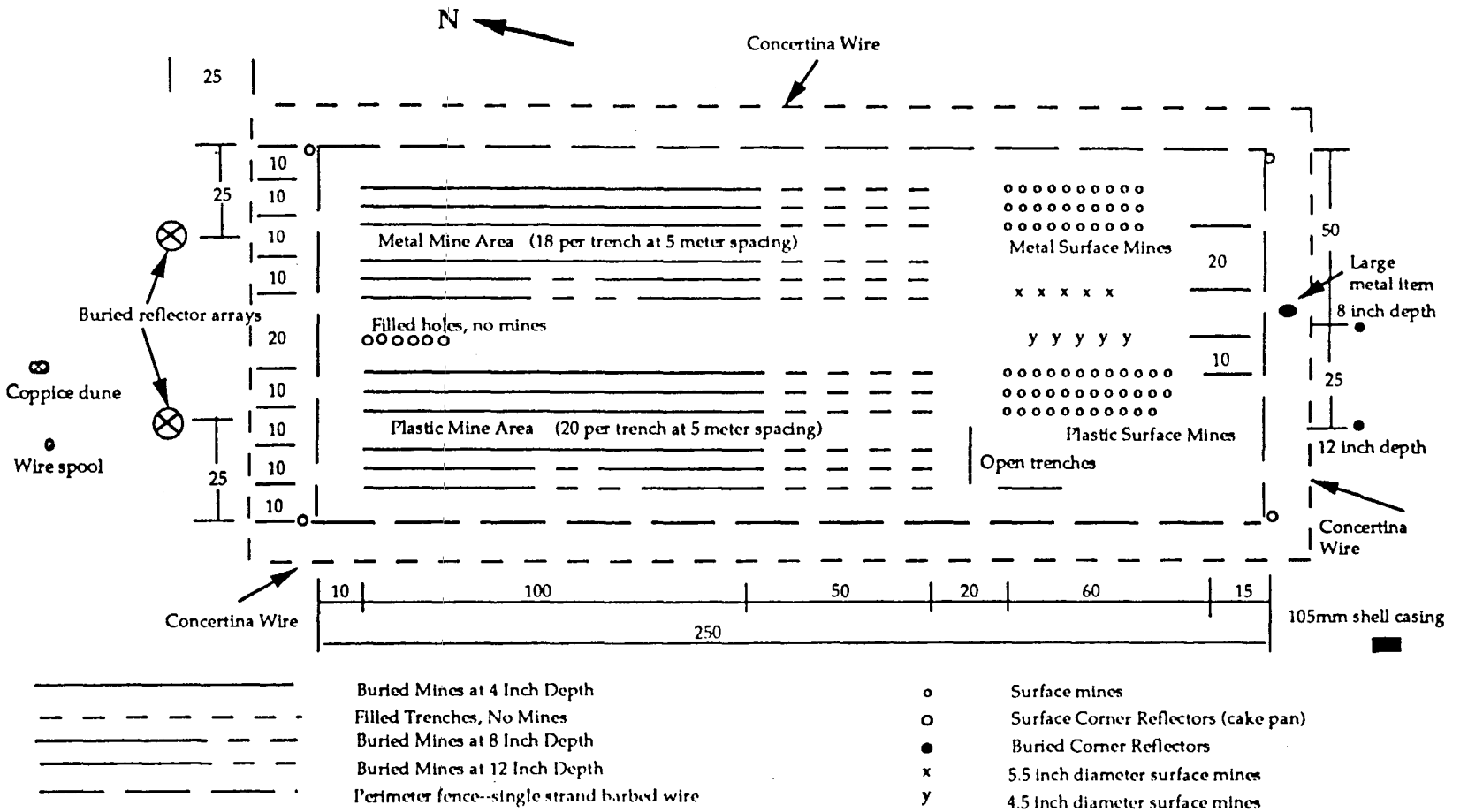

All dimensions are in meters except as indicated

Figure C9. Test site layout as of 18 January 1991.

Table C1. Physical Characteristics of Nonmetallic Surrogate Mines

	Total	Fill Mixture	Styrofoam (air gap)
Weight:	15.5 lbs 7.0 kg	15.0 lbs 6.8 kg	negligible negligible
Volume:	368 in^3 6000 cm^3	321.7 in^3 5270.0 cm^3	28.3 in^3 463.0 cm^3
Diameter:	12.5 in 31.7 cm	12.4 in 31.2 cm	6.0 in 15.2 cm
Height:	3.0 in 7.6 cm	2.9 in 7.1 cm	1.0 in 2.5 cm
Relative dielectric constant	3.0 to 3.1	3.0 to 3.1	1.03
Loss tangent	0.01	0.01	1.0

Schedule of Operations

Phase I Site – 10-15 October 1990

10 October

0900 - Arrived on location in the Gypsum Ridge Training Area. Took initial soil samples. Located and marked the site for construction of the test minefield.

11 October

0945-1330 - First data collection flights by the P-3 radar aircraft, with no construction. Only north-south flights made.

0900-1700 - Began construction of the test minefield.

12 October

0900-1500 - Completed construction of the test minefield.

1745-2100 - Data collection flights over completed test minefield site. Only north-south flights were made.

13 October

0700-0800 - Removed mines and metal engineer stakes from test minefield site.

14 October

1000-1300 - Final data collection flights over test minefield site. Only north-south flights were made.

Phase II Site – 14 November 1990 - Present

14 November 1990

0800-1630 - Started and completed construction of the Phase II test minefield.

6 December 1990

Scatterable mine surrogates were placed on the site.

13 December 1990

An X-shaped open trench was dug at the north end of the test site, between the Phase II test site and the Phase I test site. P-3 data collection flights were made over the Phase II test site. Both east-west and north-south flights were made.

14 January 1991

Two of the buried reflectors were dug up. Six holes were dug between the area containing metal mines and the area containing nonmetallic mines.

20 March 1991

Overflight by JPL flying a NASA DC-8 with X-, L-, and P-band radars in support of Operation Groundhog.

21 March 1991

Placed four 2-foot diameter aluminum disks near the site in support of Operation Groundhog.

30 May 1991

Flights were made over the site by the NAWC P-3 aircraft.

6 November 1991

Placed 20 M-79 scatterable mines along the first trench containing metal mines.

APPENDIX D

SOIL CHARACTERIZATION AND SURFACE CHARACTERISTICS[3]

Introduction

Two separate efforts to address the soils of the Gypsum Ridge test site were carried out during the experiment 9-14 October 1990 (Phase I). Soil samples were collected within the test site for soil moisture determinations, particle size analysis and petrographic analysis (Ehlen and Henley, 1991). Soils were also characterized in four 1-meter-deep pits around the perimeter of the test site; and surface roughness was addressed (Curtis and Tidwell, 1992). A second experiment was carried out 13-16 November 1990 (Phase II), but involved only soil characterization within the test site. Soil characterization within the test site (Phase I and Phase II) will be described prior to soil characterization done around the perimeter (Phase I only); a discussion of surface roughness follows.

Soil Characteristics Within The Test Site

Sampling

During Phase I, 9-14 October, 32 soil samples were collected at 12 locations within the 100x250 m test site (Figures D1, D2, and D3). Surface (0-4 cm), trench bottom and backfill samples were taken at 10 locations within 12 triangular-shaped, 150-m-long trenches that were dug in part by SEE (Small Emplacement Excavator), but mainly by grader. Only surface samples were collected at the remaining two locations. Eight of the 12 trenches were 8 inches deep, two were 12 inches deep and two were 16 inches deep. The second site (Phase II), identical to the first in size and layout, was located 200 m south of the first site; the two did not abut each other. Surface, trench bottom, and backfill soil samples were collected from comparable locations during both phases of the experiment, e.g. samples were collected from mine three in row 1 in both sites; one additional trench bottom sample was collected during Phase II (Figures D4, D5, and D6).

The sampling density is weighted toward the areas where the metal mines were buried because it was believed that these mines had a greater chance of being detected: three sets of samples were taken in the 8-inch deep trenches (one in an unmined trench), and one set was collected in each of the 12- and 16-inch deep trenches. Two sets of samples were taken in the 8-inch deep trenches containing nonmetallic mines; one in the 12-inch deep trench, and one in the 16-inch deep trench. One surface sample was collected where the metal mines were placed on the surface, and one where the nonmetallic mines were placed on the surface. The additional trench bottom sample collected during Phase II was taken from the short, open trench perpendicular to the initial 12 trenches (Figure D5).

[3] Part of this appendix was abstracted from Curtis and Tidwell (1992).

Percent Soil Moisture--Surface Samples: Phase I

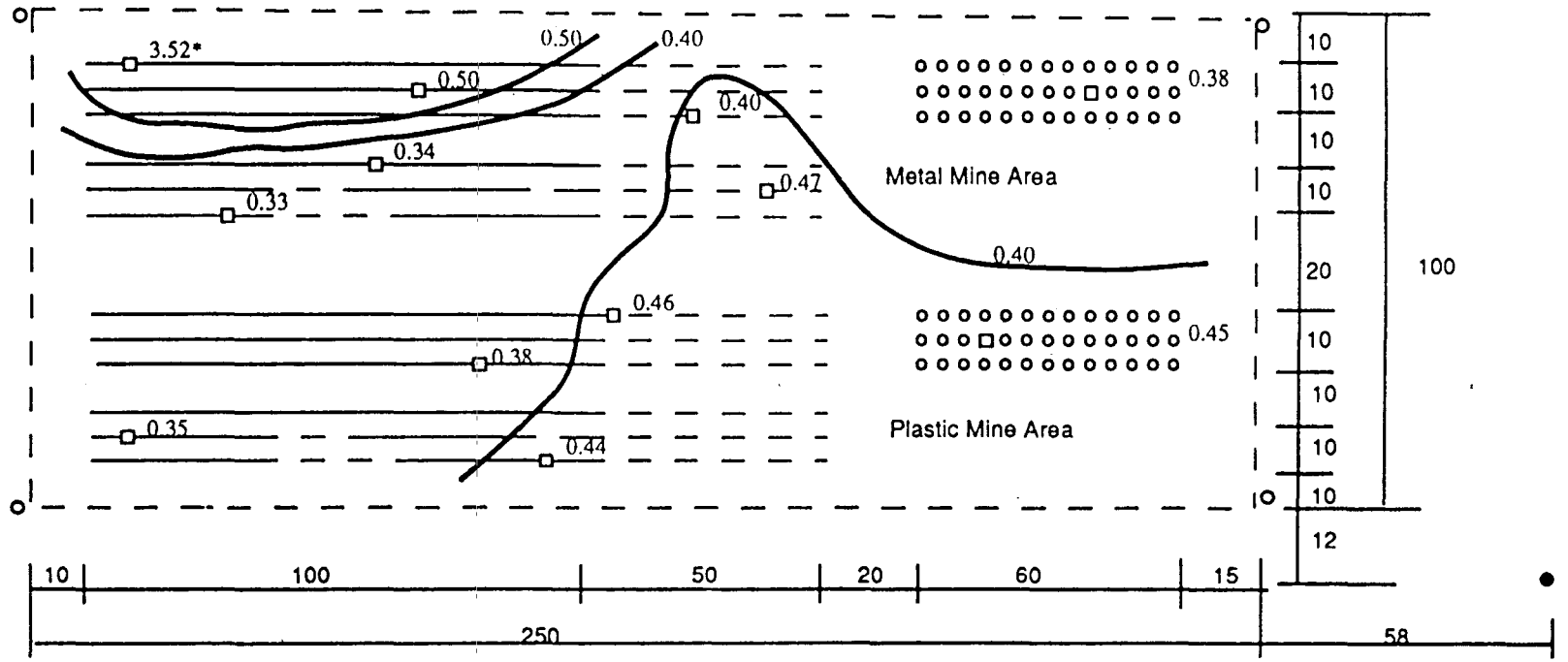

20 Buried Mines at 4 Inch Depth

Filled Trenches, No Mines

20 Buried Mines at 8 Inch Depth

20 Buried Mines at 12 Inch Depth

13 Surface mines

Surface Corner Reflectors

Buried Corner Reflector

Soil Sample Location

All dimensions are in meters

N

* Surface and bottom measurements probably reversed

Figure D1. Percent soil moisture - Surface samples: Phase I

Percent Soil Moisture--Bottom Samples: Phase I

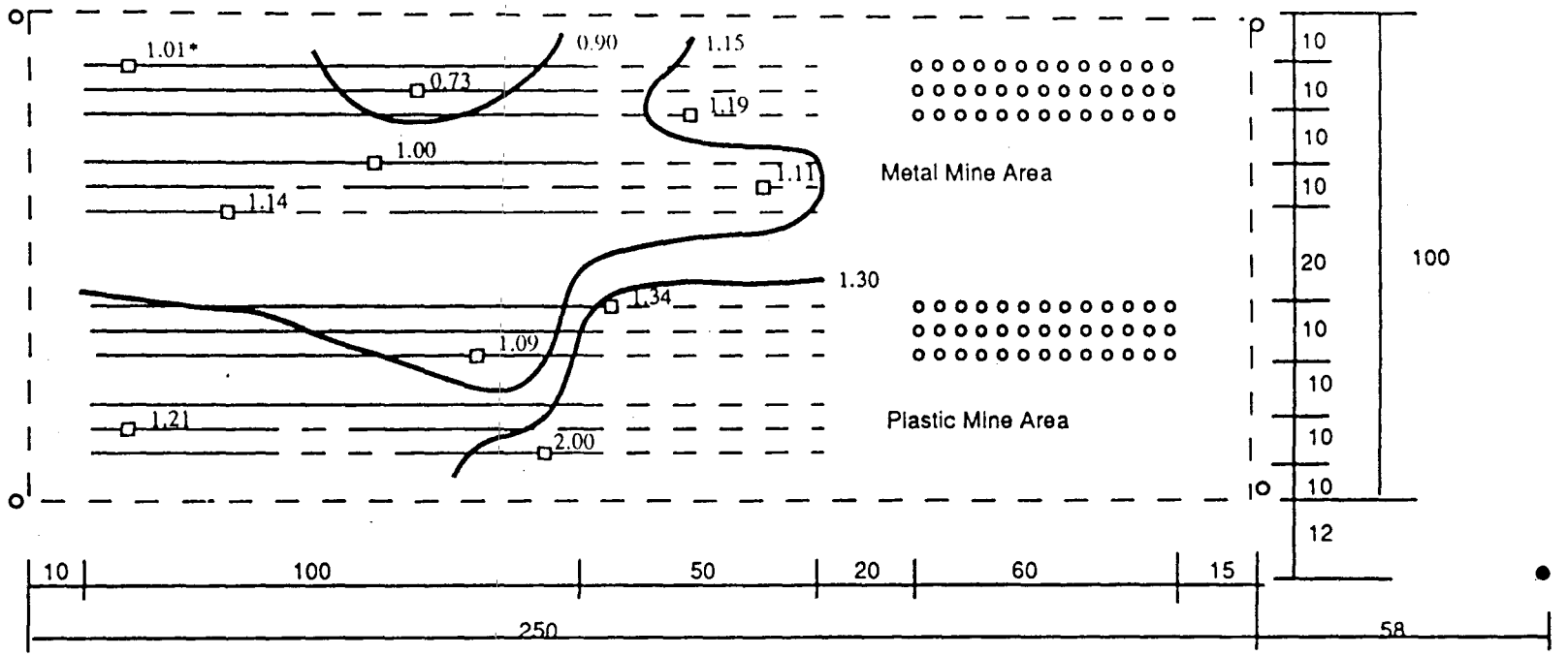

20 Buried Mines at 4 Inch Depth
Filled Trenches, No Mines
20 Buried Mines at 8 Inch Depth
20 Buried Mines at 12 Inch Depth

All dimensions are in meters

N

13 Surface mines
Surface Corner Reflectors
Buried Corner Reflector
Soil Sample Location

* Surface and bottom measurements probably reversed

Figure D2. Percent soil moisture -- Bottom samples: Phase I.

Percent Soil Moisture--Backfill Samples: Phase I

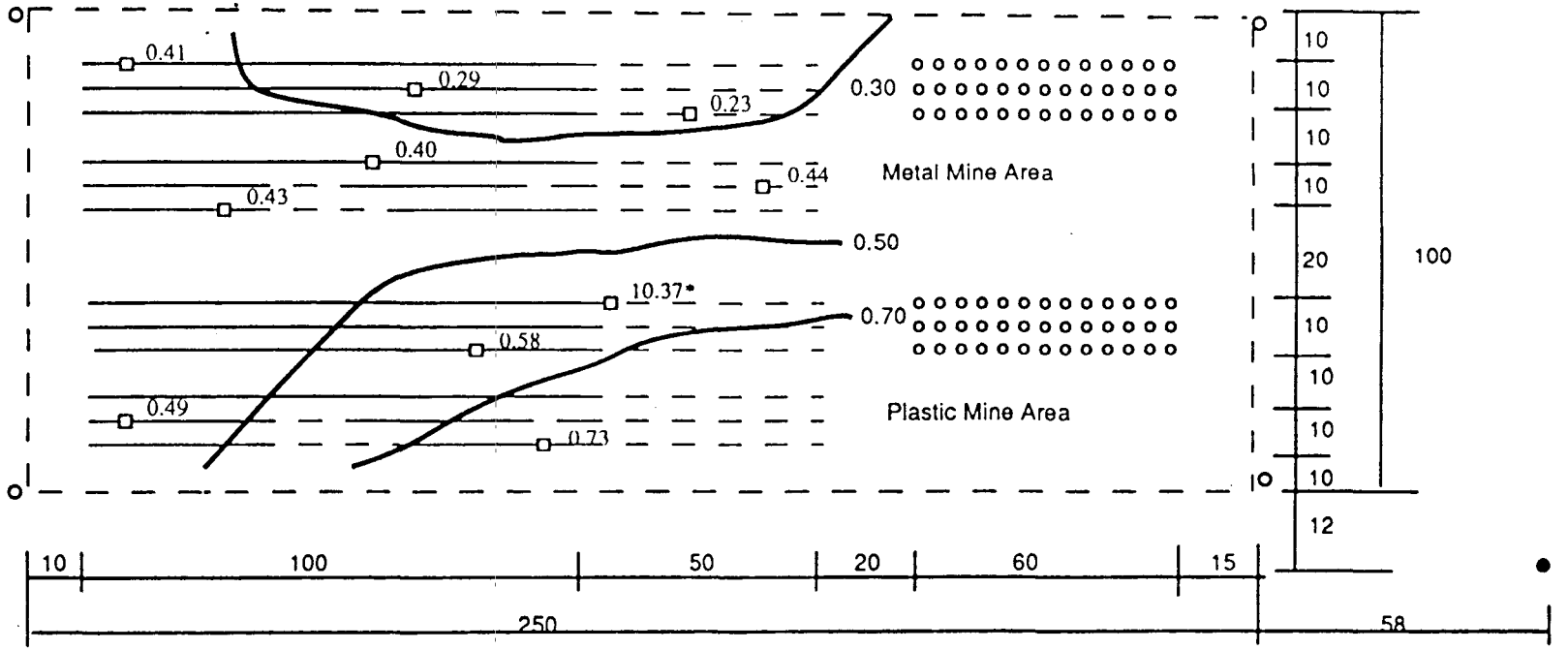

20 Buried Mines at 4 Inch Depth

Filled Trenches, No Mines

20 Buried Mines at 8 Inch Depth

20 Buried Mines at 12 Inch Depth

All dimensions are in meters

N

13 Surface mines

Surface Corner Reflectors

Buried Corner Reflector

Soil Sample Location

* Probably a bad measurement

Figure D3. Percent soil moisture -- Backfill samples: Phase I.

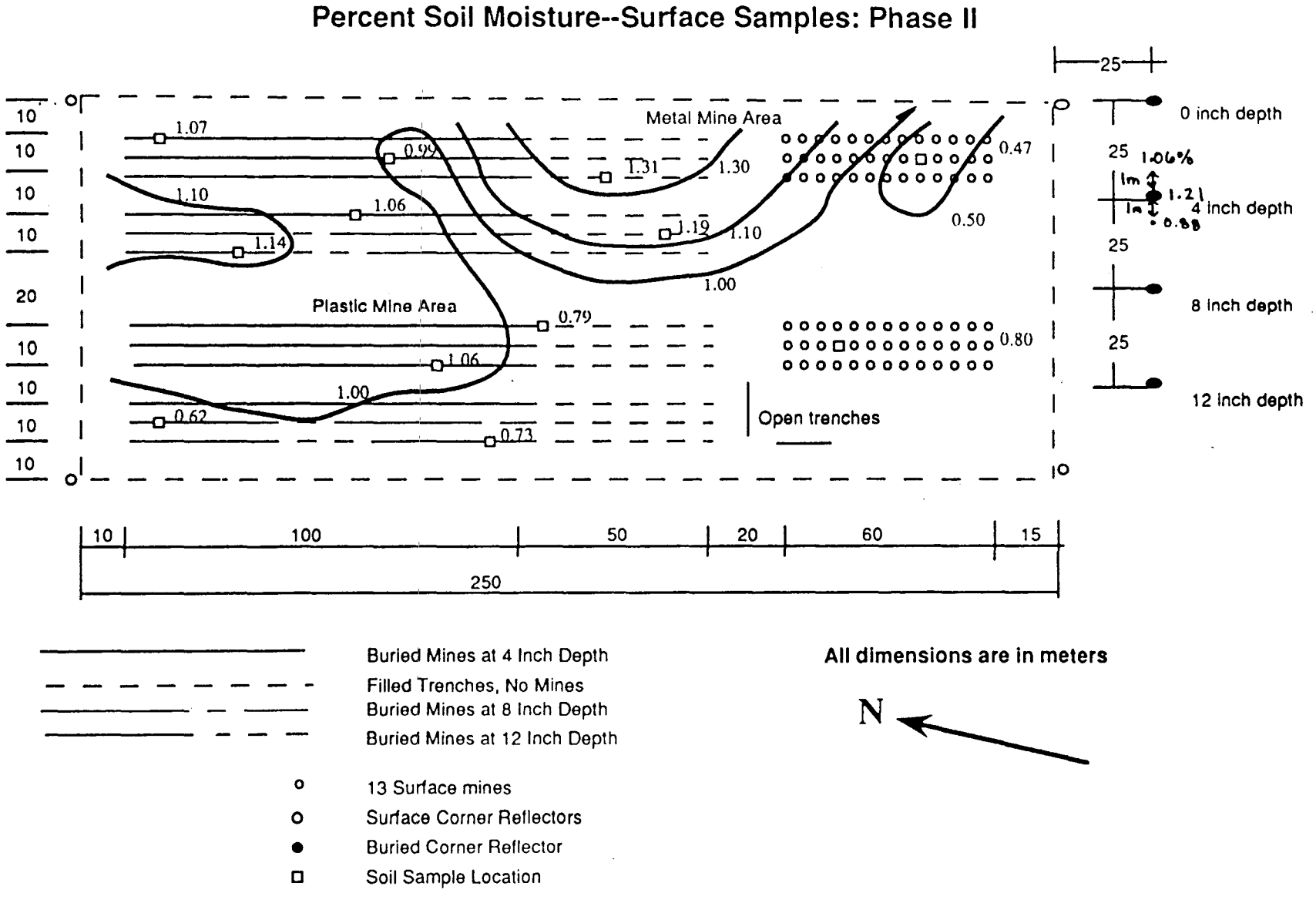

Figure D4. Percent soil moisture -- Surface samples: Phase II.

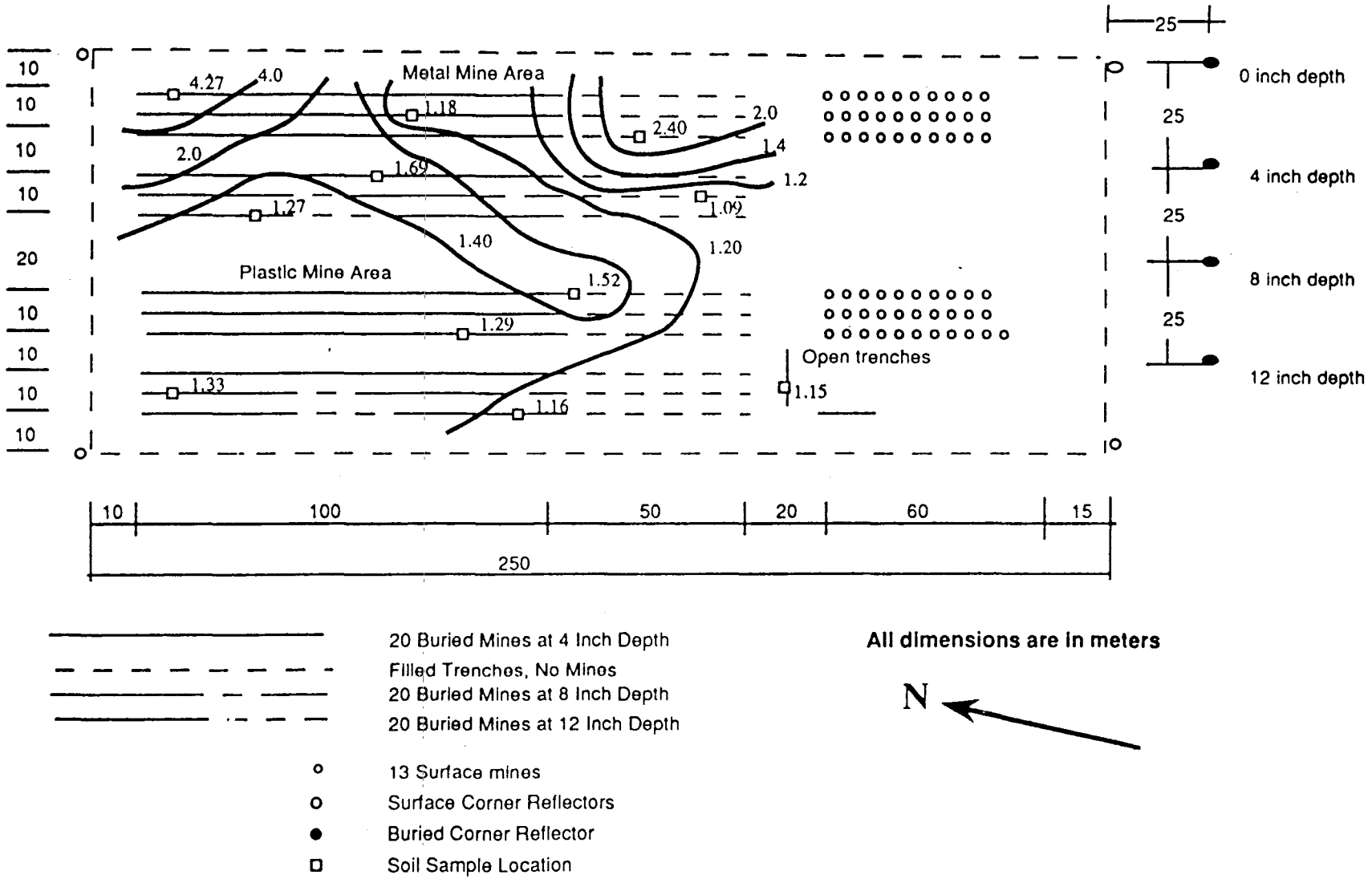

Figure D5. Percent soil mositure -- Bottom samples: Phase II.

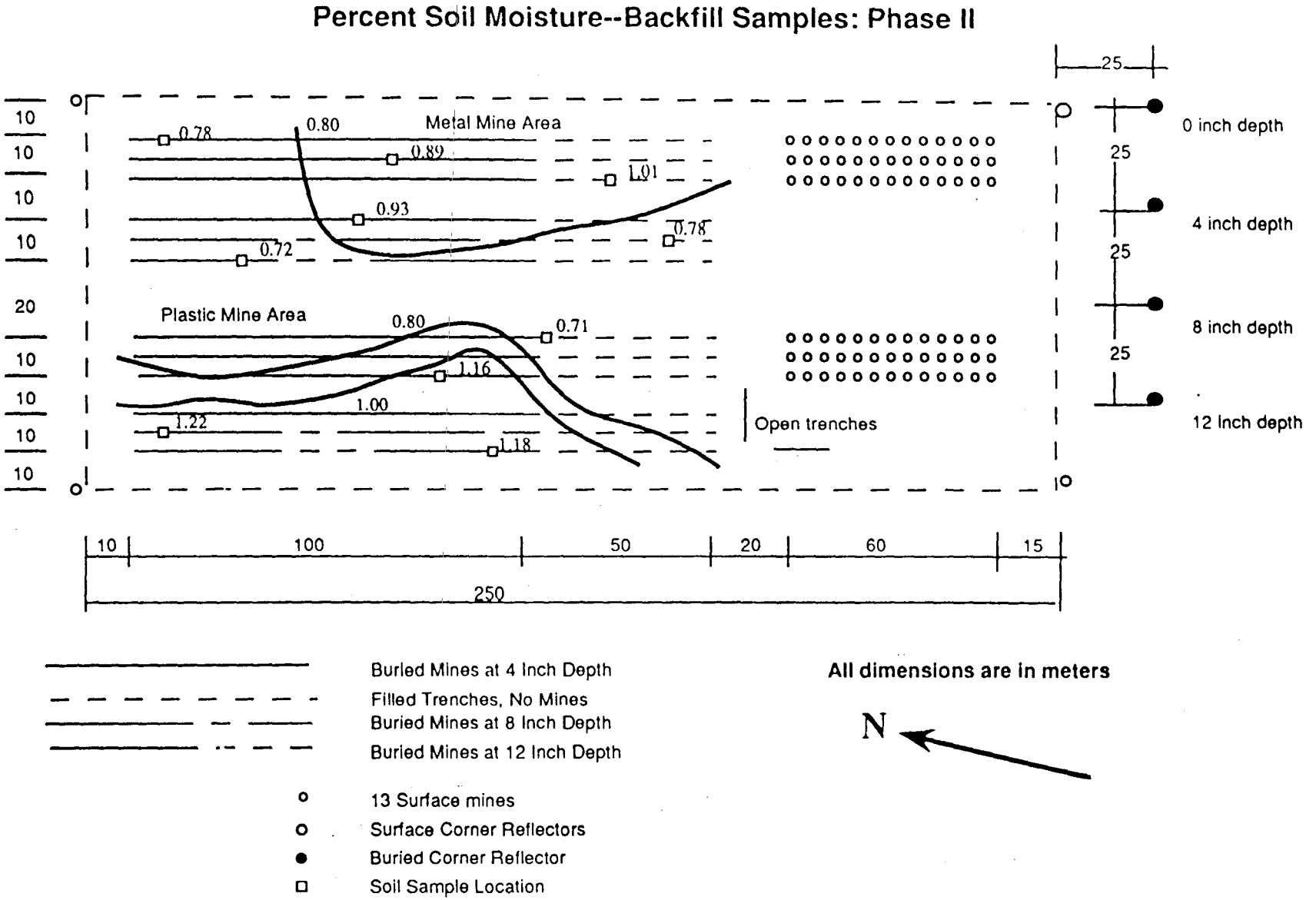

Figure D6. Percent soil moisture -- Backfill samples: Phase II.

Methodology

Surface samples were collected just before the trenches were dug and trench bottom samples were taken as soon as the mines were emplaced. Backfill samples for Phase I were collected within 1.5 hours before the flight; but for Phase II, samples were taken immediately after the trenches were filled. The soil samples were placed in cans, sealed, and weighed immediately with a triple beam balance. Upon return to TEC, the samples were oven-dried at 103° Celsius and the dry weight was determined. Percent soil moisture was then calculated on an oven-dry weight basis.

Sieve analysis was conducted in the laboratory on the oven-dried samples. The sieve sizes were >2 mm (No. 10), 1 mm (No. 18), 0.5 mm (No. 35), 0.25 mm (No. 60), 0.125 mm (No. 120), and 0.075 mm (No. 200).

Soil Moisture Determinations

All soil moisture values, except for one backfill sample and one surface sample in Phase I and one trench bottom sample in Phase II, are within the range for good penetration by radar. Measurement errors occurred with respect to these three samples. As expected, the surface samples are the driest, the trench bottom samples are the wettest, and the backfill samples are in between.

Phase I. The soil moisture data are presented in Table D1; the mines are numbered from the north. Surface soil moisture ranged from 0.33-0.50%; and backfill soil moisture ranged from 0.23-0.73%. Trench bottom soil moisture ranged between 0.73-1.34% in the 8-inch deep trenches; 1.11-1.21% in the 12-inch deep trenches, and 1.34-2.00% in the 16-inch deep trenches.

Table D1: Percent Soil Moisture, Phase I

Sample Location	Surface Samples	Bottom Samples	Backfill Samples
Row 1, mine 3	meas.error	1.01	0.41
Row 2, mine 15	0.50	0.73	0.29
Row 2, surface mine 9	0.38	-	-
Row 3, unmined trench, 25 m from N end	0.41	1.19	0.23
Row 4, mine 13	0.34	1.00	0.40
Row 5, unmined trench, 40 m from N end	0.47	1.11	0.44
Row 6, mine 7	0.33	1.14	0.43
Row 7, unmined trench, 10 m from N end	0.46	1.34	meas. error
Row 8, surface mine 4	0.45	-	-
Row 9, mine 17	0.38	1.09	0.58
Row 11, mine 3	0.35	1.21	0.49
Row 12, mine 20	0.44	2.00	0.73

Statistically, there are no significant differences at the 95% confidence level in percent soil moisture among surface, trench bottom and backfill samples.

Except for the surface samples, soil moisture tends to increase slightly from north-northeast to south-southwest in the test site; surface soil moisture is higher in the north-northeast and south-southwest than in the northwest/southeast band through the center of the site. These data are shown on Figures D1, D2, and D3.

Phase II. As shown in Table D2 and on Figures D4, D5, and D6, surface soil moisture ranged from 0.47-1.31%; and backfill soil moisture ranged from 0.78-1.22%. Trench bottom soil moisture ranged between 1.29-4.27% in the 8-inch deep trenches; 1.09-1.33% in the 12-inch deep trenches, and 1.16-1.37% in the 16-inch deep trenches. This test site is thus slightly wetter than the Phase I test site; no rain had occurred between the two experiments. Again, there are no statistically significant differences at the 95% confidence level in percent soil moisture among surface, trench bottom and backfill samples.

Table D2: Percent Soil Moisture, Phase II

Sample Location	Surface Samples	Bottom Samples	Backfill Samples
Row 1, mine 3	1.07	meas. error	0.78
Row 2, mine 15	0.99	1.18	0.89
Row 2, surface mine 9	0.47	-	-
Row 3, unmined trench, 25 m from N end	1.31	2.40	1.01
Row 4, mine 13	1.06	1.69	0.93
Row 5, unmined trench, 40 m from N end	1.19	1.09	0.78
Row 6, mine 7	1.14	1.37	0.72
Row 7, unmined trench, 10 m from N end	0.79	1.52	0.71
Row 8, surface mine 4	0.80	-	-
Row 9, mine 17	1.06	1.29	1.16
Row 11, mine 3	0.62	1.33	1.22
Row 12, mine 20	0.73	1.16	1.18
Perpendicular trench, base of row 11	-	1.15	-

Surface soil moisture was highest in the southeast corner and lowest in the southwest corner of the test site. Trench bottom soil moisture exhibited a totally different pattern, being highest in the northeast and lowest in the southwest. Backfill sample soil moisture was lowest in a central north-south band and in the northeast corner, increasing to both east and west. It was highest in the west.

Particle Size Analysis

Phase I. Sieve analyses for the Phase I soil samples are shown in Tables D3, D4, and D5. These soils consist mainly of fine sand and very fine sand: surface samples contain a mean of 45.1%

fine sand and very fine sand; trench bottom samples, a mean of 45.9%; and backfill samples, a mean of 46.8%. Gravel in the surface samples ranges from 5.4-26.1% (mean 12.2%); in the trench bottom samples, from 6.2-16.2% (mean 10.7%); and in the backfill samples, 6.1-17.0% (mean 11.3%). Surface samples contain 2.5-7.9% silt+clay (mean 5.3%); trench bottom samples, from 3.5-6.6% (mean 4.7%); and backfill samples, 2.6-7.2% (mean 4.8%). Surface samples thus tend to contain more gravel than either trench bottom or backfill samples and contain more silt and clay as well. Although all samples contain more fine sand than any other particle-size range, bottom samples contain more fine sand than either surface or backfill samples.

Table D3: Sieve Analysis, Phase I: Surface Samples (Percent total)

Sample Number	gravel >2mm	very coarse sand, 1-2mm	coarse sand, 0.5-1mm	medium sand, 0.25-0.5mm	fine sand, 0.125-0.25mm	very fine sand, 0.075-0.125mm	silt+clay <0.075 mm
327a	16.0	10.5	13.4	13.9	27.8	14.9	3.5
326a	5.4	7.4	14.1	15.7	30.2	21.8	5.3
328a	18.7	5.9	8.3	13.4	28.7	18.5	6.5
329a	11.1	8.2	13.2	14.8	31.2	16.8	4.7
330a	26.1	6.2	10.9	14.9	26.5	11.6	3.7
332a	7.5	7.6	13.1	14.1	32.4	19.7	5.6
334a	15.0	9.7	15.5	14.6	24.0	16.5	4.7
336a	9.1	9.0	10.8	11.5	28.3	23.5	7.9
338a	14.6	7.7	13.2	13.7	25.0	18.6	7.1
340a	9.3	8.1	11.5	19.9	33.5	12.8	4.9
341a	7.1	8.8	14.2	15.6	25.9	21.1	7.2
343a	6.5	14.0	23.3	20.4	20.9	10.4	2.5

Table D4: Sieve Analysis, Phase I: Bottom Samples (Percent total)

Sample Number	gravel >2mm	very coarse sand, 1-2mm	coarse sand, 0.5-1mm	medium sand, 0.25-0.5mm	fine sand, 0.125-0.25mm	very fine sand, 0.075-0.125mm	silt+clay <0.075 mm
322a	14.9	10.2	18.6	17.5	21.6	13.6	3.7
323a	9.6	6.5	13.8	20.5	32.7	13.3	3.5
324a	6.2	7.7	15.2	16.8	28.1	19.4	6.6
325a	6.7	5.8	13.9	16.8	35.3	17.5	4.0
331a	16.2	4.1	8.7	20.3	30.6	15.6	4.5
333a	9.4	8.6	16.2	16.5	26.2	17.7	5.4
335a	9.6	7.8	13.3	15.7	29.9	17.4	6.3
337a	16.0	8.1	12.8	14.0	25.3	18.9	4.9
339a	7.4	6.8	12.5	14.6	33.0	20.6	5.0
342a	10.6	10.0	17.0	16.8	27.4	14.7	3.5

Table D5: Sieve Analysis, Phase I: Backfill Samples (Percent total)

Sample Number	gravel >2mm	very coarse sand, 1-2mm	coarse sand, 0.5-1mm	medium sand, 0.25-0.5mm	fine sand, 0.125-0.25mm	very fine sand, 0.075-0.125mm	silt+clay <0.075 mm
312a	14.3	8.1	12.5	15.3	29.3	17.8	2.6
313a	6.1	7.4	13.5	17.2	33.6	18.0	4.3
314a	7.5	6.3	11.7	16.7	33.5	19.3	5.0
315a	15.2	7.0	11.6	14.6	29.7	17.1	5.0
316a	13.6	5.2	13.0	17.1	26.8	18.9	5.3
317a	17.0	7.2	15.7	18.4	27.9	11.7	2.0
318a	6.5	10.4	15.6	16.3	30.2	15.5	5.4
319a	12.3	6.8	12.1	13.3	26.8	21.6	7.2
320a	7.5	7.7	12.4	13.7	33.5	19.1	6.1
321a	13.2	12.4	18.0	13.6	21.8	16.1	5.0

Phase II. Like the samples from Phase I, the soil samples from Phase II consist mainly of fine sand and very fine sand (Tables D6, D7, and D8). Surface samples contain a mean of 41.3% fine sand and very fine sand; trench bottom samples, a mean of 42.1%; and backfill samples, a mean of 40.0%. Gravel ranges from 5.2-34.8% in the surface samples (mean 13.4%), from 4.9-25.6% in the trench bottom samples (mean 12.1%), and from 8.2-35.1% in the backfill samples (mean 15.9%). In the surface samples, silt+clay ranges from 4.1-18.1% (mean 9.3%); in the trench bottom samples, from 3.0-8.7% (mean 5.8%), and in the backfill samples, from 3.2-14.1% (mean 7.2%). Trench bottom and backfill samples contain more gravel than surface samples, but surface samples contain more silt and clay than do trench bottom and backfill samples.

Table D6: Sieve Analysis, Phase II: Surface Samples (Percent total)

Sample Number	gravel >2mm	very coarse sand, 1-2mm	coarse sand, 0.5-1mm	medium sand, 0.25-0.5mm	fine sand, 0.125-0.25mm	very fine sand, 0.075-0.125mm	silt+clay <0.075 mm
312b	9.0	13.4	11.6	10.1	23.3	22.0	10.6
321b	9.4	13.7	12.9	11.1	18.9	15.8	18.1
323b	13.3	11.4	16.0	15.5	25.1	14.7	4.1
327b	6.6	10.9	13.4	14.3	26.5	20.5	7.8
328b	13.2	9.2	14.0	14.5	22.5	17.8	8.8
331b	14.9	11.0	10.3	13.0	23.7	17.6	9.3
333b	14.5	18.8	13.2	13.8	21.9	11.1	6.8
334b	20.2	10.3	8.6	9.7	21.7	19.3	10.3
337b	7.3	9.5	10.5	10.4	30.4	22.6	9.2
339b	12.3	13.4	12.8	15.1	24.4	16.0	6.0
342b	5.2	11.6	12.9	11.3	25.7	22.7	10.6
344b	34.8	7.3	8.4	8.3	16.6	14.7	10.0

Table D7: Sieve Analysis, Phase II: Bottom Samples (Percent total)

Sample Number	gravel >2mm	very coarse sand, 1-2mm	coarse sand, 0.5-1mm	medium sand, 0.25-0.5mm	fine sand, 0.125-0.25mm	very fine sand, 0.075-0.125mm	silt+clay <0.075 mm
314b	10.8	9.5	16.7	21.9	26.2	11.0	3.9
317b	14.4	13.6	13.4	16.7	25.6	12.4	3.9
318b	11.1	8.8	12.2	15.4	27.1	17.8	7.5
322b	11.9	10.5	12.5	15.1	33.6	12.7	3.4
324b	4.9	8.1	21.4	20.1	25.3	13.6	6.7
329b	25.6	10.9	12.7	15.2	20.9	10.2	4.6
335b	17.2	12.2	17.5	13.8	19.2	13.3	6.8
336b	6.7	16.9	14.5	11.9	24.6	18.1	7.4
340b	7.2	3.5	4.6	11.1	41.4	24.0	8.3
341b	7.2	5.3	6.6	9.5	36.7	26.1	8.7
343b	16.5	15.6	24.6	16.9	15.8	7.7	3.0

Table D8: Sieve Analysis, Phase II: Backfill Samples (Percent total)

Sample Number	gravel >2mm	very coarse sand, 1-2mm	coarse sand, 0.5-1mm	medium sand, 0.25-0.5mm	fine sand, 0.125-0.25mm	very fine sand, 0.075-0.125mm	silt+clay <0.075 mm
313b	11.7	13.9	25.0	15.6	17.9	10.2	5.6
315b	8.2	7.3	10.8	14.2	45.0	11.2	3.2
316b	35.1	12.1	9.3	8.8	17.5	10.9	4.6
319b	10.3	9.2	9.5	13.4	30.5	20.5	6.6
320b	9.5	6.9	11.1	15.4	28.6	19.7	8.8
325b	17.5	12.9	14.6	11.7	16.3	13.0	14.1
326b	20.8	7.4	21.2	18.9	19.2	9.1	3.5
330b	13.8	10.2	10.5	15.0	28.7	15.3	6.6
332b	16.4	10.2	10.3	12.3	25.2	16.7	8.9
338b	15.2	8.0	8.9	12.7	27.8	19.0	8.4

Comparison of Phase I and Phase II Soil Samples

Soil moisture is slightly higher in the Phase II soil samples than it is in the Phase I samples, but this was expected. The Phase II site is down slope from the Phase I site and is located closer to

the nearby playa lake. There are, however, no statistically significant differences at the 95% confidence level between the two sets of soil samples from Twentynine Palms with respect to soil moisture. There are also no statistically significant differences (also at the 95% confidence level) between surface, backfill and trench bottom samples in Phase I, Phase II or between Phase I and Phase II with respect to particle size.

Conclusions

These results suggest that radar should penetrate the soils of the test sites at least to the depths of interest. Surface and trench bottom sample soil moistures are well within the range of known radar penetration, and as best as can be determined at this time, the fine sand to very fine sand soils should also allow penetration. The effects of gravel were not considered. Analysis of spectral reflectance curves for some of these soils suggest that gypsum is either not present or is present only in very small quantities (Ehlen and Henley, 1991); subsequent petrographic analysis confirmed this (Rubick Luttrell, 1991). The presence of salts should thus not affect radar penetration at the Twentynine Palms test sites.

Soil Characteristics around the Perimeter of the Test Site

Methodology

Four soil pits were dug just outside test site boundaries to eliminate any significant disturbance of the test site soil. The pits were dug to a depth of about 1 meter to identify any differences in the texture or structure of the soil as a function of depth. Pairs of soil moisture samples were taken at regular intervals in each pit, and bag samples were collected for soil classification and mineralogical analyses. Classification was made using the Unified Soil Classification System (USCS; Figure D7).

Qualitative Observations

In general, the soil at the Twentynine Palms test site is a typical desert soil, with a weak, thin upper layer, or horizon, and a somewhat cemented lower horizon (Ritter, 1986). The cemented material often gave way at greater depths to a loose sand. At each soil pit site, about the first 5 cm of soil could be easily removed with a shovel. There was a distinct interface between the weak sandy soil and the cemented soil beneath it. A pick axe was required to break through the cemented material, which was in a layer at least 10 cm thick.

Unified Soil Classification

Major Divisions			Group Symbols	Typical Names	Field Identification Procedures (Excluding particles larger than 3 in. and basing fractions on estimated weights)			Information Required for Describing Soils
1	2		3	4	5			6
Coarse-grained Soils: More than half of material is larger than No. 200 sieve size.	Gravels: More than half of coarse fraction is larger than No. 4 sieve size. (For visual classification, the 1/4-in. size may be used as equivalent to the No. 4 sieve size)	Clean Gravels (Little or no fines)	GW	Well-graded gravels, gravel-sand mixtures, little or no fines.	Wide range in grain sizes and substantial amounts of all intermediate particle sizes.			For undisturbed soils add information on stratification, degree of compactness, cementation, moisture conditions and drainage characteristics.
			GP	Poorly graded gravels or gravel-sand mixtures, little or no fines.	Predominantly one size or a range of sizes with some intermediate sizes missing.			
		Gravels with Fines (Appreciable amount of fines)	GM	Silty gravels, gravel-sand-silt mixture.	Nonplastic fines or fines with low plasticity (for identification procedures see ML below).			Give typical name; indicate approximate percentages of sand and gravel, maximum size; angularity, surface condition, and hardness of the coarse grains; local or geologic name and other pertinent descriptive information; and symbol in parentheses.
			GC	Clayey gravels, gravel-sand-clay mixtures.	Plastic fines (for identification procedures see CL below).			
	Sands: More than half of coarse fraction is smaller than No. 4 sieve size.	Clean Sands (Little or no fines)	SW	Well-graded sands, gravelly sands, little or no fines.	Wide range in grain size and substantial amounts of all intermediate particle sizes.			
			SP	Poorly graded sands or gravelly sands, little or no fines.	Predominantly one size or a range of sizes with some intermediate sizes missing.			Example: Silty sand, gravelly; about 20% hard, angular gravel particles 1/2-in. maximum size; rounded and subangular sand grains, coarse to fine; about 15% nonplastic fines with low dry strength; well compacted and moist in place; alluvial sand; (SM).
		Sands with Fines (Appreciable amount of fines)	SM	Silty sands, sand-silt mixtures.	Nonplastic fines or fines with low plasticity (for identification procedures see ML below).			
			SC	Clayey sands, sand-clay mixtures.	Plastic fines (for identification procedures see CL below).			
					Identification Procedures on Fraction Smaller than No. 40 Sieve Size			
					Dry Strength (Crushing characteristics)	Dilatancy (Reaction to shaking)	Toughness (Consistency near PL)	
Fine-grained Soils: More than half of material is smaller than No. 200 sieve size. The No. 200 sieve size is about the smallest particle visible to the naked eye.	Silts and Clays: Liquid limit is less than 50		ML	Inorganic silts and very fine sands, rock flour, silty or clayey fine sands or clayey silts with slight plasticity.	None to slight	Quick to slow	None	For undisturbed soils add information on structure, stratification, consistency in undisturbed and remolded states, moisture and drainage conditions.
			CL	Inorganic clays of low to medium plasticity, gravelly clays, sandy clays, silty clays, lean clays.	Medium to high	None to very slow	Medium	
			OL	Organic silts and organic silty clays of low plasticity.	Slight to medium	Slow	Slight	Give typical name; indicate degree and character of plasticity; amount and maximum size of coarse grains; color in wet condition; odor, if any; local or geologic name and other pertinent descriptive information; and symbol in parentheses.
	Silts and Clays: Liquid limit is greater than 50		MH	Inorganic silts, micaceous or diatomaceous fine sandy or silty soils, elastic silts.	Slight to medium	Slow to none	Slight to medium	
			CH	Inorganic clays of high plasticity, fat clays.	High to very high	None	High	
			OH	Organic clays of medium to high plasticity, organic silts.	Medium to high	None to very slow	Slight to medium	Example: Clayey silt, brown; slightly plastic; small percentage of fine sand; numerous vertical root holes; firm and dry in place; loess; (ML).
Highly Organic Soils			Pt	Peat and other highly organic soils.	Readily identified by color, odor, spongy feel and frequently by fibrous texture.			

(1) Boundary classifications: Soils possessing characteristics of two groups are designated by combinations of group symbols. For example GW-GC, well-graded gravel-sand mixture

FIELD IDENTIFICATION PROCEDURES FOR FINE-GRAINED SOILS OR FRACTIONS

These procedures are to be performed on the minus No. 40 sieve size particles, approximately 1/64 in. For field c screening is not intended, simply remove by hand the coarse particles that interfere with the te

Dilatancy (reaction to shaking)

After removing particles larger than No. 40 sieve size, prepare a pat of moist soil with a volume of about one-half cubic inch. Add enough water if necessary to make the soil soft but not sticky.

Place the pat in the open palm of one hand and shake horizontally, striking vigorously against the other hand several times. A positive reaction consists of the appearance of water on the surface of the pat which changes to a livery consistency and becomes glossy. When the sample is squeezed between the fingers, the water and gloss disappear from the surface, the pat stiffens, and finally it cracks or crumbles. The rapidity of appearance of water during shaking and of its disappearance during squeezing assist in identifying the character of the fines in a soil.

Very fine clean sands give the quickest and most distinct reaction whereas a plastic clay has no reaction. Inorganic silts, such as a typical rock flour, show a moderately quick reaction.

Dry Strength (crushing characteristics)

After removing particles larger than No. 40 sieve size, mold a pat of soil to the consistency of putty, adding water if necessary. Allow the pat to dry completely by oven, sun, or air-drying, and then test its strength by breaking and crumbling between the fingers. This strength is a measure of the character and quantity of the colloidal fraction contained in the soil. The dry strength increases with increasing plasticity.

High dry strength is characteristic for clays of the CH group. A typical inorganic silt possesses only very slight dry strength. Silty fine sands and silts have about the same slight dry strength, but can be distinguished by the feel when powdering the dried specimen. Fine sand feels gritty whereas a typical silt has the smooth feel of flour.

Figure D7. Unified Soil classification.

Soil Classification

Figures D8 through D11 summarize the results of on-site measurements of the soil from the soil pits and of laboratory studies of samples. For each of the four pits that were dug, a summary figure (Figure D8-A, for example) is presented that contains USCS symbology for soil classification as well as wet and dry densities and gravimetric moisture contents as a function of depth. Visual soil classification represents depth-dependent soil texture deduced from laboratory classifications of a limited number of samples (not all bag samples were analyzed to minimize costs), along with field notebook notations on changes in soil properties as the pits were being dug. Density and moisture content numbers are placed on the charts at about the depth at which the samples were collected. Moisture contents within the test site were typically $< 1\%$ at the surface, increasing to 2-3% at depths of about 50 cm.

Each summary chart is followed by a gradation curve for each of the laboratory samples that were tested (Figure D8-B, D8-C, D8-D, etc. for example). These curves show clearly that the soil found at this test site is typically a mix of sands (mostly well graded), with less than 10% fine gravels, and anywhere from 5-20% silts (possibly some clays).

Soil Petrography

A cursory petrographic examination was made of several soil samples. The results of these studies are shown in the memorandum dated 31 October 1990 (see pp. 76). Of particular relevance to the analysis of radar data for this study (as those results might compare to a future test under moist soil conditions) is the reference to the possible existence of gypsum (hydrated calcium sulfate). Under wet conditions, the presence of gypsum, a salt, could drastically affect the electrical properties of the soil.

Surface Characteristics

Surface Anomalies

In order to establish a record of surface conditions during the SAR overflights but without the advantage of a helicopter-mounted, high-resolution photographic capability, a visual inspection was conducted of the test area, which produced a test site ground-truth map (Figure D12). The 100x250 m rectangular test site was divided up into 25 m squares with imaginary boundaries. The observer was positioned roughly at the center of each square and sketched all of the surface anomalies that might result in significant returns to the SAR systems. These anomalies included such things as the orientation of significant vehicle tracks, the locations of creosote bushes, and the location of metallic trash such as flattened smoke grenade boxes and expended shell casings.[4] As indicated by the different shadings within each 25 m square, the **observer roughness** was determined by estimating visually the largest change in elevation between peaks and troughs of vehicle tracks or sand dune formations.

[4] Visible metal objects were removed before the overflights.

SITE I

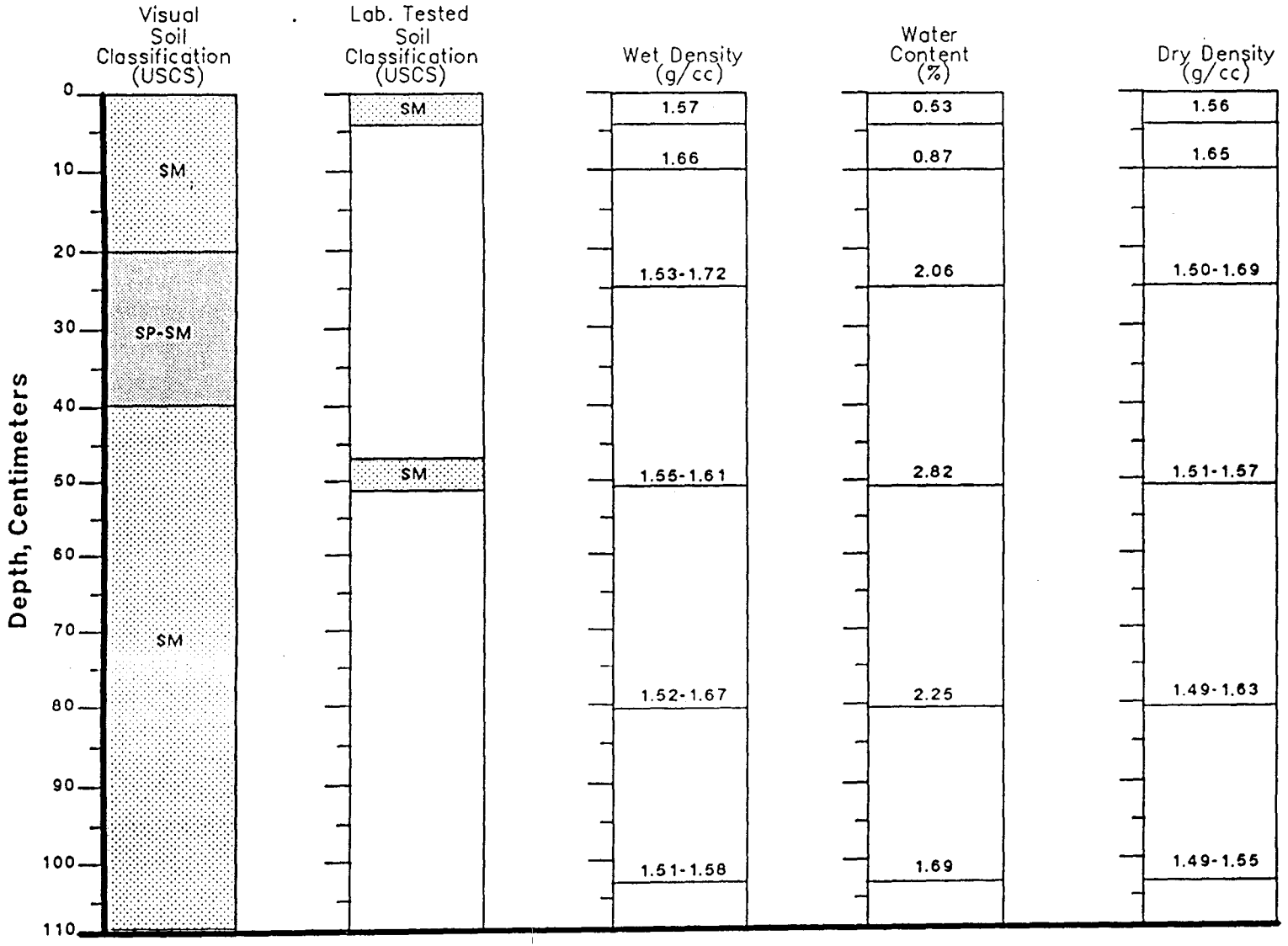

Figure D8. Site I. A. Soil classification, soil density and soil moisture content.

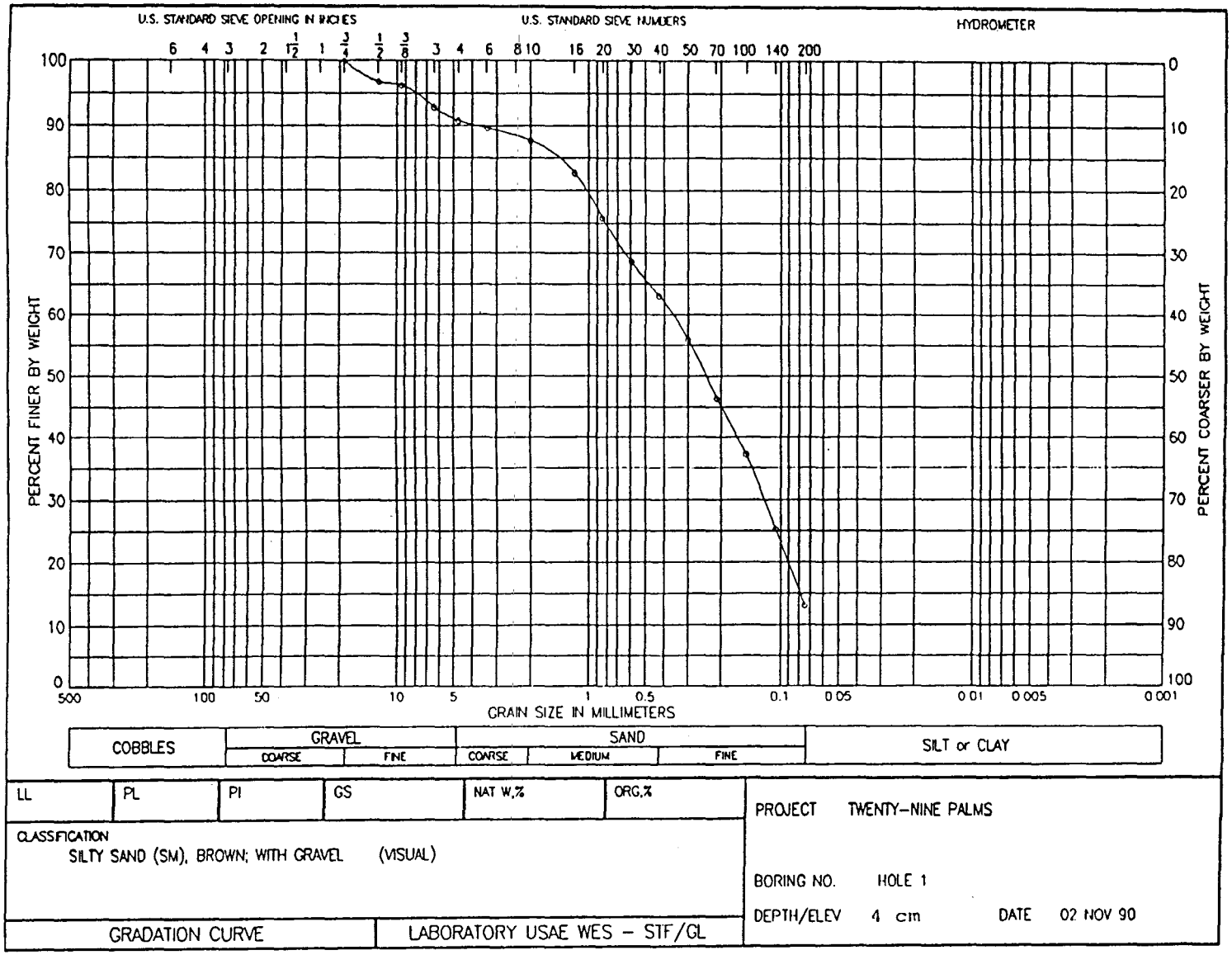

Figure D8. Site I. B. Particle size, 4-cm depth.

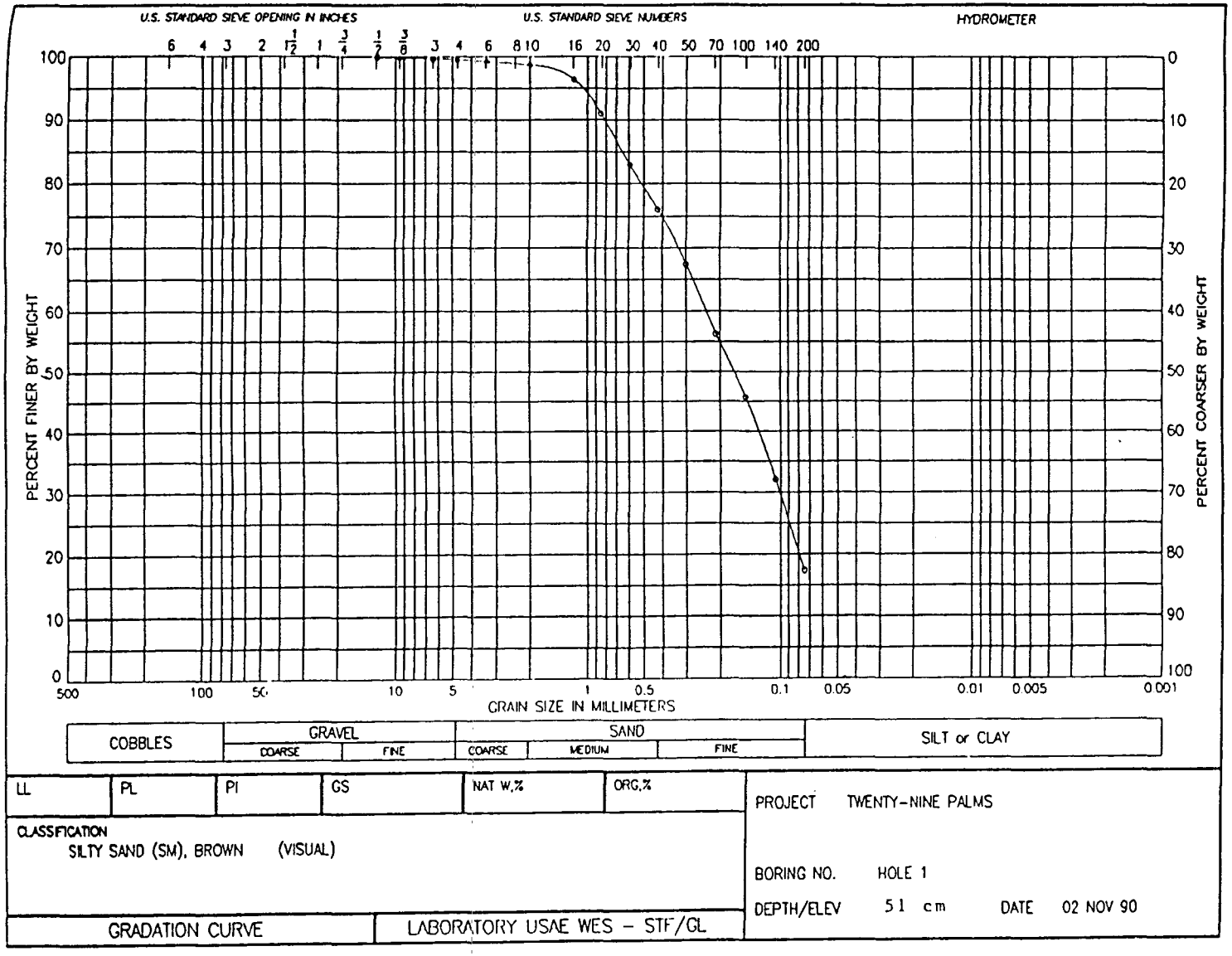

Figure D8. Site I. C. Particle size, 51-cm depth.

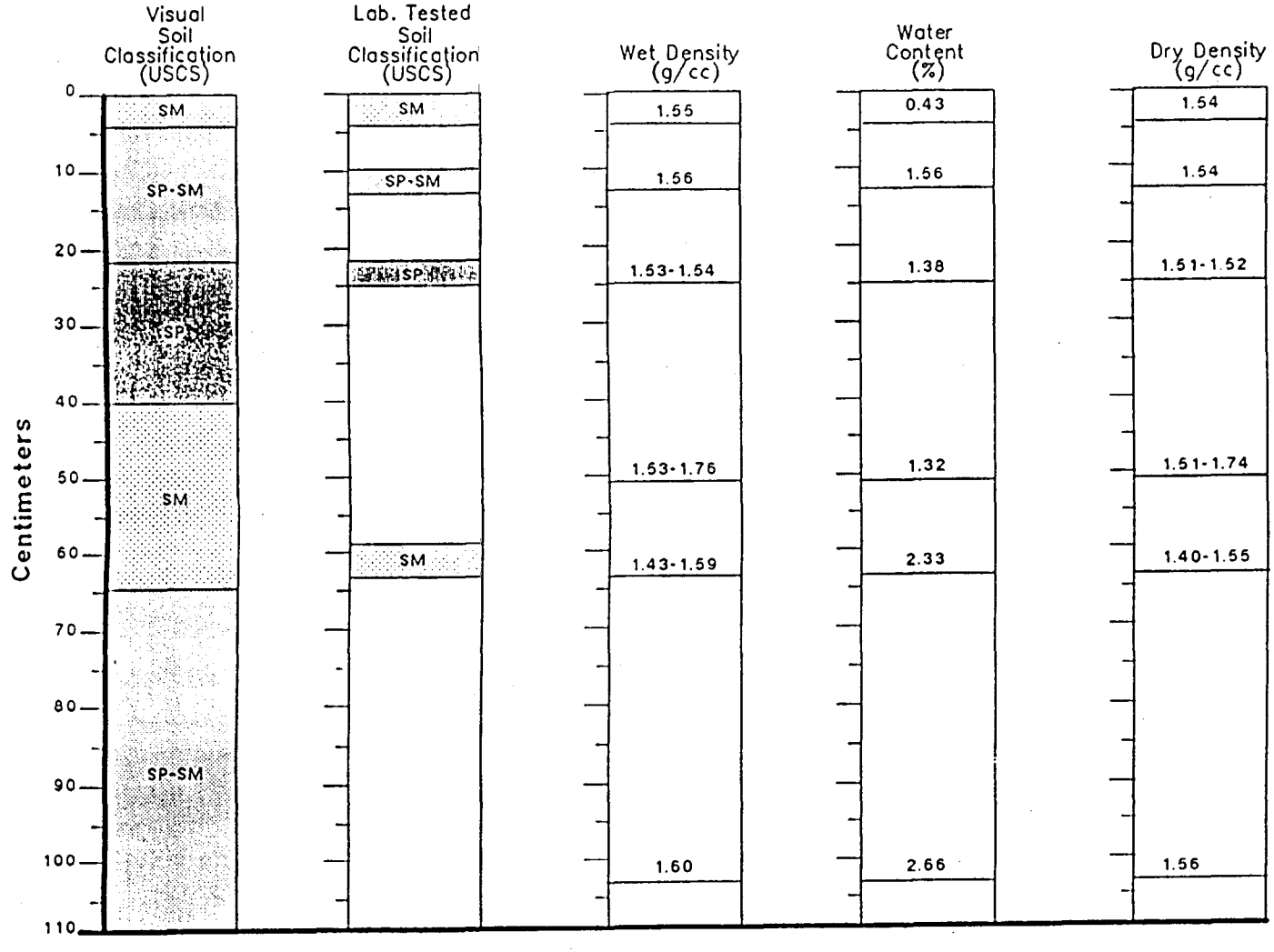

Figure D9. Site II. A. Soil classification, soil density and soil moisture content.

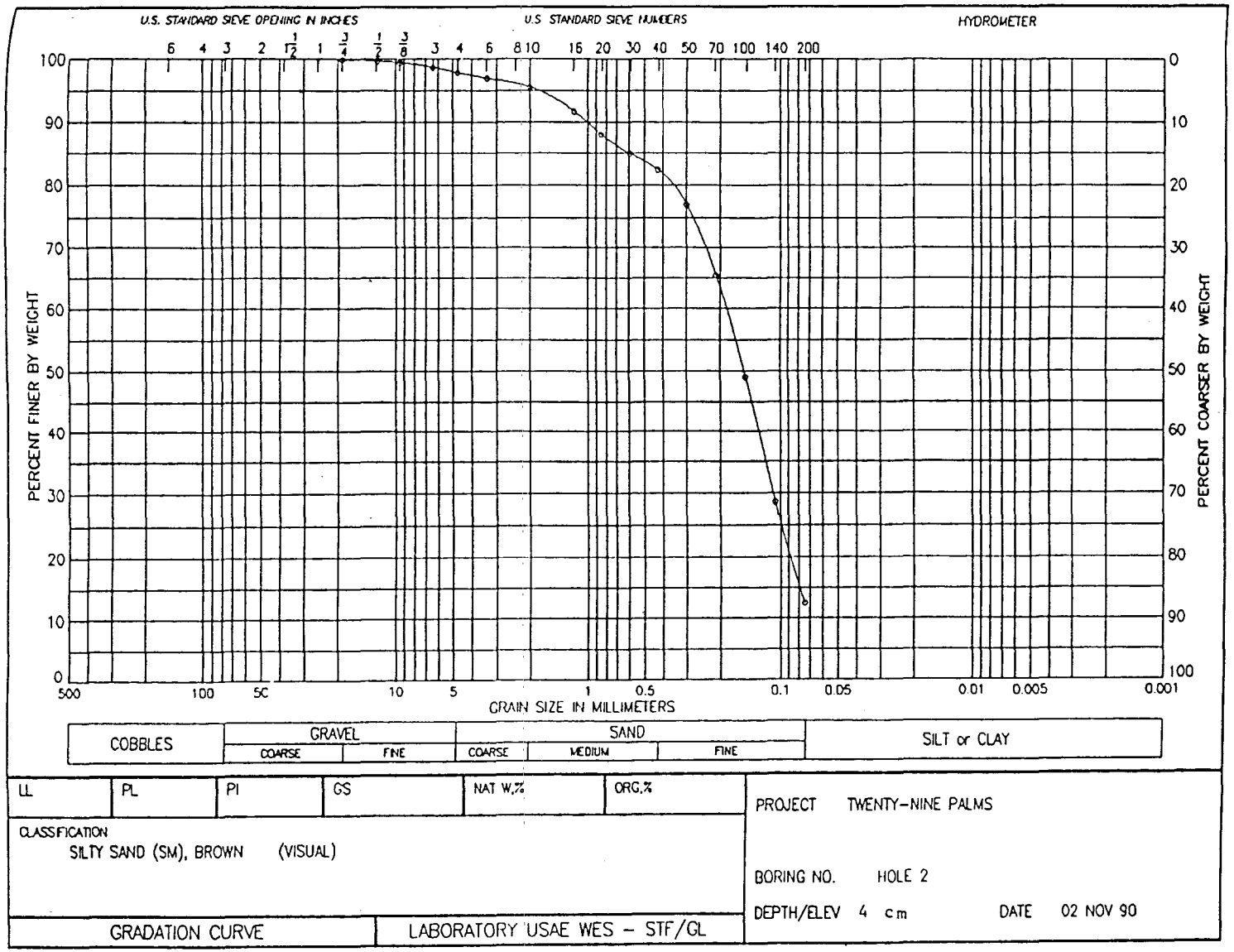

Figure D9. Site II. B. Particle size, 4-cm depth.

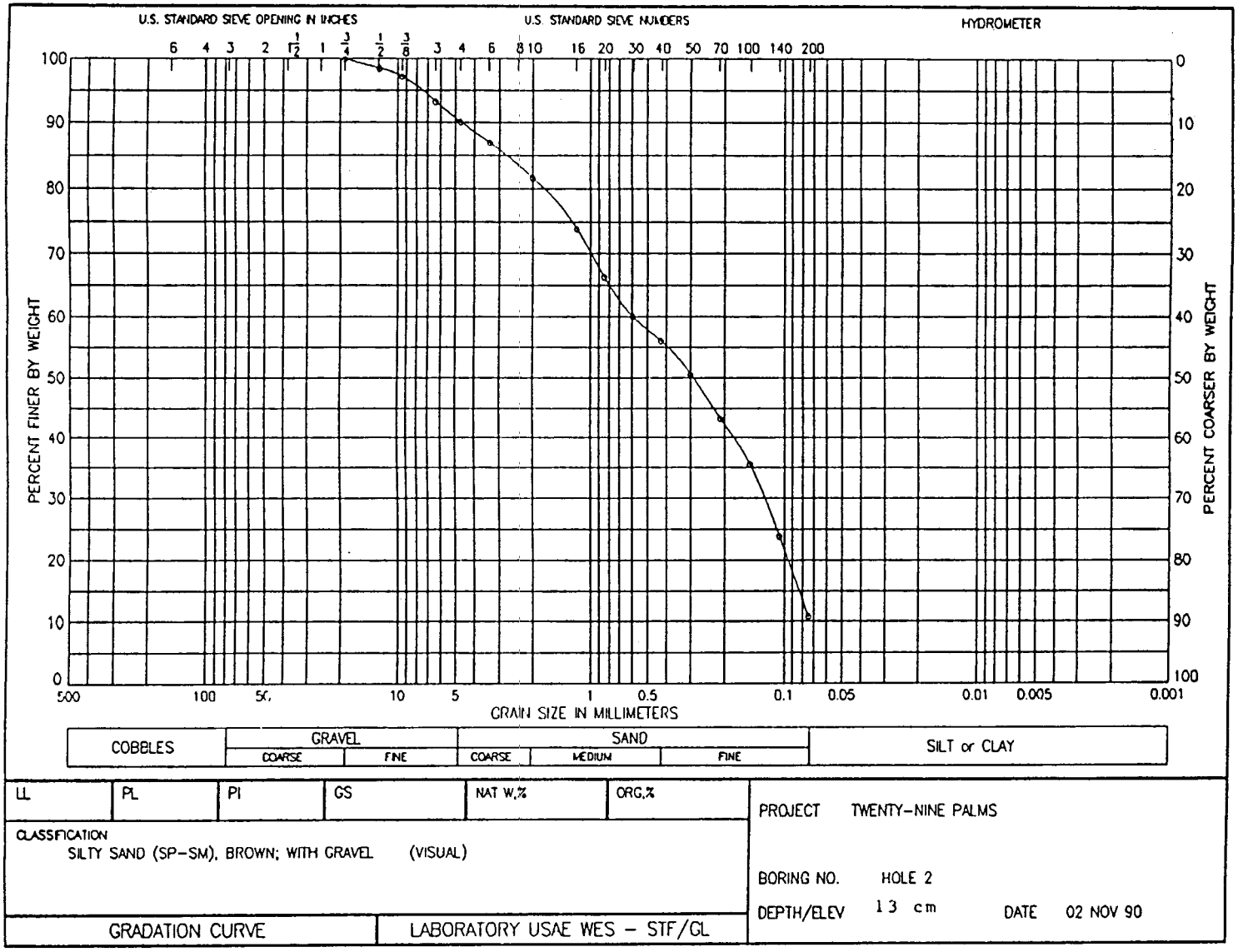

Figure D9. Site II. C. Particle size, 13-cm depth.

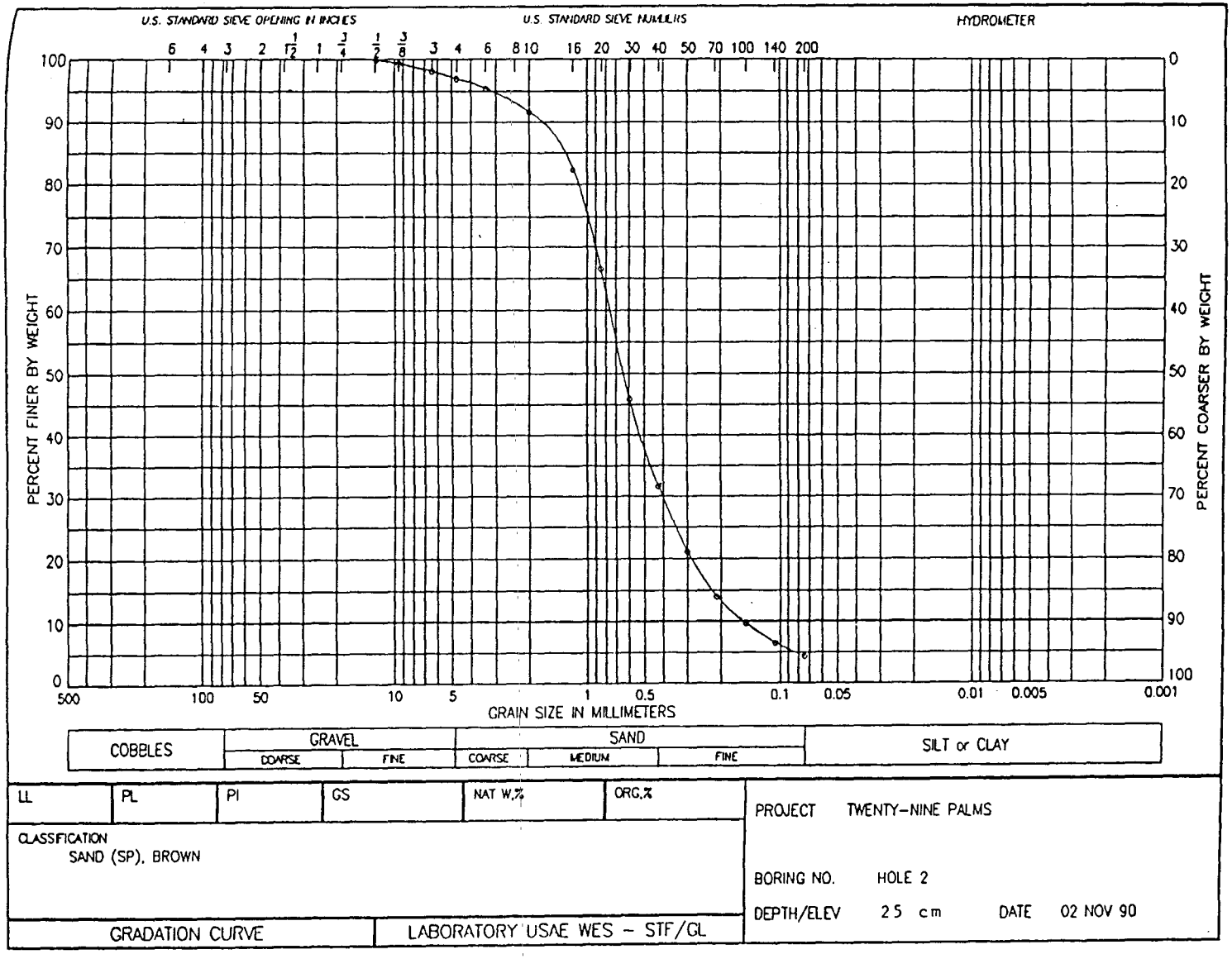

Figure D9. Site II. D. Particle size, 25-cm depth.

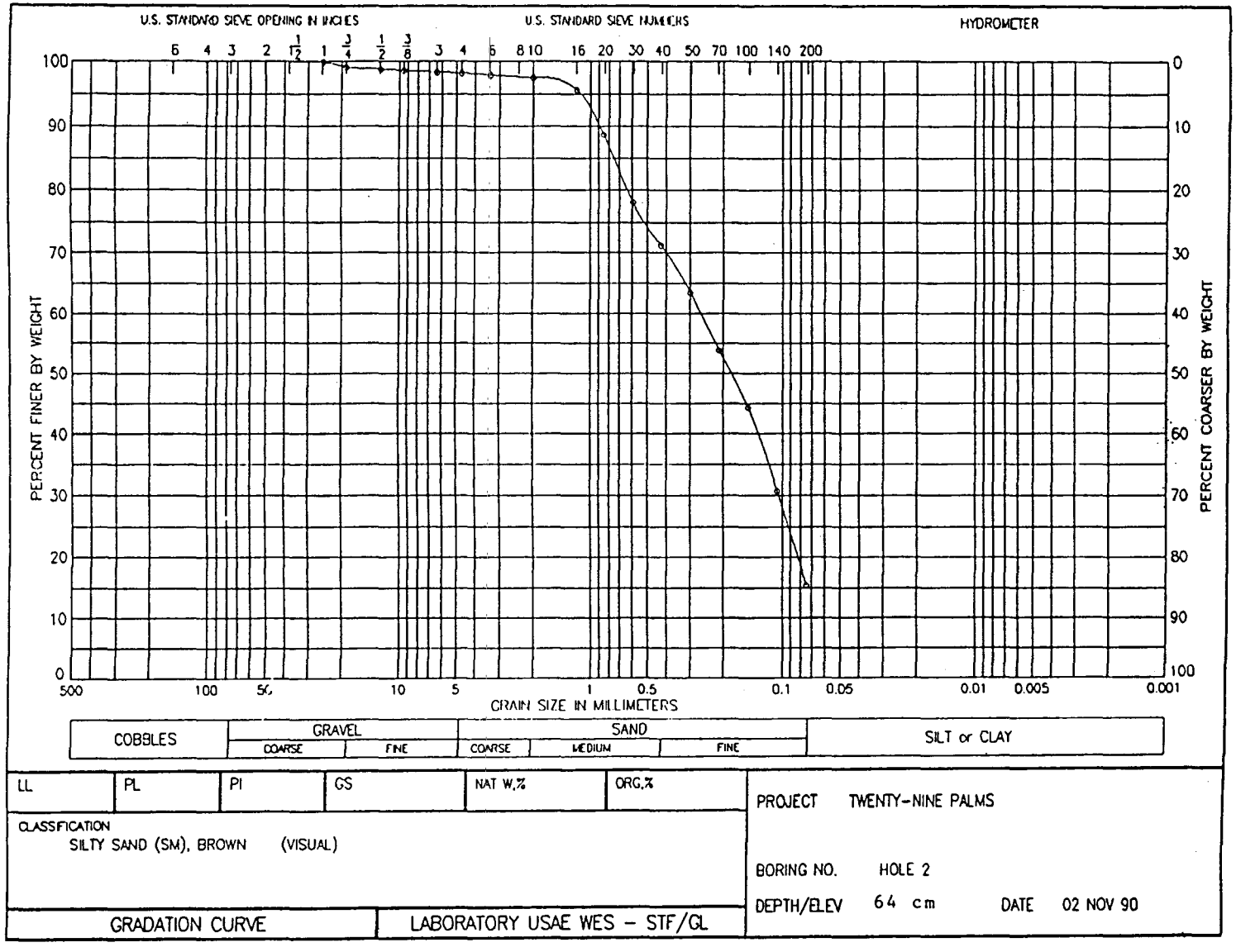

Figure D9. Site II. E. Particle size, 64-cm depth.

SITE III

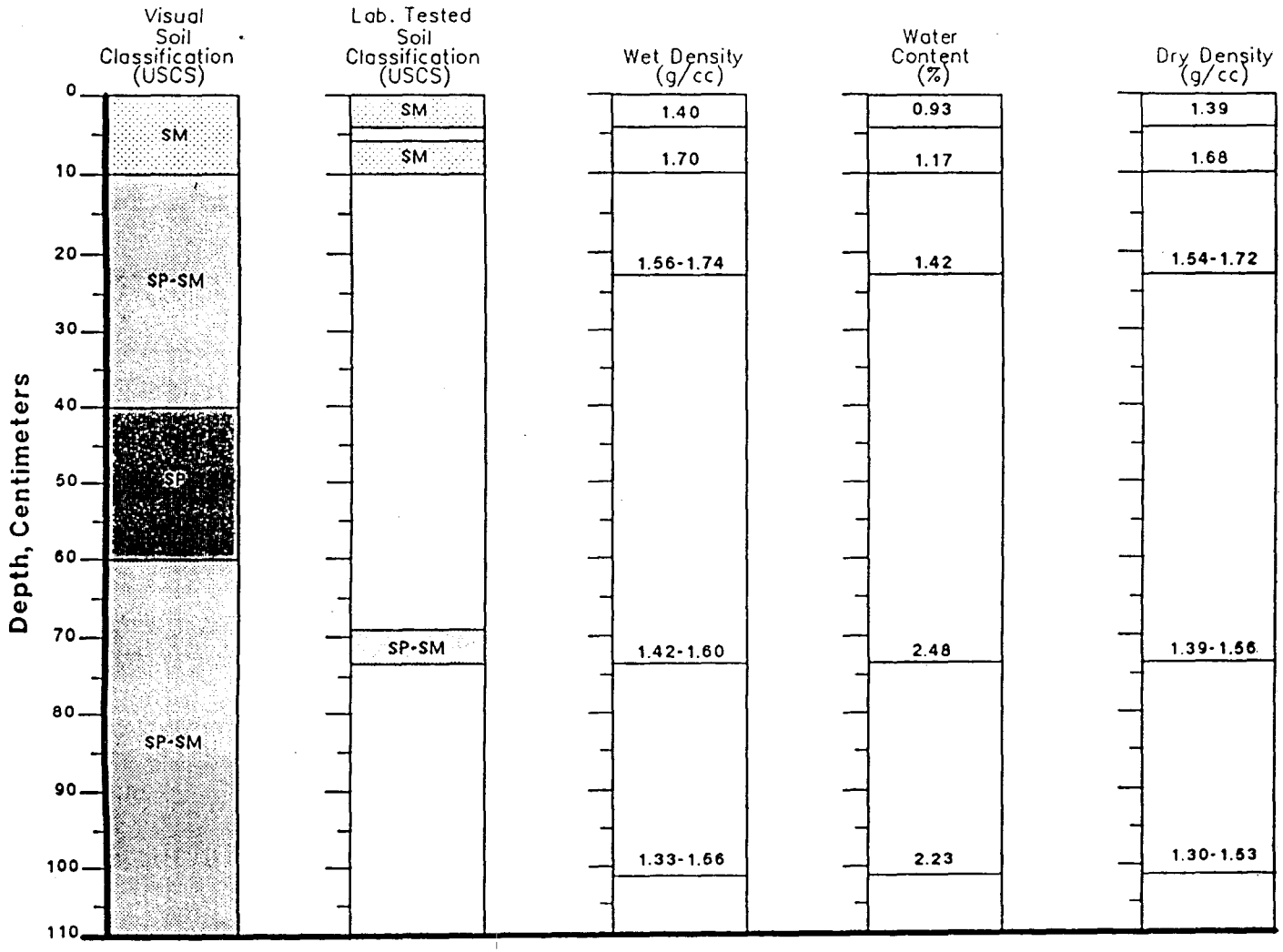

Figure D10. Site III. A. Soil classification, soil density and soil moisture content.

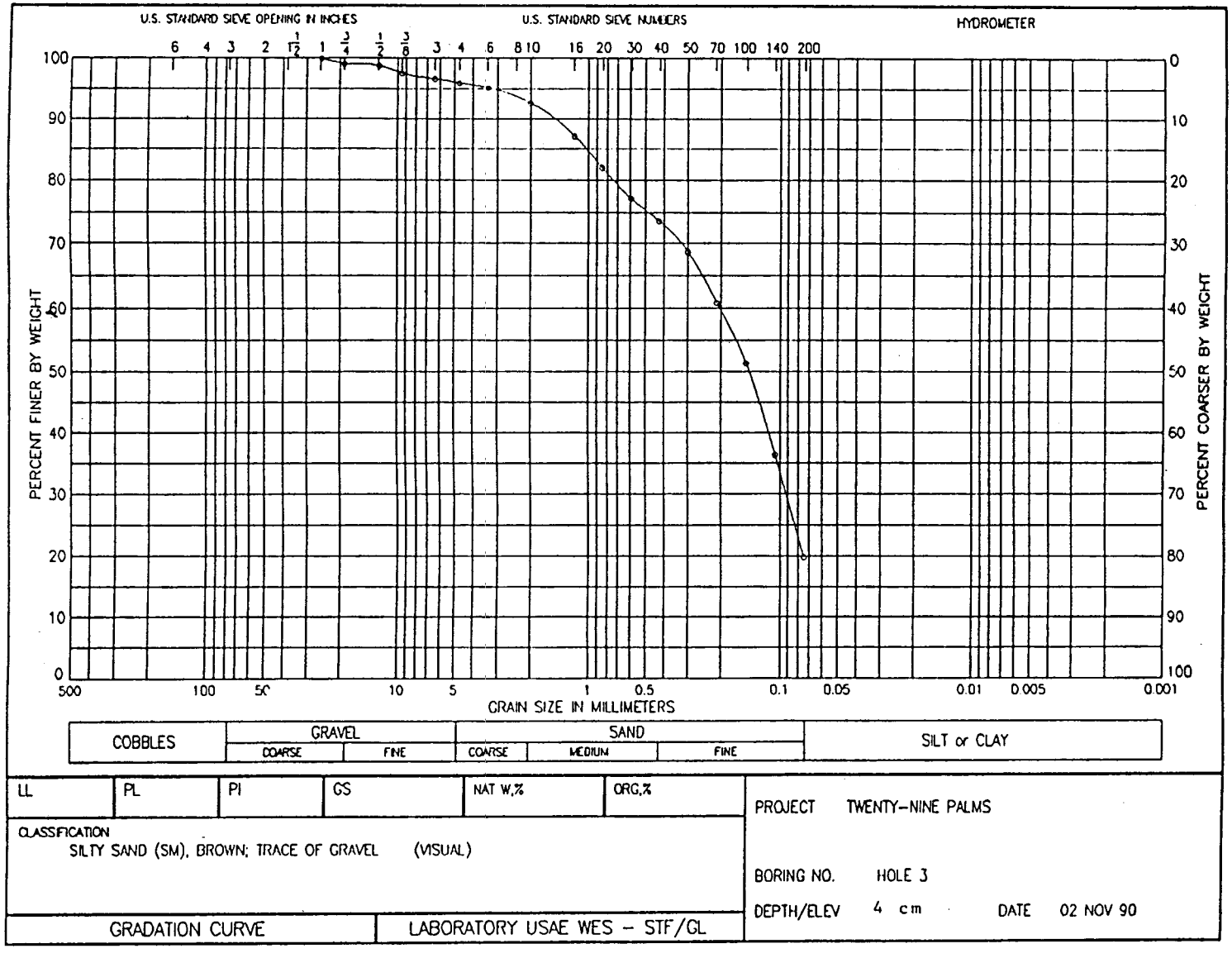

Figure D10. Site III. B. Particle size, 4-cm depth.

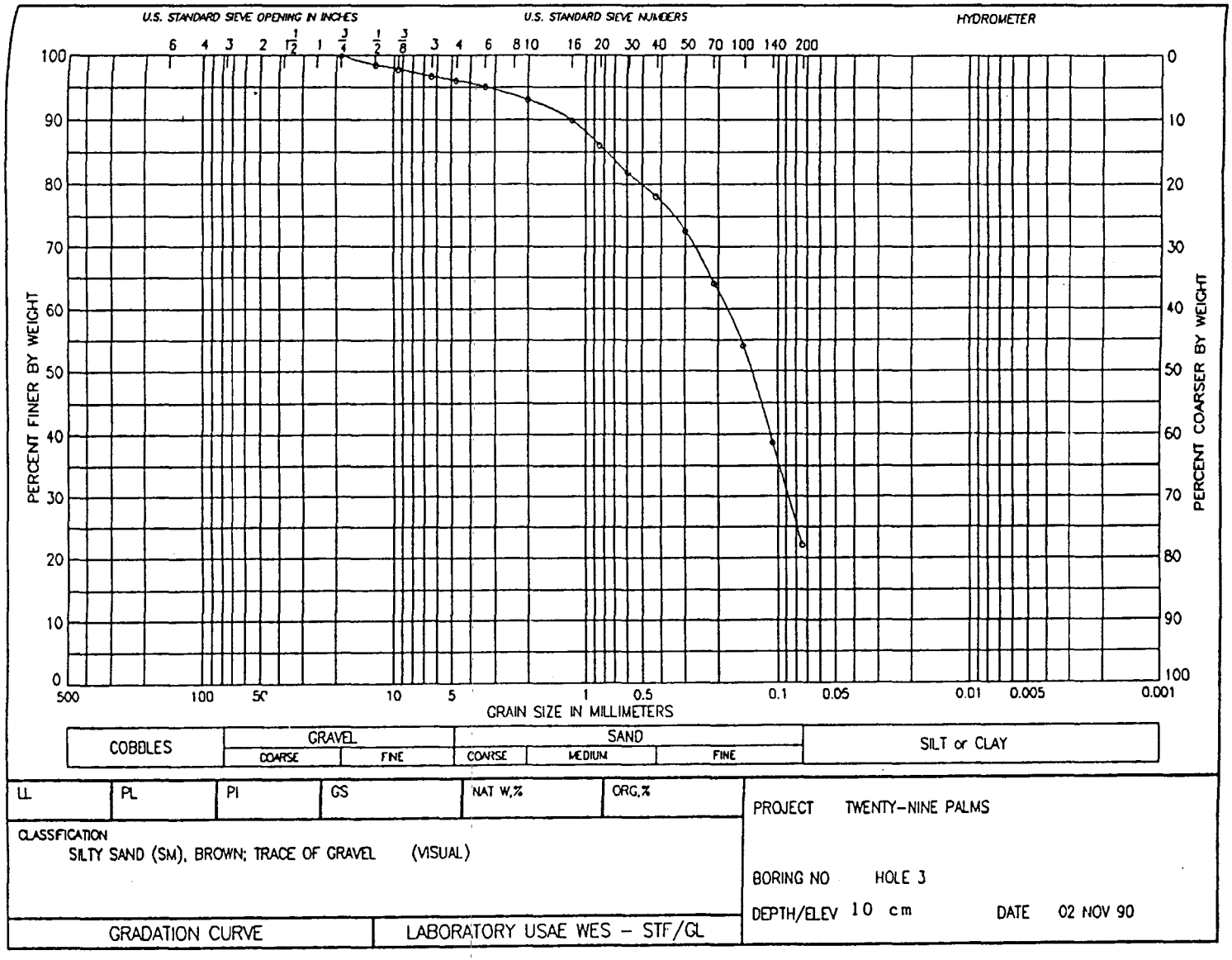

Figure D10. Site III. C. Particle size, 10-cm depth.

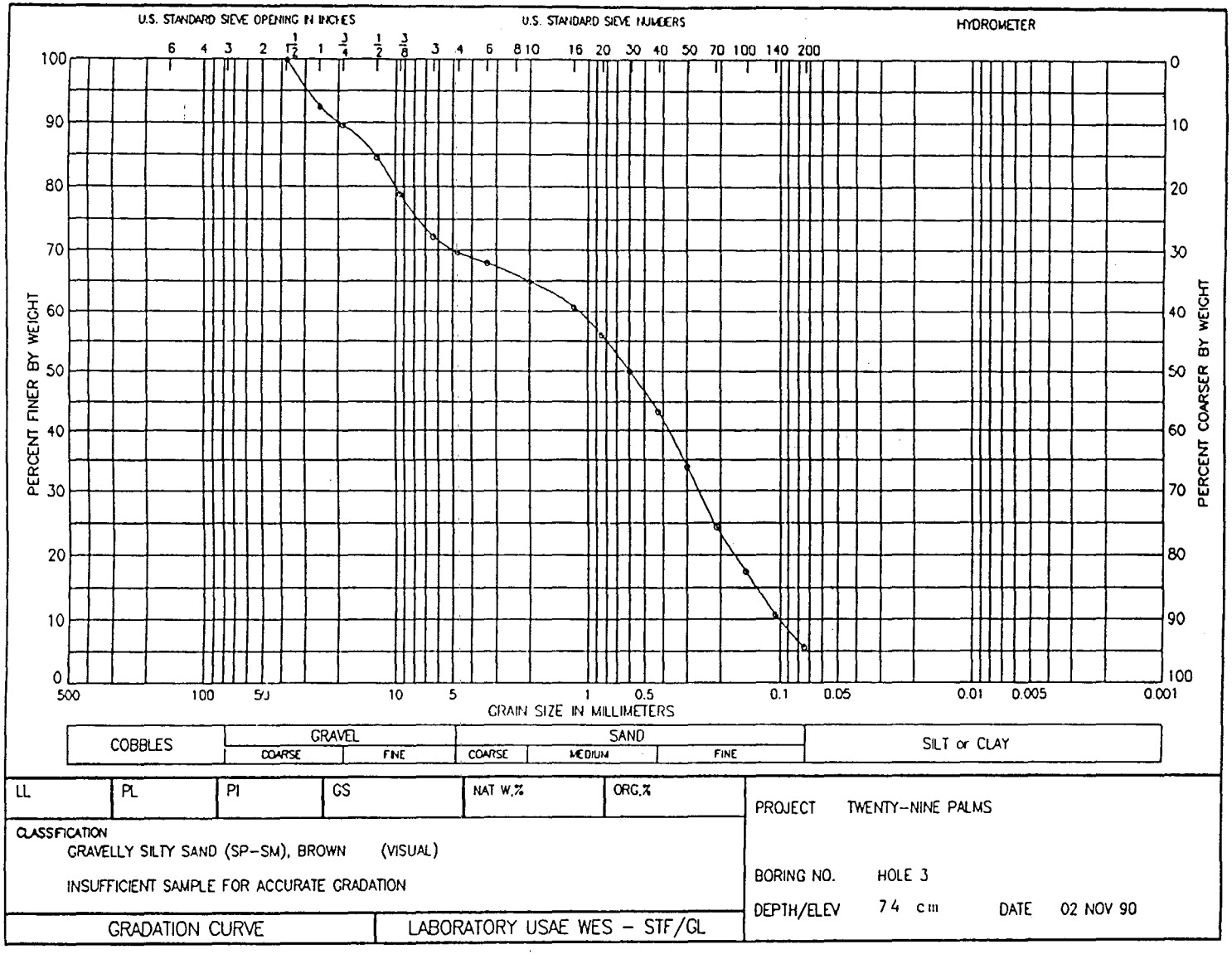

Figure D10. Site III. D. Particle size, 74-cm depth.

SITE IV

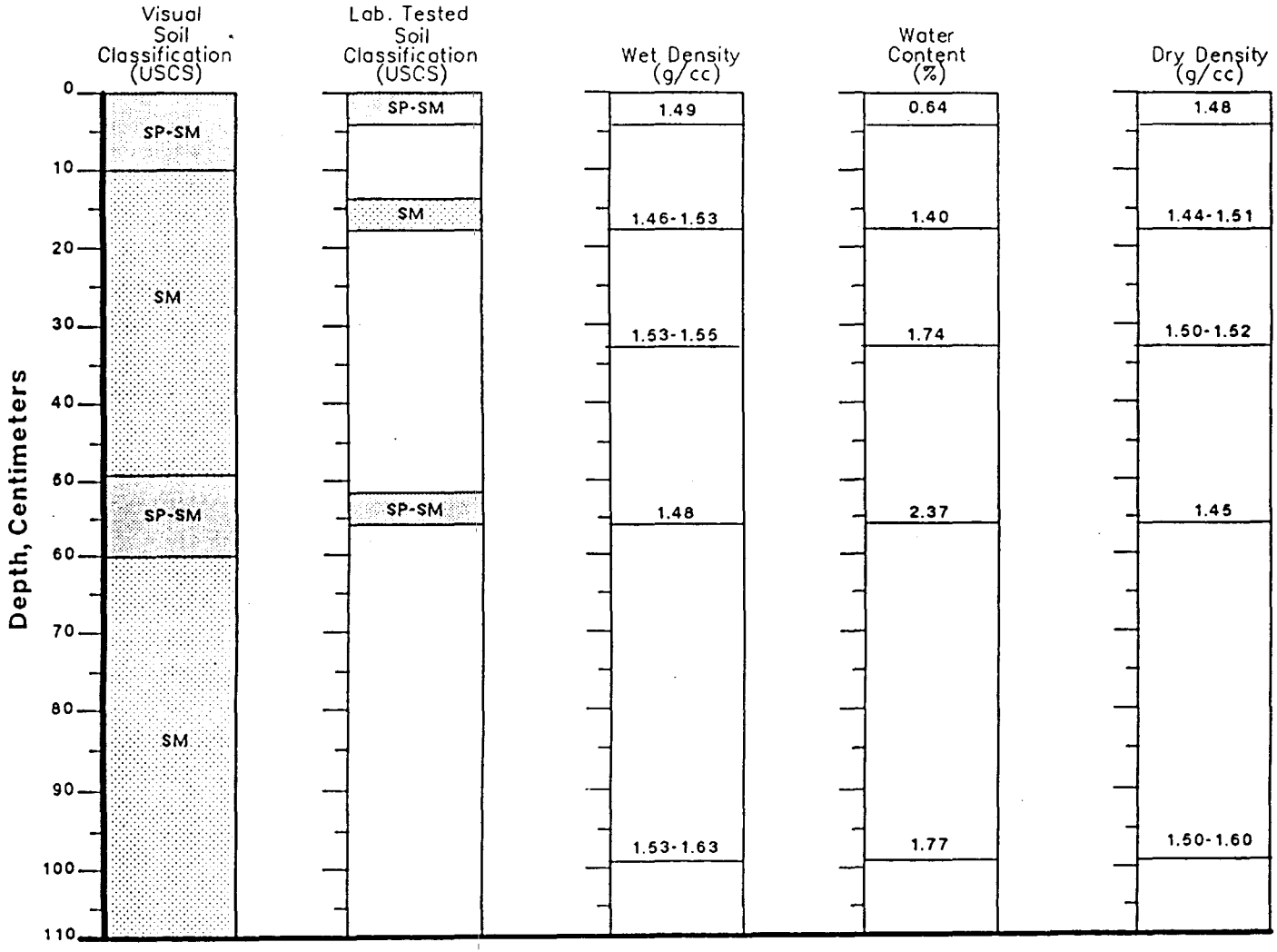

Figure D11. Site IV. A. Soil classification, soil density and soil moisture content.

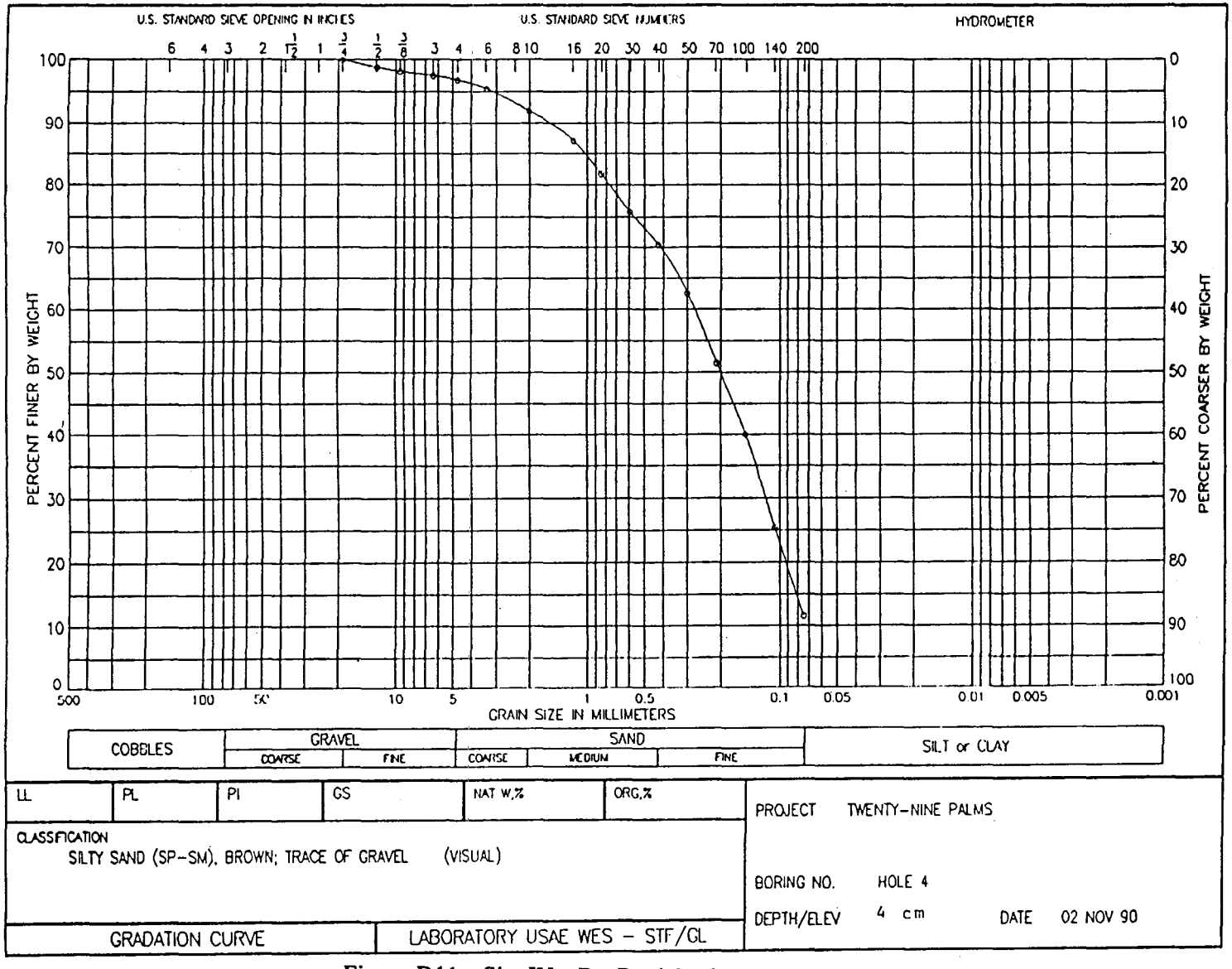

Figure D11. Site IV. B. Particle size, 4-cm depth.

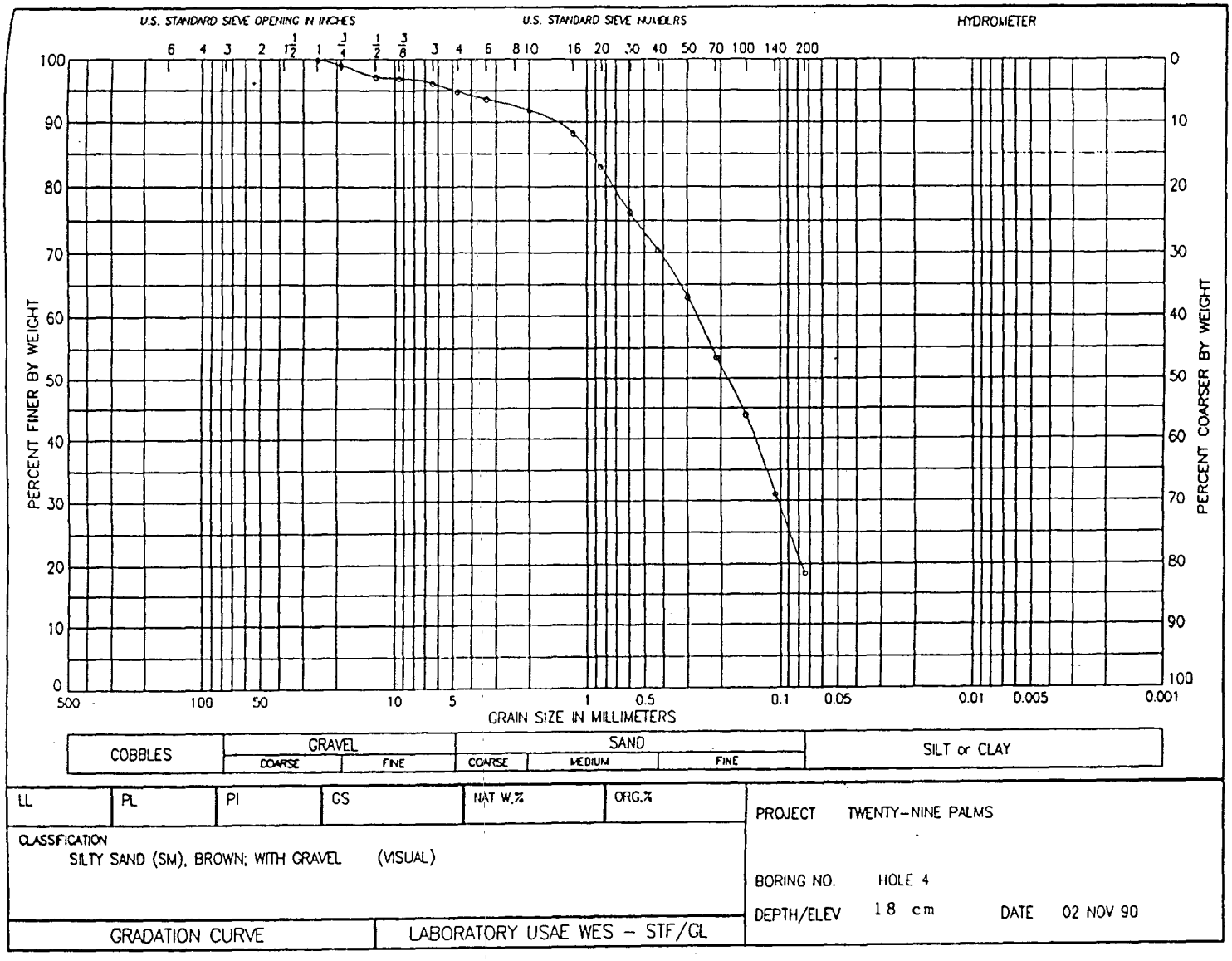

Figure D11. Site IV. C. Particle size, 18-cm depth.

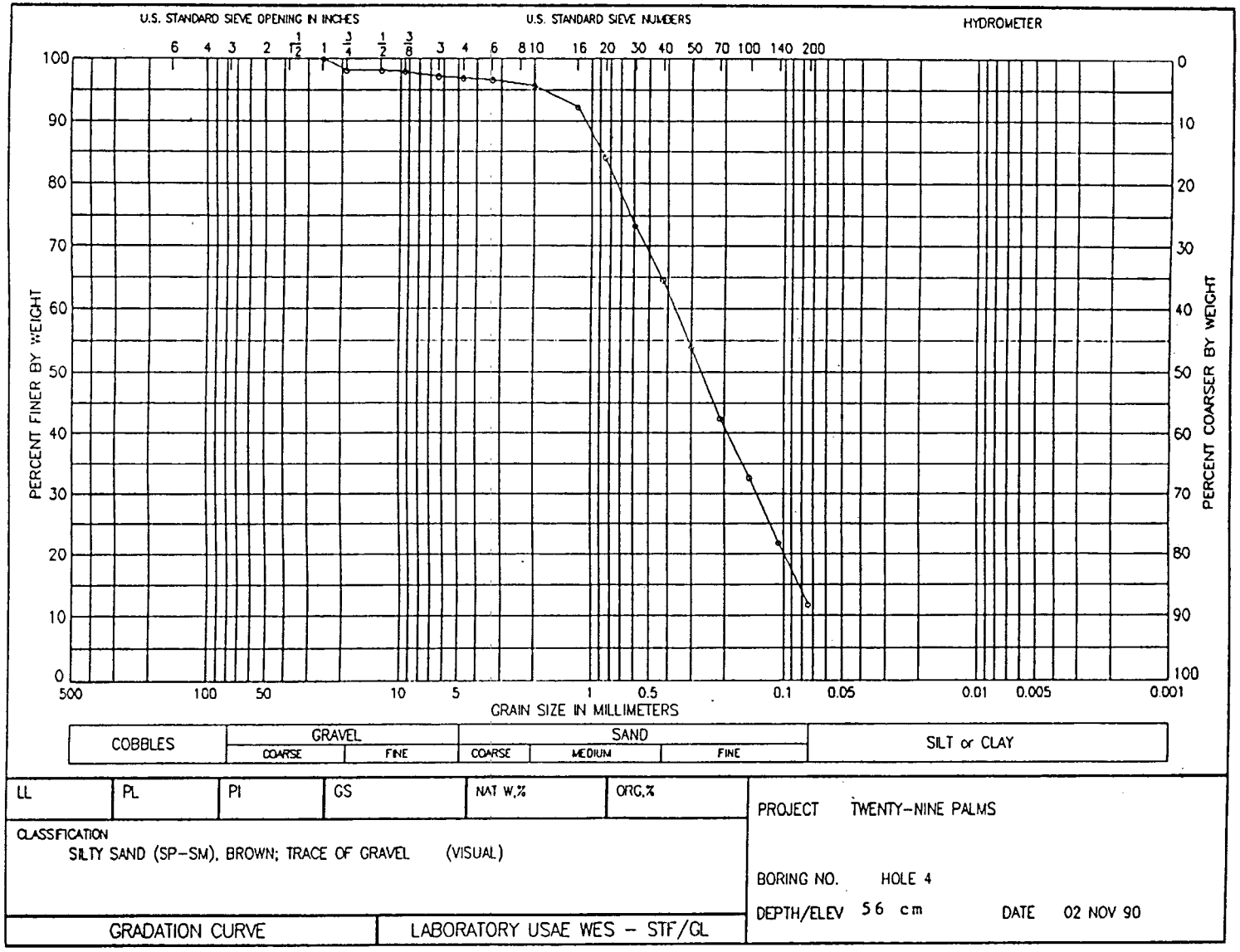

Figure D11. Site IV. D. Particle size, 56-cm depth.

Memorandum for Lee Tidwell, SD-O October 31, 1990
Subject: Examination of Soil from 29 Palms

1. Twelve samples of soil were received for examination from 29 Palms. The samples are from four different holes representing three levels in each hole. The samples are described below:

Hole Number and Depth			
#1	#2	#3	#4
4 cm	4 cm	4 cm	4 cm
10 cm	13 cm	10 cm	18 cm
51 cm	64 cm	74 cm	56 cm

2. The sand size particles in all samples were similar and tended to be subrounded to rounded. The majority of the sample consisted of quartz grains, potassium feldspars, and plagioclase feldspars. Other mineral constituents consisted of amphiboles, mica, calcite and possibly some clay minerals. There were also some white crystals in some samples that may be gypsum.

3. Some of the samples contained gravel and coarse sand size particles. These particles are igneous type rocks ranging from granites to fine grain rhyolites.

4. Agglomerates of sand size particles were evident in several of the samples. These agglomerates consisted of sand grains cemented together with a clay matrix as water was applied to these agglomerates, they disaggregated easily.

5. Calcite was present in all samples as discrete particles and did not contribute to the cementing mechanism of the agglomerates.

6. Individual description of materials found in each hole is provided as follows:

a. Hole #1. The near surface sample consisted of large agglomerates and sand grains. The other two samples from this hole contained no agglomerates.

b. Hole #2. All samples in this hole were similar with only minor agglomerates present. The deepest sample contained no large aggregate particles while the two near surface contained a few large aggregate particles but tended to be mostly sand size particles.

c. Hole #3. The near surface sample consisted mostly of sand size particles, middle sample consisted of large agglomerates, and the deep sample consisted of gravel size igneous rock particles.

d. Hole #4. All three samples were similar with only minor agglomeration and mostly sand size particles.

Conclusion

7. The composition of all samples were similar. Only differences observed were the agglomeration of sand particles and presence of gravel size particles that were present in some samples and not in others. The depth of various deposits such as agglomerates and gravel particles were not consistent and tended to be random.

8. When dry, the agglomerates were hard but when wet they disaggregated readily. Physical properties of the soil containing agglomerates is expected to be drastically different when wetted.

G. Sam Wong, WESSC-EP

The numbers, 1 through 4, at the midpoints of each side of the test site, indicate where the four soil pits were dug and where surface roughness measurements were made.[5]

Surface Roughness Measurements

Methodology. Radar backscatter prediction models require, as input, one or more parameters that characterize surface roughness. Two such fundamental parameters are the standard deviation of surface height and the surface correlation length (Ulaby et al., 1982). A very crude method was used for collecting data that could be used to generate these parameters. A 1-meter-square wire grid with a 10 cm wire spacing was positioned above an arbitrarily-selected patch of the test site terrain. A ruler was used to measure the distance from the grid intersections to the terrain surface directly beneath each intersection. These height measurements were recorded in a field notebook and later processed to calculate the desired surface roughness parameters.

A set of grid measurements was taken just inside the test site boundaries near the four numbered locations identified on Figure D12. The results of these measurements are found in Figures D13-D16. Elevation measurements are all reported in tabular form as though the measurements were taken from the south side of the grid, numbers in the first row representing measurements made along the north edge of the grid.

Analysis. Several caveats with regard to the surface roughness measurements are in order. First of all, there is the inherent assumption that a 1-meter-square sample of terrain elevations is representative of larger areas. At this site, this is probably not a bad assumption, as far as calculating standard deviations is concerned, because there are no large-scale elevation changes within the test site.

If the standard deviation calculations have merit, then they may be used to test the smoothness criteria for the SAR systems. Let the standard deviation of elevation be called σ. Then Rayleigh's criterion for the terrain to appear "smooth" to the radars is

$$\sigma < \lambda/8\cos\theta$$

while the more restrictive Fraunhofer criterion is (Ulaby et al., 1982)

$$\sigma < \lambda/32\cos\theta$$

where λ is the free-space wavelength of the radar and θ is the incidence angle of the radar (with respect to vertical). If typical average wavelength values are substituted for X-, C-, and L-band radars (3-, 5-, and 20-cm wavelengths, respectively) into these criteria, then a plot like Figure D17 can be drawn to visualize the "smoothness" conditions for this test. Comparing the average surface standard deviation of the four data sets (2.2 cm), it is clear that even for the less restrictive Rayleigh criterion, only the L-band system would see the terrain as smooth.

[5] These observations were made prior to construction of the site; changes caused by trench digging are thus not addressed.

29 PALMS TEST SITE GROUND-TRUTH

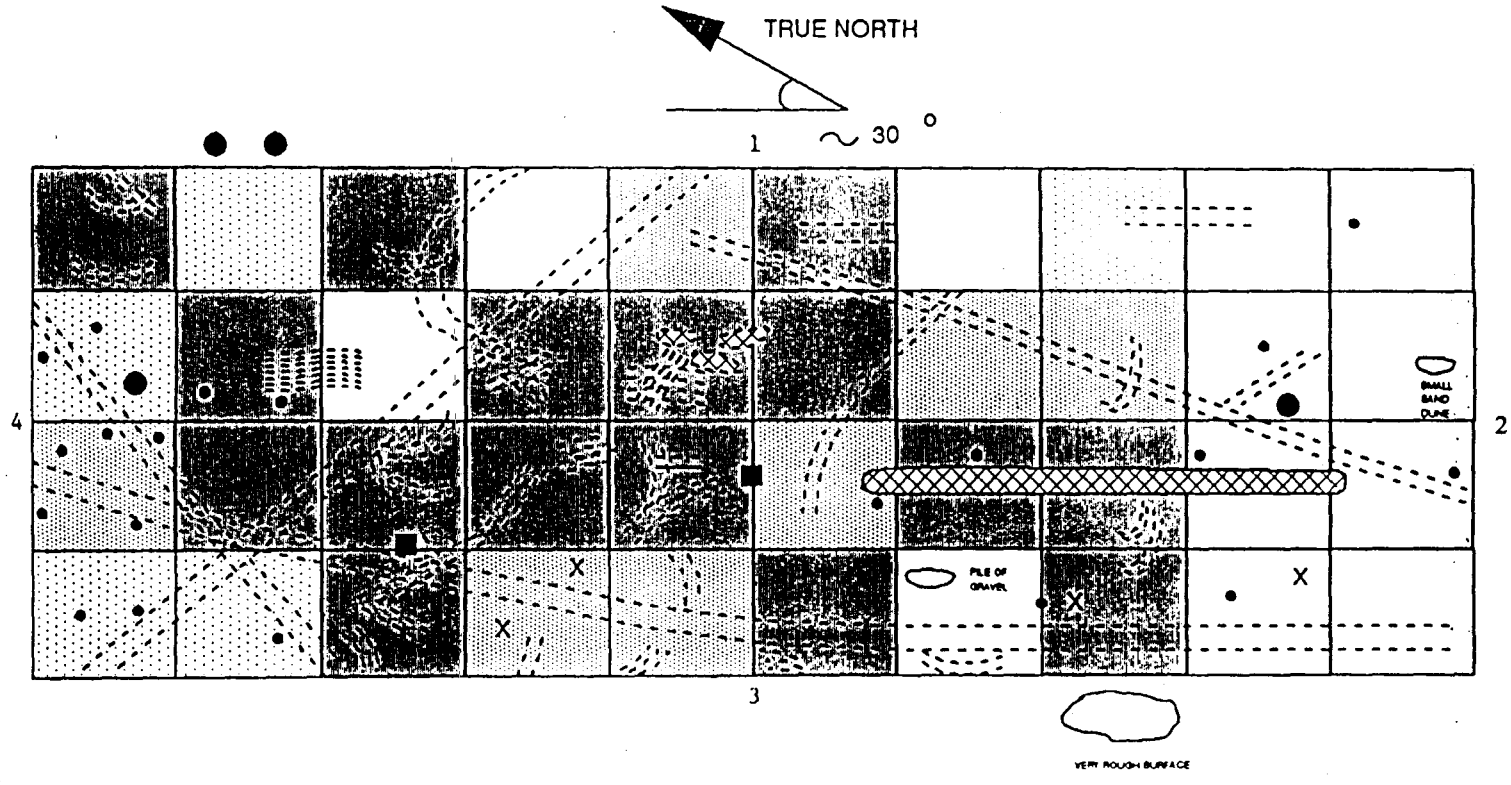

- CREOSOTE = 50cm DIAMETER
- CREOSOTE = 100cm DIAMETER
- SMOKE GRENADE BOX
- X SHELL CASINGS
- SANDY DEPRESSIONS
- VEHICLE TRACKS

MAXIMUM ELEVATION DIFFERENCE

- 0-5 cm
- 5-10 cm
- 10-15 cm
- 15-20 cm

Figure D12. Twentynine Palms test site ground truth.

As for correlation lengths, the small sampling area and relatively large sample spacing probably distorts the calculation. To obtain the reported correlation lengths, the normalized autocovariance function (or correlation coefficient function) was calculated for each of the 11 east-west transects. An average of all the east-west transects was then calculated at the grid spacing. The same was done for the north-south transects. In both directions, the 1/e value of the coefficient fell between the reported lag distances. However, because each transect involved only 11 data points, one has to believe that longer transects with the same sample spacing would give more meaningful results.

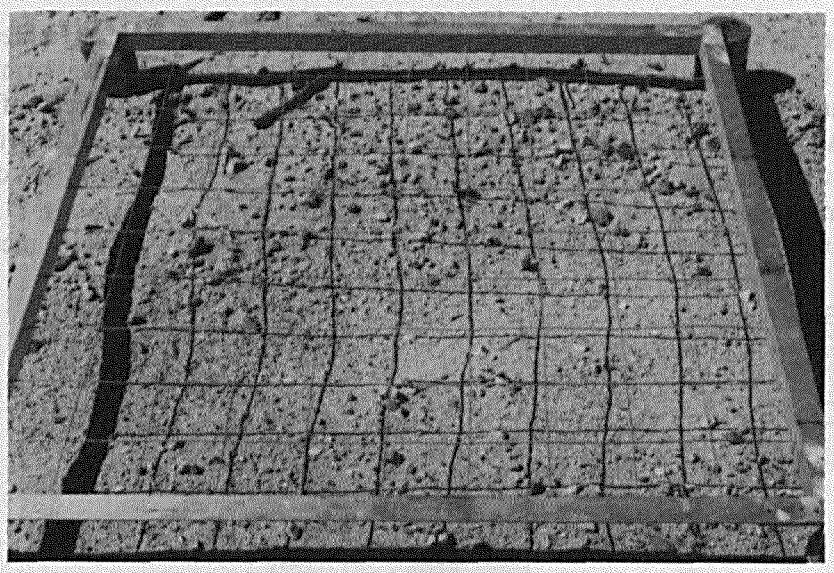

Grid Placement

11.0	9.0	9.3	9.2	8.0	8.5	8.3	7.8	8.3	8.9	9.4
10.6	9.2	9.9	9.2	8.7	8.2	8.4	7.8	8.8	9.5	10.0
10.6	9.5	9.5	9.2	9.2	8.8	9.0	9.5	9.1	10.0	11.0
10.5	9.8	9.2	9.2	10.0	9.8	9.8	10.7	11.0	12.2	12.5
8.3	9.5	9.1	9.5	10.4	10.6	11.9	12.0	13.0	13.4	13.6
8.9	9.2	10.3	11.5	11.2	12.5	12.5	13.0	12.7	13.1	13.0
10.5	10.5	11.5	12.0	12.3	12.0	12.2	12.0	11.7	12.0	12.5
11.5	11.6	12.2	12.1	11.5	9.5	10.5	11.1	11.1	11.5	10.8
12.0	12.0	11.1	11.0	10.1	10.5	10.1	9.6	9.4	9.4	9.3
10.5	11.1	10.8	10.9	10.4	9.6	9.4	9.0	9.0	9.0	9.5
10.3	10.8	10.3	9.9	9.2	9.2	9.1	9.5	9.5	10.3	10.5

Elevation Measurements in Centimeters

MAXIMUM ELEVATION DIFFERENCE = 5.8 cm

STANDARD DEVIATION = 1.4 cm

CORRELATION LENGTH = 10-20 cm

Figure D13: Site I Surface Roughness Measurements

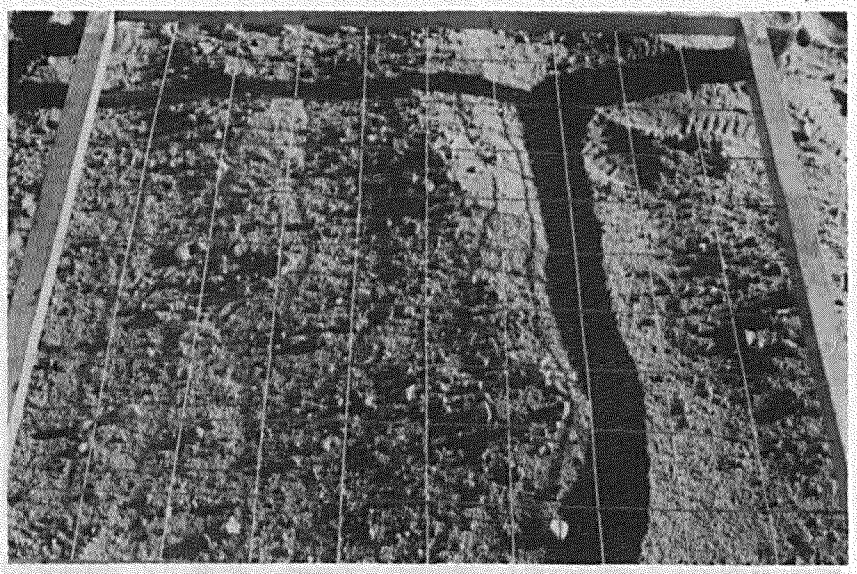

Grid Placement

11.2	11.3	10.3	9.9	9.0	9.2	10.0	9.9	10.1	10.0	9.9
11.5	11.0	9.6	8.0	8.0	8.9	9.2	9.7	9.9	10.2	10.0
9.6	9.8	8.6	7.2	7.0	7.8	9.0	9.7	10.2	10.2	10.0
8.7	9.1	8.2	6.7	6.5	7.5	8.4	9.5	9.7	10.3	10.5
7.5	8.5	8.8	7.2	7.0	8.2	8.0	9.0	9.6	10.5	10.4
7.6	8.5	8.6	7.8	7.2	7.2	8.2	8.2	8.5	10.2	10.2
8.3	9.1	9.5	8.2	6.4	6.8	7.9	8.5	8.5	9.5	9.8
10.0	9.5	9.6	8.7	5.6	6.0	7.8	8.3	8.7	9.5.	9.9
9.0	8.3	9.2	8.3	6.8	6.5	7.4	8.0	7.7	9.5	10.0
9.0	8.8	9.2	9.0	7.5	6.8	8.0	8.3	8.0	9.1	9.6
9.0	8.0	8.7	9.0	7.5	7.0	7.3	8.0	8.1	9.1	9.9

Elevation Measurements in Centimeters

MAXIMUM ELEVATION DIFFERENCE = 5.9 cm

STANDARD DEVIATION = 1.2 cm

CORRELATION LENGTH = 10-20 cm

Figure D14: Site II Surface Roughness Measurements

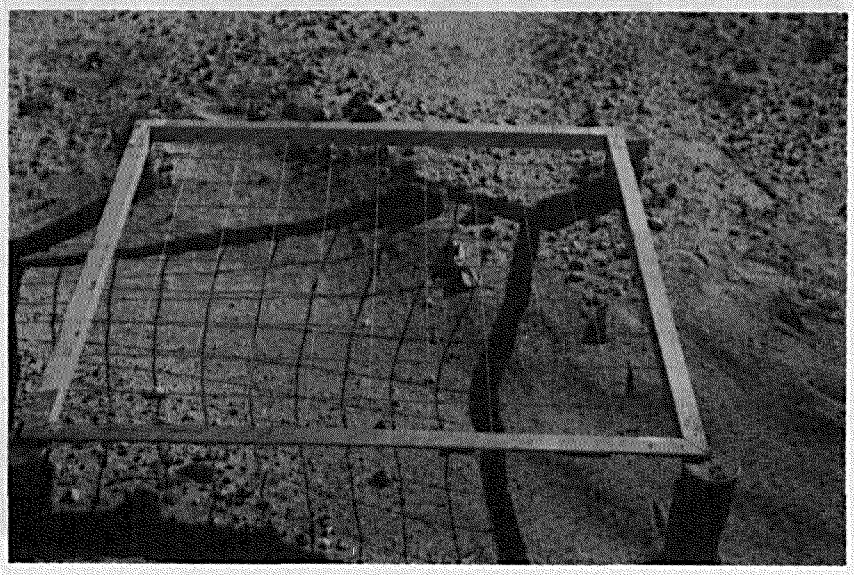

Grid Placement

9.6	9.7	11.1	13.0	14.8	16.0	17.0	17.5	17.8	17.0	16.0
9.4	10.6	12.2	13.8	15.6	16.2	17.0	17.0	17.0	15.7	15.0
9.3	11.5	13.5	15.1	15.8	16.5	16.4	16.6	15.6	14.8	14.0
11.9	13.4	15.0	16.3	17.1	16.6	16.8	15.8	15.0	14.0	12.7
14.4	15.5	17.0	17.5	17.6	17.4	16.5	15.5	14.0	12.3	10.5
16.5	16.8	18.0	18.5	19.0	17.6	16.3	14.2	12.4	10.2	8.4
18.3	18.3	18.8	19.5	19.0	18.1	15.5	13.0	10.1	5.5	7.0
19.1	19.4	19.6	20.5	20.3	18.6	14.7	12.2	10.0	9.1	8.1
20.0	20.8	20.5	20.0	19.7	18.1	15.3	14.2	12.1	10.8	9.5
21.0	20.5	20.0	20.8	19.5	18.3	16.3	14.2	13.8	12.5	11.4
20.5	20.2	20.6	21.4	19.5	18.8	17.5	15.6	14.8	14.0	12.0

Elevation Measurements in Centimeters

MAXIMUM ELEVATION DIFFERENCE = 15.9 cm

STANDARD DEVIATION = 3.5 cm

CORRELATION LENGTH = 20-30 cm

Figure D15: Site III Surface Roughness Measurements

No Photo Available

Grid Placement

14.3	12.7	13.2	12.8	12.5	13.3	13.8	13.7	14.5	14.5	14.4
13.8	14.0	13.7	13.3	13.4	14.2	14.5	14.5	14.3	14.5	13.8
14.7	14.7	15.3	15.5	15.6	15.5	15.2	14.5	13.6	13.3	12.8
14.2	15.1	15.0	15.5	15.0	14.8	14.1	13.0	11.8	11.2	10.5
13.8	14.3	14.5	14.3	14.0	13.0	11.8	11.0	9.3	8.5	10.5
13.0	12.1	12.0	11.2	10.5	10.2	8.8	8.0	7.2	8.2	11.2
13.3	12.0	11.0	9.4	8.3	6.5	5.5	5.0	6.0	9.0	11.5
14.5	13.3	12.5	11.1	8.8	7.5	6.0	4.5	7.5	11.5	12.3
15.1	14.2	13.3	12.3	10.7	8.5	6.6	7.5	10.0	12.5	12.8
14.8	14.0	13.2	12.5	11.0	9.8	8.5	10.6	12.0	13.5	13.5
14.9	13.5	13.5	13.2	12.8	11.0	10.0	12.0	13.7	14.2	14.2

Elevation Measurements in Centimeters

MAXIMUM ELEVATION DIFFERENCE = 11.1 cm

STANDARD DEVIATION = 2.6 cm

CORRELATION LENGTH = 10-20 cm

Figure D16: Site IV Surface Roughness Measurements

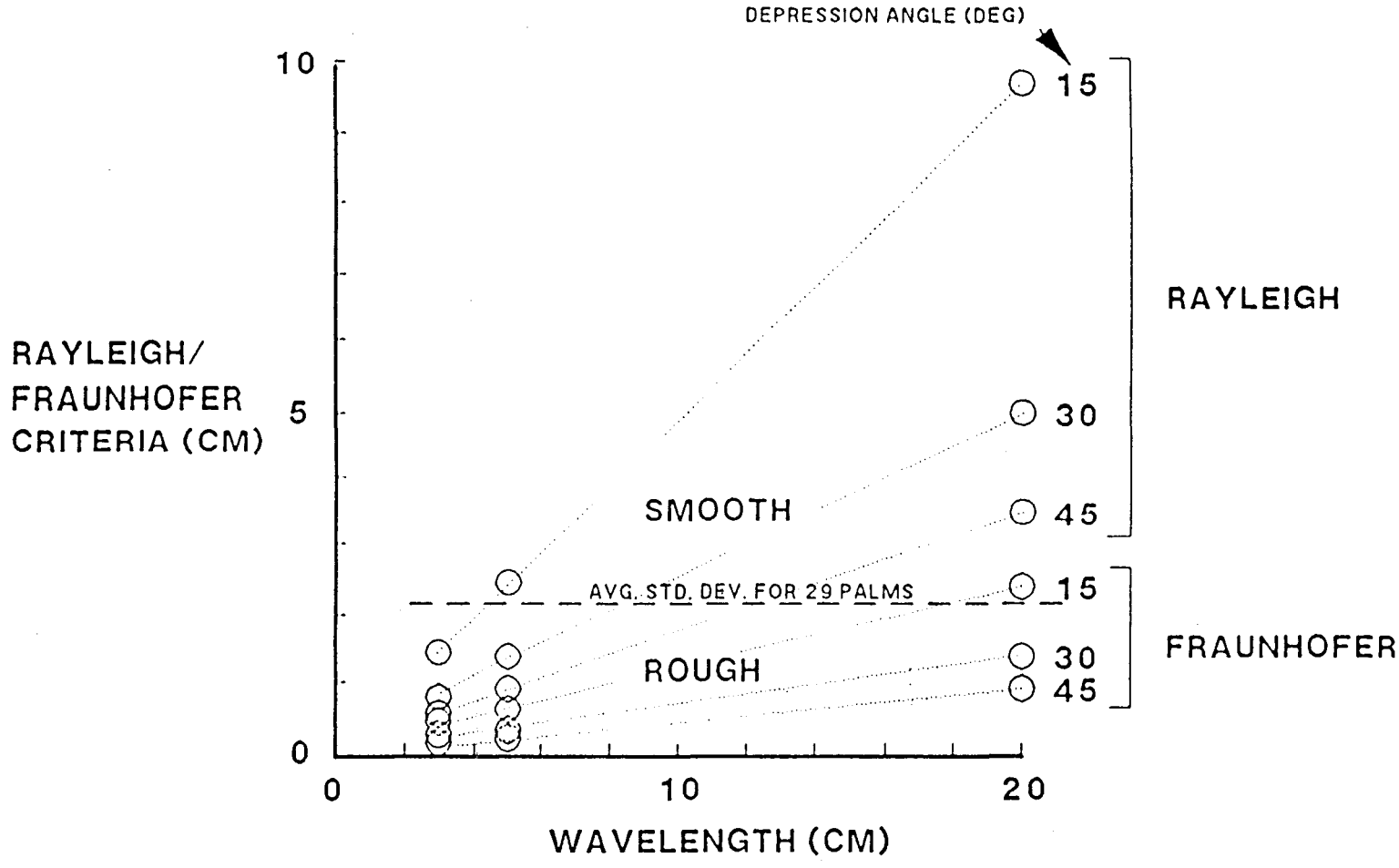

ROUGH SURFACE CRITERIA

Figure D17. Rough surface criteria.

References

Curtis, J.O. and Tidwell, L.E. 1992. *Twenty-nine Palms, California Test Site Characterization*: Vicksburg, Mississippi, U.S.A. Waterways Experiment Station, TR EL-92-14.

Ehlen, J. and Henley, J.P. 1991. *Comparison of Soils from Saudi Arabia and Twentynine Palms, CA*: Fort Belvoir, Virginia, U.S.A. Engineer Topographic Laboratories, ETL-0583, 67 p.

Ritter, D.F. 1986. *Process Geomorphology*, 2nd edition: Dubuque, Iowa, William C. Brown.

Rubick Luttrell, P. 1991. *Petrographic Analysis of Sediment Samples Collected from Field Sites in Saudi Arabia and Twenty-Nine Palms, California*: unpublished TEC contract report, 28 p.

Ulaby, F.T., Moore, R.K. and Fung, A.K. 1982. *Microwave Remote Sensing, Active and Passive, Vol. II, Radar Remote Sensing and Surface Scattering and Emission Theory*: Norwood, Massachusetts, Artech House.

APPENDIX E

PATTERN-FINDING ALGORITHMS

Introduction

Pattern-finding algorithms were developed for two specific problems. The first problem was concerned with the automatic extraction of surface metallic mines from high-resolution SAR imagery. The second problem was the automatic extraction of the disturbed soil sections of a minefield using SAR imagery. The problem of automatically extracting surface metallic mines using high-resolution SAR imagery consisted of the application of seven computer vision routines. These seven routines are (1) speckle reduction using the geometric filter, (2) thresholding, (3) connected components, (4) connected component extraction using the region property of area, (5) Hough transform, (6) connected components, and (7) centroid calculations. The connected components routine is used twice in order to obtain the final result, which consists of a square drawn around each of the surface metallic mines located in the original image.

The problem of automatically extracting the disturbed soil sections of a minefield using radar imagery required the application of six computer vision routines. These six routines are (1) speckle reduction using the geometric filter, (2) thresholding, (3) elimination of small connected components, (4) elementary fusion, (5) connected components, and (6) extraction of the disturbed soil component and superimposing it onto the original image. The final result of applying these routines is an image in which the disturbed soil section of the image is outlined in white and filled in with black. The following sections discuss the pertinent portions of the various computer vision routines and present the results for the two problems solved.

Methodology for Extracting Surface Metallic Mines

Speckle Reduction

All SAR images suffer from the results of speckle noise. This noise comes as a result of the coherent nature of the radar system. It is very desirable to reduce the speckle noise in SAR images to assist radar image interpreters and/or to digitally process images with automatic recognition algorithms on computers. The objective is to eliminate speckle, but at the same time to preserve important features of interest such as edges, strong returns, etc. The geometric filter developed by ERIM provides a good approach to speckle reduction. Speckle noise in a radar image appears as bright narrow spikes located randomly throughout the image. The geometric filter provides for the sharp reduction in amplitude of these high narrow spikes in the imagery. Other high peaks and plateaus that are associated with real terrain features are also reduced, but not as much or as fast as the high narrow spikes. Also, the geometric filter is iterative in nature, i.e. the output of one application of the geometric filter can be used as the input to another application. For this problem, two iterations of the geometric filter were used to eliminate most of the speckle.

Thresholding

A single-level thresholding routine was used to create a binary image. The threshold level depends upon the particular radar system being used. In this case, a threshold level of 45 was used. Every pixel that had a gray value less than 45 was set to 0, and every pixel that had a grey value equal to or greater than 45 was set to 255. For an 8-bit image, there are 256 gray levels, with 0 representing black and 255 representing white. The reason that thresholding is performed at this time is that a binary image is required as the input for a connected components routine.

Connected components

A binary image can be considered as consisting of 1's and 0's. The 1's can be associated with white, and the 0's with black. The purpose of the connected components routine is to provide a unique label for each pixel in a component of 1-pixels in the binary image. This is done by using a recursive routine in which each pixel in a given connected component is visited and assigned the unique label. Once all of the pixels in a given connected component have been labeled, the label is incremented and the next connected component in the image is analyzed. Eight connectivity was used for 1-pixels and four connectivity was used for 0-pixels.

Mine (Region) Extraction using Area

The area of a connected component is defined simply as being equal to the number of pixels in that component. It was found that the surface metallic mines always had areas of between 3 and 30 pixels. All connected components that had areas outside this range were eliminated. Although many other region properties could be computed, this was not necessary because the property of area was sufficient to eliminate connected components that were obviously not mines.

Hough Transform

The purpose of the Hough transform is to find those pixels in the image that form lines. Since the metallic surface mines were laid out in straight lines, it appeared that the Hough transform would be appropriate. The normal representation of a line was used and an accumulator array was formed that was initially set to all zeros. A particular point in the image plane formed a sinusoid in the transform or accumulator-array plane. When a large number of pixels fell into a particular cell of the accumulator array, they provided strong evidence that these pixels formed a line on the original image. In this case, 40 pixels were required in order to define a line. The Hough transform can find lines in a binary image regardless of their orientation.

Centroid Calculations

The purpose of the centroid calculations is to compute the centroid of each connected component and to draw a 17- by 17-pixel square around each centroid and place these squares on the original image. These squares indicate the final location of the mines.

Methodology for Extracting the Disturbed Soil Sections

It was discovered that on the L-band imagery, the disturbed soil sections of the minefield (Phase I), particularly around the area of the buried mines, was easily seen. This disturbed soil effect

was not present on the imagery from the Phase II site. Also, the exact reason for the disturbed soil effect at the Phase I site on the L-band imagery is not completely understood. It was found that on this L-band imagery, the disturbed soil effect was brighter for the VV polarization and for the smallest angle of incidence. The speckle reduction technique used on this imagery was the same as that used for the previous problem except that three iterations of the geometric filter were used instead of two.

Thresholding

A single-level thresholding routine was used to make a binary image. The threshold level varied with the angle of incidence. There were three angles of incidence associated with the L-band imagery: 35°, 50°, and 70°. The threshold levels used with each of these angles were 150, 120, and 100, respectively.

Elimination of Small Connected Components

The elimination of small connected components consisted of setting to zero all pixels in any connected component that had an area smaller than 16 pixels by 16 pixels. A 16x16 mask is moved across the image,and if any connected component is entirely contained within this mask,the component is then eliminated.

Elementary Fusion

The fusion operation used here consisted of two elementary operations, contraction and expansion. For a given binary image, the following operation is called contraction: all the 1-pixels located within a given distance t ($t > 1$) from all 0-pixels are negated (changed to 0-pixels). The following operation is called expansion: all the 0-pixels located within a given distance t ($t > 1$) from the 1-pixels are negated (changed to 1-pixels). In this case, an expansion was performed first, followed by a contraction and the value of t was set at 4. The fusion operation was used in order to fill in the holes that occurred in the connected component resulting from the disturbed soil effect.

Extracting the Disturbed Soil Component and Superimposing it on the Original Image

After the applying a connected components routine, the three region properties of area, elongation, and the measure of region spread were used to extract just the connected component associated with the disturbed soil portion of the minefield. The area of a connected component is simply equal to the number of pixels in that component. Elongation is calculated in terms of the maximum and minimum moments of inertia. It is equal to the difference between the maximum and minimum moments of inertia divided by their sum. A measure of region spread can be found by taking the sum of the maximum and minimum moments of inertia and dividing this result by the area squared. The maximum and minimum moments of inertia are computed using the principal axes of the connected component. The disturbed soil component could easily be isolated from all other components in the image using these three region properties. Once the disturbed soil component was found, a border-following algorithm was used to outline this component in white and to place it on the original image.

Results

The following results were obtained for each of the two problems discussed:

1. Extracting metallic mines located on the surface:

   a. The metallic surface mines were clearly located by the algorithm.

   b. The algorithm also found points located on the fences that surrounded the mines.

   c. The Hough transform worked well in finding the surface metallic mines that were laid out in a linear pattern.

   d. The geometric filter did a good job of eliminating speckle noise.

2. Extracting the disturbed soil sections:

   a. The disturbed soil portions of the Phase I minefield were easily visible on many, but not all, of the L-band radar images.

   b. The disturbed soil portions of the minefield were brighter for the smallest angle of incidence and for VV polarization.

   c. The disturbed soil portions of the minefield were extracted automatically using the algorithm discussed above. An example of this extraction is shown in Figures E1 and E2 in which the polarization was VV and the angle of incidence was 70°. Figure E1 is the original radar image of the test site, and Figure E2 shows the extracted disturbed soil section of the image.

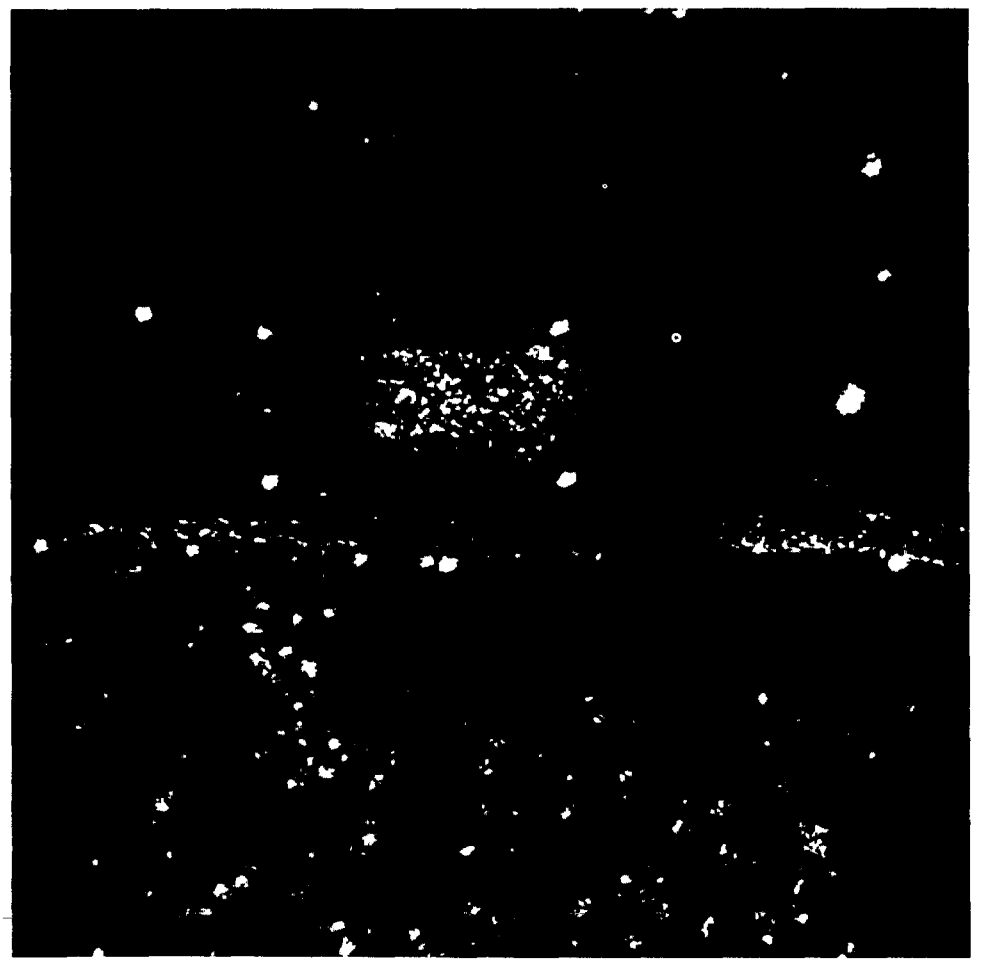

Figure E1. L-band radar image of the Phase I test site.

Figure E2. L-band radar image of the Phase I test site with disturbed soil section extracted.

APPENDIX F

DETECTION OF SUBSURFACE MINES[6]

Introduction

The objective of Project Ostrich, as stated previously, was to detect buried metallic or nonmetallic mines/objects. To deal with the problem of subsurface mine detection, various sensors were used to fly over two test sites. This section describes the procedures and results of using conventional SAR.

SAR Imagery Description

The NAWC SAR system collected X-, C-, and L-band imagery of the first minefield test site in October 1990 (Phase I). The data delivered to TEC by ERIM came in digital form and was 16-bit data that had to be converted to 8-bit data in order to be processed by TEC's computers. Some of the imagery was provided as 512x512 pixel images and could be processed and analyzed directly after 16-to-8-bit conversion. However, the majority of the images were larger (1024x1024 and 2048x2048) and had to be partitioned into 512x512 images. The test site area was always the focus of the partitioning, and any partitioned images lying outside the test site were generally not processed further. The initial X-, C-, and L-band images had been smoothed and had a resolution of 3.24 m (azimuth) x 2.4 m (range). Higher resolution (0.54 m, azimuth x 1.2 m, range) C-band and L-band images were obtained later from ERIM and were analyzed in detail. Polarizations (HH, VV, HV, VH) of the radar were noted during analysis as well as grazing angles of the radar beam.

All three bands of radar data for the first site were analyzed at TEC with special emphasis placed on the C- and L-band higher resolution data. The C- and L-bands have longer wavelengths (lower frequency) than X-band (X = 3 cm, C = 5 cm, L = 23 cm). Generally, they have the capability to penetrate the soil surface to a greater depth than X-band depending on various factors such as soil moisture, vegetation/ground cover and the soil surface roughness properties. Both the C- and L-band images of the Phase I test site show a disturbed soil area (area of trenches and machinery tracks) in the area that contained the buried mines. This part of the image was analyzed in detail.

The NAWC SAR system collected data over the second test site in December 1990 (Phase II). Of the ERIM data (X-, C-, and L-band), only the L-band higher resolution images of the second test site were analyzed. These data were selected because it was theorized that a longer wavelength like L-band might penetrate the soil surface deep enough to detect a metallic mine buried at a shallow depth. The data were also analyzed for detection of disturbed soil patterns. Data from both test sites were analyzed by doing a statistical analysis and profile analysis. The techniques of these analyses and the results are discussed in the next section.

---

[6] Verner Guthrie and Ed Simental prepared this appendix.

Subsurface Mine Analysis and Methodology

Profile Analysis

The expected signal returned from subsurface mines is very weak at best, and the presence of noise obscured the return. Attempts to detect these returns by analysis of line profiles proved unsuccessful. The intensity of the pixel values was plotted against the pixel coordinates. If the ground surface returns were constant with very little noise, one would expect that a signal return from the buried mines would show up as peaks on the plot. If in fact there is a return from these mines, it is so weak that it is lost in the noise. This profile algorithm was applied to C-, X-, and L- band radar images of various grazing and squint angles and various polarizations. The only thing clearly observed by using this algorithm was that L-band images seemed to be noisier than C- or X-band images. Although a speckle reduction algorithm was applied to the images and worked well, other noise reduction algorithms did not help because they removed too much of the image along with the noise.

Statistical Analysis

A statistical analysis was also conducted in an attempt to detect the buried mines. The analysis consisted of taking a small window (16x16 pixels) of the image and computing the mean, variance, and standard deviation of that window. If the image background is near constant in intensity and there are few features, windows that contain a buried mine return will differ statistically from those that do not. This algorithm worked very well with surface mines where it was easy to detect the windows that contained mines. For the subsurface mines, it was not possible to know conclusively which windows contained mines because the mine signal was either very weak or there was no signal at all. In addition, image artifacts and random noise distorted the statistics. In some images, especially L-band images, the image resolution is such that the window covers an area much bigger than a mine.

Conclusions

1. The profile and statistical analyses conducted in this investigation did not provide any indication of buried mines (metallic or nonmetallic).

2. No determination of optimum radar parameters (angle of incidence, polarization, squint angle, etc.) to detect buried mines could be made since none were detected on any imagery analyzed.

3. The signal from the buried mines, if it exists, appears to be lost in the noise.

4. The image quality of many images was poor and inconsistent.

5. Image resolution varies from image to image.

6. The complex dielectric constant of nonmetallic mines is very close to the complex dielectric constant of dry soils, and therefore little reflection occurs at the interface between the two.

Recommendations

1. Further analysis in this area should emphasize combinations of the polarizations HH, HV, VV, VH and/or combinations of different wavelengths.

2. Any future work in trying to detect buried mines with radar should emphasize very high-resolution systems.

3. The application of electromagnetic propagation in soil to detect buried objects is not well understood. Therefore, it is recommended that an in-depth theoretical study of the electromagnetic scattering mechanisms be conducted to include the effects of polarization, surface roughness, frequency, angle of incidence, depth, shape, and size of the buried mines. Such an analysis should provide quantitative recommendations for future experiments.

4. The buried mine problem may be alleviated by studies in the development of efficient noise reduction algorithms and/or the improvement of signal-to-noise ratio in the sensor system.

GLOSSARY

ASPO	Army Space Programs Office
BRDEC	Belvoir Research, Development and Engineering Center
C-Band	Radar wavelengths extending from 3.75 cm to 7.5 cm
DOD	Department of Defense
ERIM	Environmental Research Institute of Michigan
ETL	U.S. Army Engineer Topographic Laboratories
FSTC	Foreign Science and Technology Center
HH	Horizontal polarization transmitted and horizontal polarization received
HV	Horizontal polarization transmitted and vertical polarization received
JPL	Jet Propulsion Laboratory
LANDSAT	Multispectral earth-orbiting imaging satellite imaging land areas
L-band	Radar wavelengths extending from 15 cm to 30 cm
MCAGCC	U.S. Marine Corps Air Ground Combat Center
NASA	National Aeronautics and Space Administration
NAWC	Naval Air Warfare Center
OSD	Office of the Secretary of Defense
P-band	Radar wavelengths extending from 30 cm to 100 cm
Pixel	Unit of an observed digital image (picture element)
Polarization	Orientation of the electric field strength vector
RTV	Part of the designation for the silicon rubber in the nonmetallic mine
SAR	Synthetic Aperture Radar
SDA	Subterranean Detection and Analysis
SEE	Small Emplacement Excavator

GLOSSARY (continued)

SIR-A/B	Shuttle Imaging Radar, Mission A/B
SPOT	Système Probatoire d'Observation de la Terre, signifying Earth Observation Test System
TEC	U.S. Army Topographic Engineering Center (formerly ETL)
TTADB	Tactical Terrain Analysis Data Base
USCS	Unified Soil Classification System
USGS	U.S. Geological Survey
USMC	U.S. Marine Corps
USMC 173 MWSS	U.S. Marine Corps 173 Marine Wing Support Squadron
USMCCDC	U.S. Marine Corps Combat Development Center
VV	Vertical polarization transmitted and vertical polarization received
VH	Vertical polarization transmitted and horizontal polarization received
WES	U.S. Army Waterways Experiment Station
X-band	Radar wavelengths extending from 2.4 cm to 3.75 cm